IEEE Access
Multidisciplinary | Rapid Review | Open Access Journal

Received 21 March 2023, accepted 13 April 2023, date of publication 17 April 2023, date of current version 21 April 2023.

Digital Object Identifier 10.1109/ACCESS.2023.3267673

SURVEY

LED Systems Applications and LED Driver Topologies: A Review

MORTEZA ESTEKI[1], (Student Member, IEEE), S. ALI KHAJEHODDIN[1], (Senior Member, IEEE), ALIREZA SAFAEE[2], (Senior Member, IEEE), AND YUNWEI LI[1], (Fellow, IEEE)

[1]Department of Electrical and Computer Engineering, University of Alberta, Edmonton, AB T6G 1H9, Canada
[2]OSRAM Innovation, Beverly, MA 01915, USA

Corresponding author: Morteza Esteki (mesteki@ualberta.ca)

This work was supported by the Canada First Research Excellence Fund through the University of Alberta's Future Energy Systems Research Initiative.

ABSTRACT High-power light-emitting diodes (LEDs) and high-brightness LEDs have revolutionized the lighting industry. The availability of cost-effective LEDs with high luminous flux, efficacy, and reliability has expanded their application to replace incandescent and fluorescent light sources. They have also enabled many new applications that were considered infeasible before, due to the inherent limitations of traditional sources of light. This survey provides a comprehensive overview of ac- and dc-supplied LED lighting systems and their applications, corresponding specifications and their similarities to/differences from regular power supplies. Restrictions imposed by LEDs characteristics, safety considerations, and dimmers are discussed. Also, LED driving approaches are categorized and their suitability for different applications is provided.

INDEX TERMS Light-emitting diodes, LED drivers, LEDs applications, LED systems, power converters.

I. INTRODUCTION

Following the trend of other semiconductor devices, the price and performance of high-power LEDs (HP-LEDs) and high-brightness LEDs (HB-LEDs) have been continuously improving, and now the total cost of LED-based lighting products is dominated by other components of the system, especially the driver. Although the definition may vary, HB-LEDs refers to LEDs with a luminous efficacy greater than 50 lumens/watt [1], [2] while HP-LEDs refers to LEDs that typically have a single chip size of at least $1mm^2$, require a drive current of more than $350mA$, and consume over $1W$ of power [3], [4], [5], [6]. The early LED products were hardly more efficient than the mature incandescent lamps. Recent products, however, are more efficient, reliable and cost-effective gaining higher market share, and standards facilitate their adoption [7], [8].

High control-ability and fast dynamics of LEDs combined with powerful low-cost controllers provide unprecedented possibilities for futuristic LED-based products. The high efficacy [9], [10], customizable wavelength spectrum, directionality [11], [12], [13] and fast dynamics of LEDs have enabled them in data transmission applications such as Li-Fi. LEDs can also emit in non-visible parts of electromagnetic spectrum enabling applications such as ultraviolet sanitation systems and infrared night-vision, which were previously limited due to high energy demand of traditional light sources. Small form-factor, ease of drive and low-temperature operation of LEDs allow unprecedented flexibility in lighting applications. Micro-LEDs can be assembled in unconventional shapes, non-flat or flexible arrangements to make displays with no backlight [14]. LEDs compactness, their insensitivity to mechanical shock, vibration, and moisture and their long lifetime have enabled their application in the automotive industry both for interior and exterior lights [15]. Especially, steerable LED headlights can provide unique adaptive directionality of light to enhance the safety and user experience [16], [17].

Flexibility in the control of LEDs can improve light experience and quality [18], [19]. LEDs enable tunable color temperatures, e.g. in the lights that change color temperature from warm white (higher wavelengths) to cool white

The associate editor coordinating the review of this manuscript and approving it for publication was Ton Duc Do.

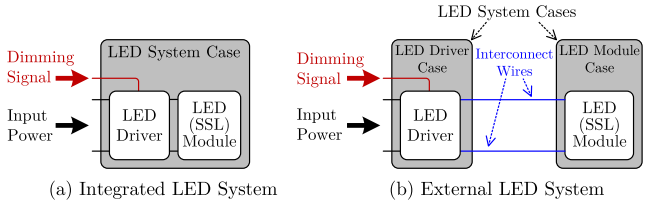

FIGURE 1. Configurations of LED lighting systems: (a) Integrated, (b) External LED driver.

(shorter wavelengths). The tunable light color/intensity feature is important in vertical farming industry, horticulture, which enables customized light color/intensity/duration optimized per plant or vegetable type [20], [21]. LEDs are also essential in human-centric lighting compatible with the circadian rhythm of human beings [22]. All these have shifted the lighting industry from a slow-paced mature state to a rapidly changing field with various new applications and possibilities.

Fig. 1 shows general configurations of LED lighting systems designed for solid-state lighting (SSL). A typical LED system has three essential parts: an SSL light source, a dedicated power supply called ''LED driver'' (which is the interface between the power source and the SSL), and a system case (including the required electrical, thermal, optical, and mechanical components to support the light source). The light source or LED module is usually composed of several LEDs and mounted to a thermally conductive base.

LED lighting systems can be implemented as Integrated or External configurations. In an Integrated system, Fig. 1(a), the LED driver is housed in the same case as the LED module, while in External configuration, Fig. 1(b), the driver and modules are housed separately. Integrated systems are commonly used in residential applications and can be installed as ''Plug and play'' or ''Internal drivers''. Internal drivers are built into the LED fixture itself, whereas plug-and-play drivers are separate components that can be connected to the fixture via a plug or a screw-in socket. Internal drivers are typically used in new LED fixtures that are designed to be hardwired into the building electrical system. These drivers are permanently installed inside the fixture, which means that they cannot be easily removed or replaced. LED downlights and LED troffer lights are examples of internal drivers. Plug-and-play drivers, on the other hand, are designed to be more flexible and versatile. These drivers can be connected to the fixture via a plug, which means that they can be easily removed or replaced if needed. This makes them ideal for retrofitting existing fixtures with LED lighting. Examples are LED bulbs and tubes compatible with old incandescent bulbs and electronic ballast tubes, respectively. In both of the Integrated methods, there is thermal coupling between LED module and the driver, as well as limitations on the size and weight of the whole product that make component and heat transferring more challenging. The external LED systems, Fig. 1(b), are normally used for applications such as outdoor, commercial, and street lighting, where better reliability, longer life span and safer product are more important than retrofitting. The heat transfer of the driver and LED module can be dealt with separately, however, running wires between them brings new challenges such as EMI or protection issues. These all impact the driver design process specific to LED products. This paper describes specific needs of Integrated or External configurations for different applications and their impact on topology and protection selection.

As LED-lighting systems were initially introduced for the largest market i.e. general lighting, the primary power source was limited to ac-grid. With the expansion of LEDs applications, there are now many LED systems compatible with dc power sources. In addition to automotive applications, the development of renewable energy systems with dc outputs has opened possibilities toward dc-distribution concepts where LED light sources can be directly driven from dc [23]. Another development initiated by information technology is the concept of Power-over-Ethernet (PoE) enabling the network infrastructure to provide dc power via an Ethernet cable to an endpoint device, which can be an LED luminaire. A luminaire or a light fixture is a complete lighting unit consisting of a light source(s) and driver(s) or ballast(s), together with the parts designed to distribute the light, position and protect the light source(s), and connect the light source(s) to the power supply [24], [25]. The emerging interest in Internet-of-Things (IoT) also brought LED drivers into attention [26] as they can provide power not only to LEDs but also to adjacent IoT systems. This is especially true for LED drivers in outdoor lighting poles which have both the strategic properties: being close to where people are, and having permanent energy availability [26]. The extended-feature that makes LED drivers in demand is to power up sensor boards, wired and wireless pole-pole networks and even micro-cell telecommunication stations installed in the poles, all as parts of ''Smart City'' landscape [27]. Although power over Radio Frequency (RF) has been used in a variety of applications, such as applications such as wireless sensor networks (WSNs) and Internet of Things (IoT) [28], [29], [30], [31], to the best of our knowledge, RF power harvesting has not been reported to be used for delivering power to LEDs.

In this paper, a comprehensive categorization of LED lighting applications is provided and their unique needs are discussed in detail. Providing more application-oriented insight can help engineers and product designers develop better products with fewer iterations. As a subcategory of power supplies, LED systems have many similarities to other power electronic converters. This review provides both similarities and differences of LED drivers from other power supplies. A balanced coverage of both ac-fed and dc-fed LED systems, their application needs and proper driver topologies is contributed. Driver topologies for each of ac-fed and dc-fed systems are categorized and the common properties of each category are described based on applications. Some features unique to LED products are discussed in more depth, for example, phase-cut dimming methods and related topology

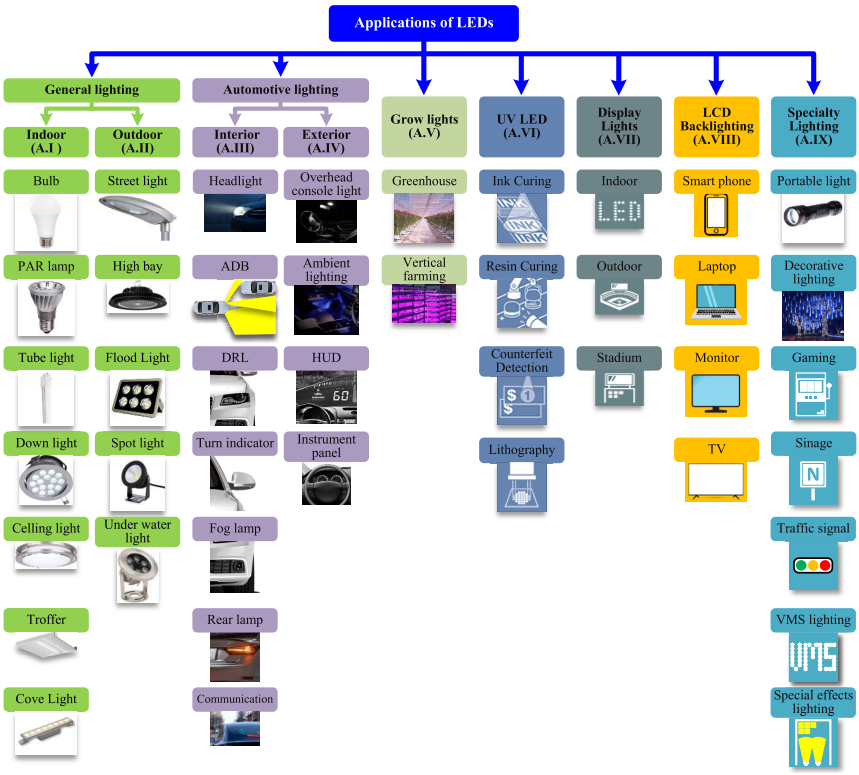

FIGURE 2. Main LED lighting applications.

compatibility, bleeder circuits and constraints for satisfactory customer experience. Double Frequency Power decoupling strategies to compensate power pulsation in ac-fed LED drivers are provided and the passive and active methods for reduction of energy storage components are described. Also for dc-supplied LED systems, partial power processing solutions are discussed, including the systems based on switched capacitor concepts. Finally, a list of topologies per application is recommended as a possible starting point for practicing engineers.

This paper is organized as follows: LED system applications are discussed in section II, and LED module configurations are given in section III. The specifications of LED systems are discussed in section IV. Ac-supplied and dc-supplied LED driving approaches are presented in sections V and VI, respectively. Finally, the suggested starting topologies and conclusions are provided in section VII and section VIII, respectively.

II. LED SYSTEMS APPLICATIONS

LED technology has been progressing and replacing traditional light sources. As LEDs capabilities increase, their applications expand as well. In Fig. 2 LEDs applications are classified into seven main categories (A.I to A.IX): general lighting, automotive lighting, grow lights, UV LED lights, displays, LCD back-lighting and specially lighting. In each of these applications, LEDs with specific properties are required, and drivers need certain features or requirements to effectively meet the application needs. In the following, considerations and limitations of LEDs and driver circuits per application are briefly discussed.

A. GENERAL LIGHTING-INDOOR (A.I)

General lighting or ambient lighting is to illuminate a space in accordance with its function with a comfortable level of brightness and is widely used in various applications and environments, as can be seen in Fig. 2.

General lighting LED systems are ac-supplied, and depending on power level, system configuration, and location their input voltage range, power quality limitations, and safety concerns are subject to norms such as ENERGY STAR Program requirements product specification for luminaries, IEC 61000-3-2.

LED bulbs and lamps are extremely cost-sensitive as they compete with a technology that had a century for cost optimization. This fact directly impacts the driver topology selection and many topologies with high component count are cost-prohibited. Also, topologies requiring feedback components such as optocouplers, current sensors, or even extra windings on magnetics are not acceptable options. Often a primary-side current regulation is needed. The space envelope is also constrained. In incandescent light bulbs, most of the heat leaves the bulb via radiative heat transfer, however, in LED lamps the heat is generated in both the LED driver and LED modules. Thus, even though the higher efficiency, the

lower heat, heat must be transferred via conductive transfer which means the components will run hot. Heatsinking is limited due to cost, space, and weight limitations, impacting the topology selection as well as the physical realization.

To replace fluorescent tubes, there are two types of LED tubes: (a) the ones directly replacing the fluorescent tube without modifications to the luminaire circuitry and (b) the types that require modification of the luminaire. Considering their ancestors price, LED tube lights are under extreme cost pressure. They must run as long as fluorescent tubes, with limited terminals heat transfer. Also, fluorescent tubes are not sensitive to line voltage surges while LED tube lights should have sufficient means to tolerate such surges. The total weight and uniform weight distribution are also critical to match the sockets designed for fluorescent tube weight. Moreover, with many LEDs in series, the aging of LEDs can require a gradual increase of voltage to maintain the lumens level. The drivers often record the hours of operation and compensate for the aging, which adds to the design considerations.

B. GENERAL LIGHTING-OUTDOOR (A.II)

Flood lights are designed for both indoor and outdoor applications i.e. they must tolerate constant high temperatures when used indoors due to the limited heat transfer of the housing and large temperature fluctuations in outdoor usage. To reduce their sensitivity to humidity they need better sealing, which makes heat transfer even more challenging resulting in half a day of operation at high temperatures. As they are not turned on and off frequently, higher inrush currents are permitted. Upon their installation location, flood lights can be fed by thin long wires and their screw-type sockets can develop high impedance due to humidity and dust. Therefore the driver topology should accept a wider input voltage range. Similar to other general lighting lamps, flood lights often need to be phase-cut dimmer compatible.

Street lighting is another type of general lighting system. Installed on top of poles, they face severe temperature fluctuations during each day and from summer to winter. Therefore, heat transfer and magnetic designs are critical, as using cooling fans is not allowed due to cost pressure and reliability concerns. Besides costly installation and maintenance of streetlights require provisions to compensate effects of aging in these systems. Although streetlights are often fed by a dedicated line, EMI from different lights fed on the same line should not impact other LED systems. In streetlights, there is a high chance of lightning strikes to light poles. Hence proper surge protection is a must.

C. AUTOMOTIVE LIGHTING-EXTERIOR (A.III)

Automotive exterior lights are important subsystems of a vehicle.

1) Front headlights (low-beam, high-beam, and fog lights) and Tail lights are safety and security critical and they need to operate reliably and efficiently as the lights may be on for several hours [32], [33], [34]. Automotive dc distribution system experiences large variations, from lowest during cold-crank from an old battery in cold weather, up to jump start from a new battery with a higher nominal voltage, and transients from various intermittent loads [35]. If an integrated LED system approach is used, Fig. 1(a), the LEDs may be floating with respect to the car chassis potential. On the other hand, the external arrangement, shown in Fig. 1(b), requires two or more wires between the LED driver and LED module. It is preferred to keep the return wire at the chassis voltage. This eliminates a malfunction in case of a short circuit to the car body [36], [37].
2) Daytime running lights, (DRL), can use the same LED module as the front headlights driven with lower current, some LEDs from that LED module, or a completely separate one. They also need to be efficient, however, the reliability requirement can be less stringent compared to front headlights [38], [39], [40].
3) Brake lights, Indicator lights, and Backup lights can also share the same LED module as tail lights or have separate ones. They are also safety-critical and must be reliable, however, can have a lower efficiency as they are not running for a long time [41], [42].

D. AUTOMOTIVE LIGHTING-INTERIOR (A.IV)

Automakers expand the safety, convenience, and appearance of newer models by expanding interior lighting. Designers have more opportunities to differentiate their products by taking advantage of design freedom enabled by LEDs. Similar to exterior ones, interior lights are subject to various transients present on vehicle dc lines. In addition, they are required to have a low quiescent power consumption not to drain the battery during extended parked periods [43].

E. GROW LIGHT (A.V)

There is a growing trend toward vertical farms, hydroponic greenhouses, and small gardening systems. A grow light is an artificial light source used to stimulate plant growth [20]. Grow lights are useful for both greenhouses where the sunlight is insufficient or indoor farming (e.g. vertical farming) where there is little natural light [21]. LEDs are specifically suitable as grow lights as they are more energy efficient and durable. LED grow lights can be designed and controlled to resemble the sunlight full spectrum, or provide a customized spectrum to the needs of the plants being cultivated. As LED grow lights are tunable to emit the best spectrum of light, they can provide a desirable spectrum (color temperature) for each plant type and its stage of growth to meet the plant's needs. Far-red and blue lights are of colors that most plants prefer for optimum growth. LEDs ability to offer strong peaks in these colors has made them a strong competitor.

Greenhouses use grow lights to speed up the growth, while vertical farming completely relies on them. In greenhouses usually, ceiling mounted grow lights are used and in vertical farming, rack lights are preferred. In both applications, due to

humidity, dc voltages beyond 60V are prohibited and lower dc levels or ac distributions are required. Besides, as many lights operate close to each other, selecting driver topologies with low light ripple is needed to eliminate visual beating effects. The beating effect refers to the phenomenon that occurs when two or more light sources with slightly different frequencies are superimposed on each other, resulting in fluctuations in the intensity and quality of light [44]. The beating effect in LED grow lights can occur when two or more light sources with slightly different PWM dimming frequencies are used in the same grow light system. Usually, light intensity and colors are controlled via computer programs. The I2C bus is commonly used which is sensitive to EMI. LED grow lights often have at least four strings of LEDs to provide different color/intensity combinations. In each string same color LEDs are used. However, the number of LEDs for different colors is not the same, and thus drivers capable of running multiple strings are preferred. Also, as vertical farming grow lights are installed on racks, low-profile designs are needed to keep room for more farming and thus design for natural cooling becomes more important, especially for magnetic components. It should be noted that fans cannot be used in humid and warm environments on farms.

F. UV LED (A.VI)

The ultraviolet (UV) portion of the electromagnetic spectrum refers to wavelengths between 100 to 400 nm. There are several applications for UV LED lights in processing light-sensitive materials, e.g. in lithography, resin, and ink curing processes [45]. UV-C includes wavelengths of 100 to 280 nm and is highly effective for disinfection. Power levels vary widely from 10-100 watts for handheld disinfecting lights to kilowatts for integrated UV lights used in water processing plants. The UV for sanitation is one of few applications that light ripple out of a lamp is not important and allows using chopped current via LEDs to control the light.

G. DISPLAY LIGHT (A.VII)

LEDs are gaining popularity for displays providing advantages such as high-quality images, the possibility to form non-flat screens, higher contrast levels, and no backlight. The driving schemes are often based on the right combination of time-multiplexing and hardware parallelization [46], [47], however more details on this topic are beyond the scope of this paper.

H. LCD BACKLIGHTING (A.VIII)

LCD display require a backlight that can be implemented by high-power LEDs. In portable applications, the backlights are fed from the battery therefore, maintaining the high efficiency and capability of dimming for one order of magnitude (for day and night use) is important. Another important challenge for a backlight driver is the visual light beating effect that can occur when the display is used under ambient light controlled by chopped currents that require an almost dc current drive. Another major necessity for backlight drivers is electromagnetic compatibility, as the backlight is a large piece electrically connected to the driver and it can contribute to radiated emissions significantly [48].

I. SPECIALTY LIGHTING (A.IX)

Many applications can be considered specialty lighting as can be seen in Fig. 2 and discussed here:

1) Portable lights are battery driven and their main feature is low weight and high efficiency. They often provide blinking features, therefore lower loss during transients is required. They will be used in a wide range of temperatures and sometimes are considered a security-providing device, therefore high reliability is of significant importance. Robustness against the impact of mechanical shock or vibration is also needed, which makes drivers with fewer components preferable.
2) Decorative lights are mostly required to be inexpensive. Some may have multiple strings of LEDs, one per color, and a single driver with multiple outputs is favorable.
3) Signage and traffic lights are safety and security-critical and this requires high reliability, long life as well as high efficiency, and low power consumption when LEDs are off. They need to function under wide temperature variations, and shock and vibration.

III. LED MODULES CONFIGURATION

There are many different types of LEDs available to suit a wide range of applications. The color and brightness of the light depend on the semiconductor materials used in the LED and the amount of current flowing through it. The forward voltage is the minimum voltage required for the LED to start emitting light. Different colors have different forward voltages, ranging from 1.2V for infrared LEDs to 4.0V for some blue and white LEDs. Hence, LEDs forward voltages are normally less than 4V depending on LED technology and color.

Some common types of current LED technologies are: Traditional LEDs with a forward voltage range of 1.8V to 3.3V, Miniature LEDs with a similar forward voltage range as traditional LEDs, High power LEDs with a forward voltage range of 2.0V to 4.0V, RGB LEDs with forward voltage range of 2.0V to 3.5V per color, Quantum Dot LEDs (QLEDs) with a similar forward voltage range as high power LEDs, UV LEDs with a forward voltage range of 2.8V to 4.0V, and IR LEDs with a forward voltage range of 1.2V to 1.7V.

Several LEDs should be used together to achieve the desired light intensity and pattern. LED modules can be driven by both ac and dc voltages or currents. Hence, LED modules can be divided into dc-LED and ac-LED modules as shown in Fig. 3.

A. DC-LED MODULES

Dc-LED modules should be driven by a dc voltage or current. There are three main configurations for dc-LED modules:

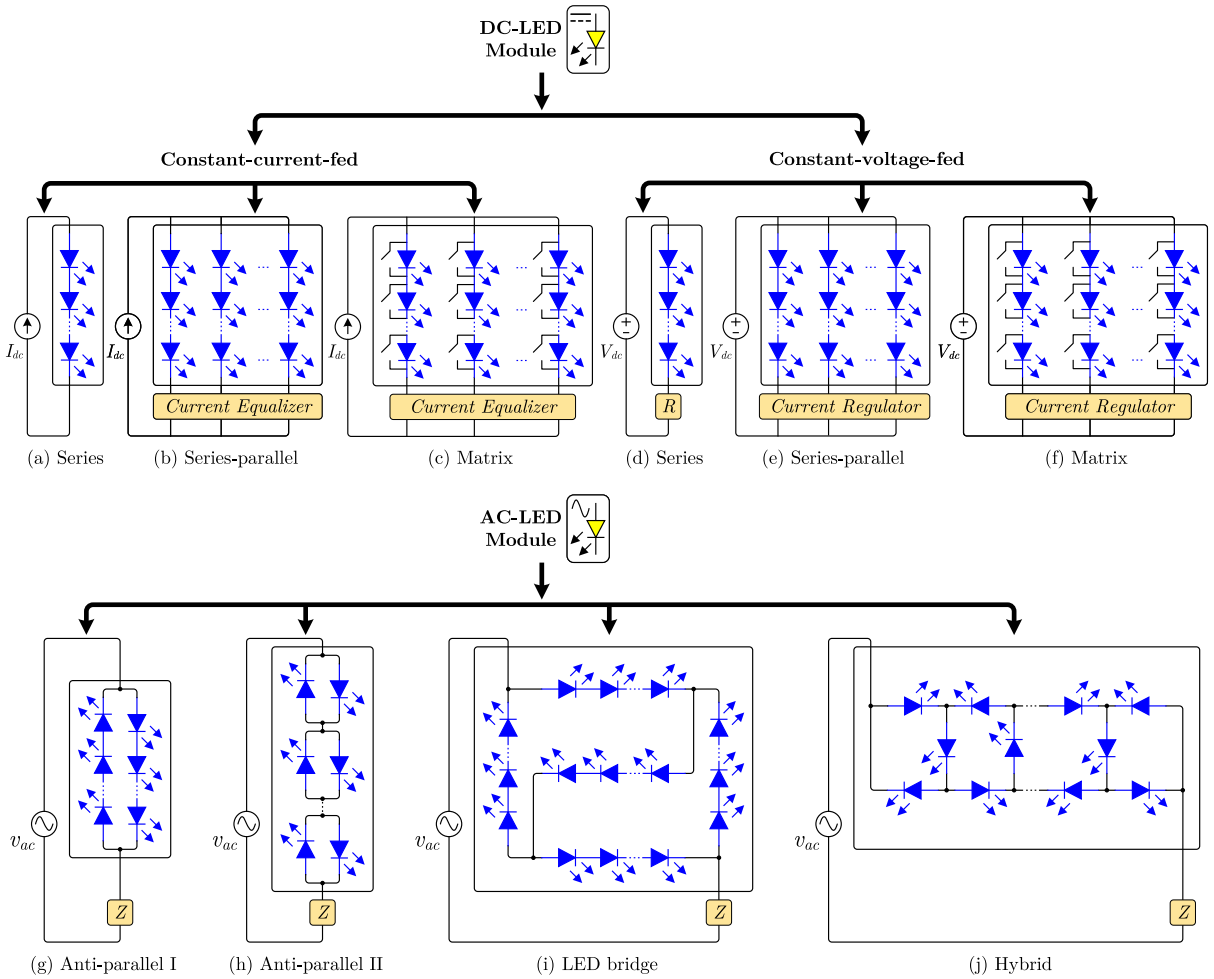

FIGURE 3. Examples of LED modules configurations. [49], [50], [51], [52]. "Z" referrers to an impedance that is often utilized to limit the current and stabilize the module operation point for a specific range of ac voltage and ambient temperature [53].

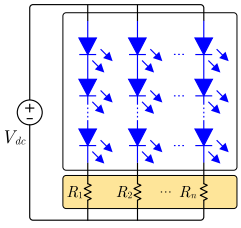

FIGURE 4. Series-parallel LED module configuration connected with shunt resistors ($R_1 = R_2 = \ldots = R_n$) [54].

series, series-parallel and matrix configuration as described below.

1) SERIES CONFIGURATION

In the series configuration, unlike the case of Constant Current (CC) drivers, Constant Voltage (CV) LED drivers would require an impedance to keep the string current in the allowed range which might not be preferable in high-power applications with efficiency restrictions. Using series configurations has the advantage of almost uniform light out of LEDs which might even have different forward voltages (V_f). The excessive string voltage for high number of LEDs brings challenges to designing a reliable and efficient constant current driver. In case of failure in any individual LEDs the whole string stops functioning.

2) SERIES-PARALLEL CONFIGURATION

In this configuration, LEDs can be arranged in several smaller strings connected in parallel using shunt resistors in each branch, as shown in Fig. 4. This configuration provides more fault tolerance and less output voltage for the driver, but introduces current-sharing issues, especially in applications where CC LED drivers are utilized. When CC LED drivers are used, the driver current is divided among the strings and small differences in (V_f) of the LEDs can cause significant unbalance current sharing, which leads to both non-uniform light and thermal distributions in the lamp. Such an unbalance sharing can be improved by the pre-screening or binning of LEDs. While this approach may mitigate the issue, it is expensive and does not guarantee a fully balanced current sharing. Hence, a current equalizer unit should be utilized

to help the current sharing between branches to be more uniform, as shown in Fig. 3. The current sharing methods for CC LED drivers are well documented [55], [56].

On the other hand, when CV LED drivers LED drivers are used, the same voltage will be placed on LED strings and a current regulator unit is needed to limit and regulate the current of LED strings Fig.3. Current regulation of series-parallel LED modules that are fed by CV LED drivers are similar to series LED modules and are performed usually using shunt resistors at the expense of lower efficiency. The current regulation methods for CV LED drivers are discussed in [57] and [58]. In parallel strings, the failure of one LED, either open circuit (OC) or short circuit (SCi), can cause stress on the remaining LEDs. There is another variation of series-parallel configuration in which LEDs with similar vertical positions in all strings are also connected together. This configuration provides better current sharing and fault tolerance as in case of SC all the LEDs in the row will cease to operate and in case of OC all LEDs in the row will experience increased current by a factor that is a function of the number of columns.

3) MATRIX CONFIGURATION

In a matrix configuration, LEDs are arranged similarly to the series-parallel configuration with the difference that each LED has a parallel switch. The parallel switch can be used to intentionally SC its parallel LED. Matrix configurations are generally more fault tolerant and often produce better current sharing. The LED string voltage is comparable to that of the parallel configuration. In case of SC in any LED, the rest of LEDs in that string will operate as normal. In case of OC in any LED, the parallel switch will be turned on and the rest of the LEDs in that string will operate as normal. In both SC or OC cases, changes in the brightness of the lamp and the currents of LEDs are dependent on the type of current equalizer or current regulator used in the system and the feedback type.

B. AC-LED MODULES

1) ANTI-PARALLEL I AND II CONFIGURATIONS

The conventional anti-parallel configuration, anti-parallel I, is composed of two anti-parallel strings of LEDs as shown in Fig. 3 [49]. In the anti-parallel II configuration [59], multiple pairs of anti-parallel LEDs are connected in series. In this configuration, the peak reverse voltage of each LED is equal to its own forward voltage drop. However, each LED string operates only half of the line cycle and hence theoretically the maximum possible utilization factor of each LED would be 50% which is not cost-effective. In Ac-LED configurations, an impedance referred to as "Z" in Fig. 3, is often utilized to limit the current and stabilize the module operation point for a specific range of ac voltage and ambient temperature [53]. This impedance can be either a resistor [51], a capacitor [60], [61] or a series inductor-capacitor (LC) [62].

2) LED BRIDGE AND HYBRID CONFIGURATIONS

These configurations are presented to lower the cost of ac-LED modules. In the LED bridge rectifier configuration, the rectifier LEDs work at half of the line cycle, while the other LEDs work during the entire line cycle [50]. Therefore, the utilization rate of LEDs can be increased up to 67% with this configuration. However, the peak reverse voltage of LEDs in the bridge is high. In the hybrid configuration, LEDs are assembled in the ladder form [51] and LEDs peak reverse voltage can be reduced. In other to further increase the LEDs utilization factor, rectifier diodes can be used instead of LEDs in LED bridge configuration. This configuration is similar to dc-LEDs and gives a maximum theoretical utilization of 100%. In practice, as LED arrays have nonzero turn-on threshold voltage and the conduction time of arrays is less than half a cycle, the utilization factors are less than mentioned percentages.

IV. LED SYSTEMS SPECIFICATIONS

A. CATEGORIES OF LED SYSTEMS

Considering their input power source LED systems are divided into two categories: ac-supplied and dc-supplied systems. As shown in Fig. 5, the ac-supplied LED systems require different types of blocks compared to dc-supplied counterparts, and also may be used to drive either a dc-LED module or an ac-LED module, while, dc-supplied systems are usually utilized to drive dc-LED modules. In the next sections, most important LED module configurations and ac-supplied and dc-supplied systems architecture and typologies are reviewed.

B. CHALLENGES IMPOSED BY LEDs CHARACTERISTICS

The luminous power of an LED is roughly proportional to its current and equal luminosity from several LEDs is commonly achieved by series connection. Similar to diodes, LEDs are heavily nonlinear and thus when the voltage across an LED is below its threshold voltage, the current and power are negligible. As the voltage exceeds the threshold, a slight voltage variation can cause a large change in LED current and luminous output.

In DC-LED modules, the nonlinear characteristic of LEDs complicates the light adjustments via voltage control and becomes straightforward via current control which can be implemented as constant voltage (CV) or Constant Current (CC) modes. A CC driver regulates the LED current regardless of the LED voltage (up to a certain voltage limit). However, due to the cost pressure, sensor less current control methods are preferable. The nominal output current of commercial CC drivers is typically 350mA, 700mA, 1050mA, etc. LED modules designed for CV usually include several series strings of LEDs, connected in parallel which may require current-sharing methods to ensure LEDs share the current equally. Both constant current control methods and PWM dimming methods are applicable to CC drivers. A CV driver regulates the voltage across the LEDs, regardless of

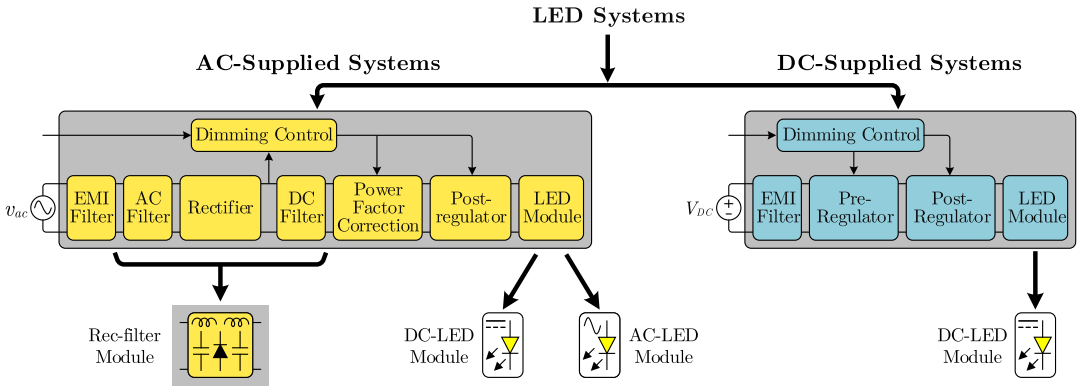

FIGURE 5. General LED systems categories.

the LED current (up to a certain current limit). Since LEDs require a specific current, many CV LED loads also include an impedance between the driver and the LEDs to control current flow. The output voltage of commercial CV LED drivers is typically 12V, 24V, etc. CV drivers can only be dimmed via the PWM method.

AC-LED modules were initially presented to eliminate the need for bulky and expensive LED drivers. Low-frequency AC-LEDs are driven directly from an AC voltage (grid) using a series impedance, usually a resistor, to limit the peak current. Although AC-LED systems usually do not require large passive components like electrolytic capacitors, due to the LEDs relative low forward voltage and non-linear behavior, long series strings of LEDs are typically needed. Additionally, the system suffers from high current distortion because the input current is high near the voltage peak and very low at lower voltages [63]. AC-LED modules can operate from 12 to 277 V AC, depending on the number of LEDs connected in series [64]. To achieve features like active current control and power factor correction without using bulky passive devices, commercial linear current control ICs have been developed that change the number of LEDs by cutting off some LEDs as the line voltage varies to maintain a sinusoidal current over the majority of the line cycle [65]. In addition to linear solutions, some converters have also been used to realize power factor correction and active current control by driving AC-LED modules with a high-frequency square-wave current. These drivers allow LEDs to have a significantly higher and imperceptible flicker frequency and brighter light at equivalent peak-current levels.

V. AC-SUPPLIED LED DRIVING APPROACHES

In the lighting industry, the cost is often the most important factor for the success of a low-end product. The main idea of ac-supplied LED drivers is to energize a high-voltage LED string directly or indirectly through some passive or active components from the grid. The specification of ac-fed LED drivers includes input voltage and frequency ranges, output voltage and current ranges (dimming range), maximum current ripple, maximum power, startup time, protections, galvanic isolation level, environmental (temperature, humidity, altitude), and mechanical info (dimensions, IP rating) and standards to comply. Data sheets normally provide graphs such as operating range, total harmonic distortion (THD), power factor, efficiency curves, as well as information regarding the inrush current and connections.

Fig. 6 depicts a general categorization for ac-supplied LED lighting systems. The driver topologies are categorized based on the LED module configuration. Categories T1 and T2 are for ac-LEDs while T3 to T5 is for dc-LEDs, respectively. Each category is further split based on the location of the energy storage and the double-frequency power decoupling (DFPD) methods they use.

A main challenge in ac-fed LED drivers is the double-frequency power oscillations that affect the LED drivers life span, maintenance cost, size, and also the quality of LEDs output light, shown in Fig. 7. Therefore, the design of LED drivers should address these issues. To deal with the double-frequency power oscillations, energy storage components are used to decouple the power delivered to the LED module from the input power.

A. DOUBLE-FREQUENCY POWER DECOUPLING) IN AC-SUPPLIED LED DRIVING APPROACHES

In ac-supplied LED drivers, the input voltage, v_{ac}, is ac and there are some regulations for limiting the input current harmonics (such as IEC 61000-3-2), which impose power factor (PF) requirements. In order to meet these requirements, near-unity PFs must be achieved. In an ideal ac-supplied dc-LED system with $PF = 1$, the input current, i_{ac}, is a sinusoidal waveform with the same phase and frequency. The input power, p_{ac}, of such system, is the product of v_{ac} and i_{ac}. Hence, as can be seen in Fig. 7, the input power is pulsating at double line (grid) frequency, while the power delivered to the LED module can be either pulsating or dc. If the power delivered to LED modules is pulsating with the same frequency as the input power, such as in T1(a) and T1(b) shown in Fig. 6, no double-frequency power decoupling (DFPD) is needed.

In other types of LED drivers, the power delivered to the LED module can be either dc or pulsating with a

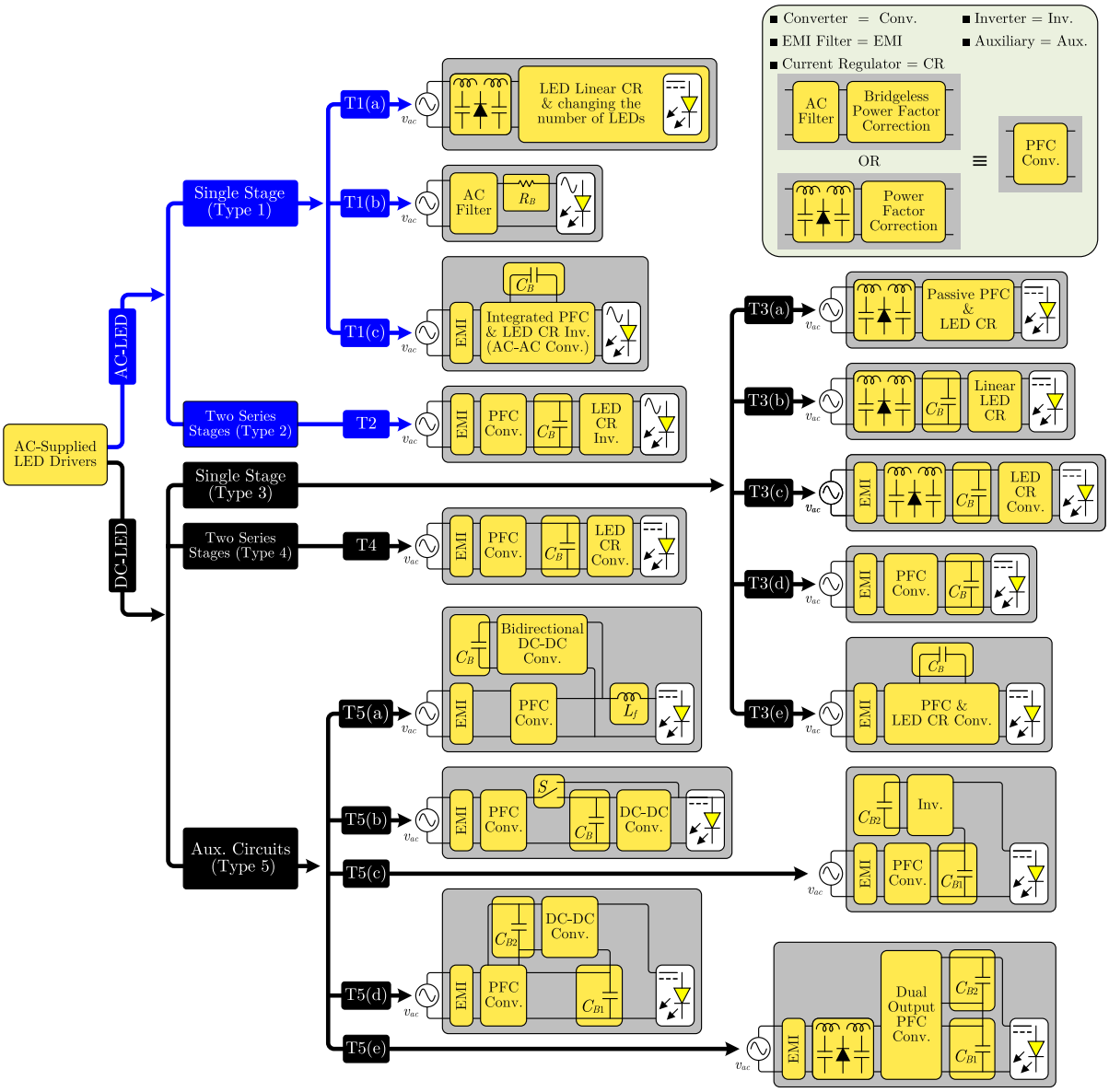

FIGURE 6. Block diagrams of different solutions for ac-supplied LED systems.

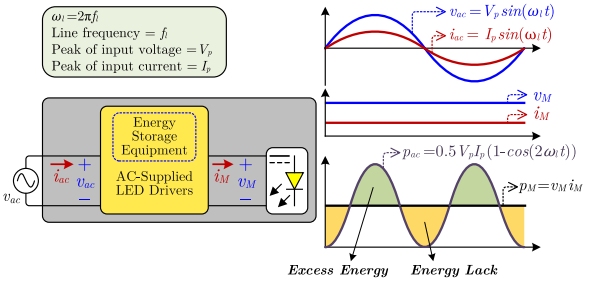

FIGURE 7. Waveforms of an ideal ac-supplied dc-LED system.

higher frequency. In this case, an energy storage component is needed to decouple the unbalanced power between the input and output. This unbalanced power for an ideal ac-supplied dc-LED module driver is shown in Fig. 7. Generally, capacitors or inductors can be used as energy storage components in LED driver applications for decoupling purposes. Magnetic components can offer higher reliability and lower failure rates than capacitors, however, their continuous power loss and power density are much higher and lower than capacitors, respectively. Hence, inductors as energy storage components are mostly used in low-power passive LED drivers, T3(a), which are suitable for applications in far-to-reach locations where high reliability is more important than high efficiency and high power density. Capacitors, on the other hand, are the most common energy storage components for decoupling. The amount of required energy storage capacitor (C_B) can be obtained from the following equation:

$$C_B = \frac{P_o}{\omega_l V_{CB} \Delta V_{CB}}, \tag{1}$$

where, P_o is the power delivered to load, ω_l is the line frequency, ΔV_{CB} is the capacitor peak to peak voltage ripple and V_{CB}=$(V_{CB_{max}} + V_{CB_{min}})/2$. According to (1), for specific power, to reduce the size of required capacitance, either V_{CB} or ΔV_{CB} should increase.

Based on the location of the energy storage capacitor(s), the LED driver approaches can be categorized as follows:

1) C_B can be placed right after the input rectifying diode bridge and ac filters as in Fig. 6, T3(b), or T3(c). V_{CB} is equal to the input peak voltage. By selecting a larger ΔV_{CB}, a smaller capacitor can be used and a linear regulator referred to as "Linear LED CR" or a converter referred to as "LED CR Conv." should suppress the side effects of the large ΔV_{CB} on the LED module current. There is no control over the input current harmonics.
2) C_B can placed after a PFC converter, as in Fig. 6, T3(d). C_B is paralleled with the LED module, and ΔV_{CB} should be small. Therefore, to decrease the capacitor size, high V_{CB} should be selected. High V_{CB} imposes high voltage on the PFC converter switches, and the LED module and hence limits the type of LED module.
3) C_B can be placed between a PFC converter and an LED CR converter, Fig. 6, T2 and T4. To make C_B smaller, either high V_{CB} or large ΔV_{CB} or both can be selected. High V_{CB} will impose high voltage stress on the components of both converters. To avoid high V_{CB}, larger ΔV_{CB} can be selected and both PFC converters should suppress the side effects of the large ΔV_{CB} on the input PF and LED module current. However, two control circuits and at least two switches are needed.
4) The PFC converter can be integrated with the LED CR converter and form a single-stage converter as in Fig. 6 where C_B can be placed inside the converter. Similar to the previous case, smaller C_B can be selected by either increasing V_{CB} or ΔV_{CB} or both. Compared to the previous case, the minimum number of switches, and the number of control circuits are reduced to one.
5) C_B can be connected through an auxiliary circuit. More than one energy storage capacitor might be needed. The following sub-categories are based on the location and the type of the auxiliary circuit:
    a) The auxiliary circuit connected in parallel with the LED module as in Fig. 6, T5(a). Both ΔV_{CB} and V_{CB} can be increased to further reduce the capacitor size. A bidirectional dc-dc converter as the auxiliary circuit produces a pure dc voltage to drive the LED module by absorbing the second harmonic component in the output current of the PFC converter. High V_{CB} will only be imposed to the bidirectional converter.
    b) In the previous case, the power processed by the auxiliary circuit can be as high as the LED module power and the auxiliary circuit must be a bidirectional dc-dc converter. To reduce the power processed by the parallel auxiliary circuit, a three-mode switch can be added to the system as in Fig. 6, T5(b). The three-mode switch controls the power delivered to C_B, and an LED module and a unidirectional dc-dc converter can be used as the auxiliary circuit to produce a dc voltage for the LED module.
    c) The auxiliary circuit connected in series with the LED module, Fig. 6, T5(c). Two capacitors, C_{B1} and C_{B2}, are needed. To reduce the sizes of the capacitor, a large voltage ripple can be selected and the auxiliary circuit produces an ac voltage which can fully cancel the voltage ripple across C_{B1}. The sum of these two voltages which is a net dc voltage is provided to the LED module. The voltage stress on the auxiliary circuit is lower than in the previous cases. As the auxiliary circuit is connected in series with the LED module, it can not provide any active power, so the auxiliary circuit must be an inverter containing at least four switches.
    d) To avoid using an Inv. in the previous case, a dual-output PFC converter can be used and C_{B2} can be connected to the second output of the PFC converter as shown in Fig. 6, T5(d). In this case, C_{B2} can provide some active power and the auxiliary output voltage can have a small dc value. Hence, the auxiliary circuit can be realized by using a dc-dc converter. The auxiliary circuit can also be integrated with the dual output PFC converter as shown in Fig. 6, T5(e) to reduce the number of required components.

B. VOLTAGE RANGES AND REGULATIONS

LED systems as a category of power supplies are subject to certain regulations and standards for power quality, surge current, protection, and safety. For ac-supplied systems, the input voltage range should be compatible with one or more utility power line voltages. NEMA SSL 1-2016 standard recommends 120, 127, 208, 220, 230, 240, 277, 347, and 480 Vac at 50 or 60Hz. These values usually have a typical ±10% tolerance in different geographic locations. Ac-supplied LED systems that cover only one specific range of line voltages are considered limited input voltage ranges. The systems that cover more standard voltages are a wide input voltage range.

C. DIMMING AND DIMMERS

Dimming implies varying the luminous intensity by controlling the power delivered to the light engine. LEDs are dimmable from 100% lumens output to less than 1% with a proportional reduction in energy consumption and LED dimming does not reduce the luminous efficacy. Lamp life is not shortened and can even increase since the dimming reduces the p-n junction temperature, a leading determinant of LED life. LEDs dimmability can boost their energy efficiency and lighting systems design flexibility. Generally, dimming

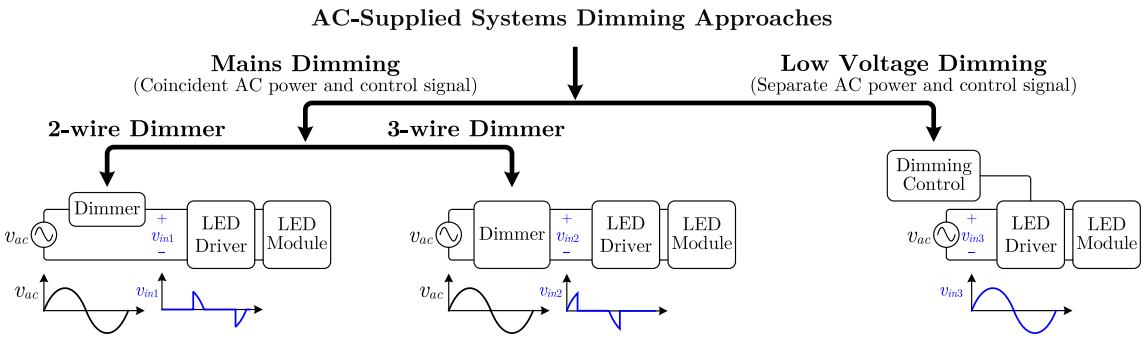

FIGURE 8. Ac dimming approaches.

can be achieved by either modulating the power waveform connected to the LED system or through controlling the LED driver. Modulating power waveform, or mains dimming is applicable to ac-supplied LED systems while controlling the LED driver, low-voltage dimming is applicable to both ac and dc-supplied LED systems in most of the applications. Fig. 8, shows different dimming approaches [66]. In the following, these dimming methods will be discussed.

1) MAINS DIMMING

Mains dimming is achieved through external dimmers that are placed in series with the LED system input. The dimmer itself modulates the power waveform and can be used for both Incorporated and External Drivers. Modulating power waveform can be done in different ways. One possible approach is scaling the waveform, i.e. amplitude modulation, or it can be accomplished by altering the waveform without changing the amplitude. A popular approach for waveform modulation is phase-cut dimming where the dimmer chops up the electrical signal from the mains, as depicted in Fig. 9. There are two common types, Leading-edge dimming and Trailing-edge dimming. The leading-edge dimming, where the energy flows only during the last portion of each power-line half cycle, can be realized using robust and low-cost Triac-based designs. This is one of the most common approaches due to compatible operation with traditional lighting systems, including incandescent lamps and magnetic transformers, and some dimming ballasts. The dimmers of this type are widely installed in buildings, therefore phase-cut dimmable LEDs are often designed for compatibility with as many leading-edge dimmers as possible. Sometimes noise reduction devices are applied to reduce the audible noise generated with leading-edge dimmers. In the Triac-based dimmers, the minimum dimming level is limited due to the need of maintaining sufficient current above the holding current of the Triac [67]. In trailing-edge dimmers, on the other hand, the energy flows only during the initial portion of each power-line half cycle and they usually are more expensive because of more complex electronics. These dimmers can function with a wider variety of lamps and especially electronic drivers and are more sophisticated than leading-edge dimmers. They usually use a MOSFET or an IGBT switch rather than a Triac and coil which benefits the user with smooth, silent dimming control, absent of any buzzing noise. The majority of dimmers are leading-edge and a smaller percent are trailing-edge or have two capabilities. The selected topology for any ac-fed LED should consider compatibility with existing and future dimmers. System-level compatibility of lamps and dimmers should be considered in power topology selection for dimmable lamps. Standard SSL7A provides a pathway toward compatibility of leading-edge dimmers (not trailing-edge ones) and LED lamps with global scope (50/60Hz; 100/120/230/277V) [68]. In leading-edge dimming drivers, the incompatibility and challenges of Triac-based phase-cut dimmers with the LED drivers have been tackled by various methods as follows:

Controlling the input reactive power: The input current is programmed to be lagging, in-phase, or leading the input voltage so that the active and reactive power drawn from the input voltage is controlled and the input current is kept higher than the holding current of the Triac on dimming. An example is proposed in [69], where a small amount of reactive power is injected by a four-quadrant ac-dc converter followed by an LLC resonant converter.

Active damping circuits: At firing instances, input current ringing, voltage spikes and light flicker can happen which normally are prevented using dampers. Resistive dampers have widely been used to address this issue, but they all suffer from low efficiency. To improve efficiency, in [70], an active damper has been proposed which stabilizes converter operation during dimmer firing with minimized components.

Bleeding circuits: A common phase-cut dimmer assumes the minimum lamp power to be such that the Triac in the dimmer operates correctly. This bounds how low the lamp current can be and makes the design of a low-power LED with a wide dimming range very challenging. This problem can be addressed by adding a bleeding circuit, Fig. 10. A bleeder is a circuit that helps maintain sufficient current during chopped intervals of ac voltage waveform beyond the holding current of the Triac in the dimmer, often at the expense of efficiency [71]. Bleeders are classified into active and passive ones. A passive bleeder can be used for very low-power LED

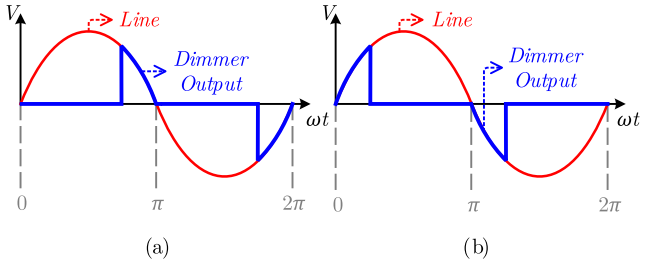

FIGURE 9. Ideal phase-cut dimmer waveforms. (a) Leading-edge. (b) Trailing-edge.

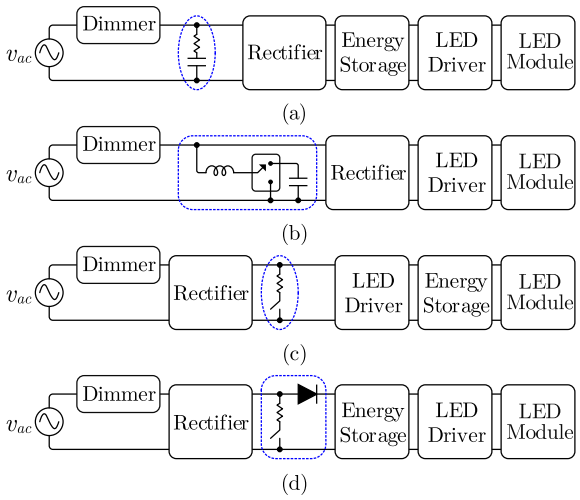

FIGURE 10. Block diagrams of common bleeding circuits. (a) Conventional bleeder. (b) Circuit presented in [73]. (c) Circuit presented in [74]. (d) Circuit presented in [69].

bulbs. An active bleeder consists of a resistor and capacitor, but the resistor is only on when needed. The trade-off is that this solution requires an active switch to turn the resistor on and off, but the efficiency will be improved [72]. Fig. 10 shows block diagrams of different LED systems and their suitable Bleeding circuits.

2) LOW VOLTAGE DIMMING

There are two principal methods for low voltage dimming of LEDs: constant current reduction; and pulse-width modulation (PWM). Constant current reduction dimming is the cycle-by-cycle adjustment of LED current at a desired level. Both constant current reduction and PWM dimming methods can be applied to either linear regulators or switching converters. CC drivers can be designed to employ either method, whereas PWM is the only method that can be employed by CV drivers. The constant current reduction technique produces flicker-free light and high luminous efficacy but poor dimming function and energy efficiency, whereas the PWM technique offers better dimming flexibility but an inherent flicker in comparison to the dc technique. Further information on these methods is provided below and summarized in TABLE 1.

a: CONSTANT CURRENT REDUCTION DIMMING

This dimming method can be done by either resistive dimming or external dc control voltage. As the current level is adjusted for brightness level, inherently the color temperature (desired spectrum) variation can occur which makes analog dimming not suitable for applications where the color of the LED is critical. In [75], analog dimming with linear regulators is proposed while analog dimming with switching converters has also been presented in [76].

b: PWM DIMMING

In PWM dimming method, the brightness of the LED is controlled via the duty cycle of the control pulse. Therefore, when LED is on the current level is constant and the color will not change in different output light brightness [77]. PWM dimming can be applied to both linear regulator [78] and switching converter [79], [80]. In [80], the authors proposed the use of phase-shifted PWM dimming methods so as to avoid EMI and pulsating current issues introduced by the PWM approach. In order to reduce flicker, the authors in [81] distribute PWM pulses over the dimming period. The frequency of disturbed PWM in this paper changes with luminance value, not the duty cycle.

D. AC-SUPPLIED AC-LED MODULE DRIVER SYSTEMS

Ac-LED modules are normally composed of high voltage LED strings in order to be driven directly from the grid or high-frequency sources with no or very small energy storage component. These modules are supplied from AC mains. Systems that are used to drive these modules are either single-stage (Type 1) or multiple stages (Type 2) drivers as shown in Fig. 6. Single-stage systems can be categorized into three subtypes: single-stage linear CR-based drivers (T1(a) in Fig. 6), simple single-stage driver (T1(b) in Fig. 6), and single-stage PFC converter-based drivers (T1(c) in Fig. 6).

1) T1(a) AND T1(b) - SINGLE-STAGE CR-BASED AC-LED MODULE DRIVERS

Single-stage linear CR-based drivers feed LED strings directly from the grid. In these drivers, the current of LEDs is limited or controlled using linear active (T1(a) in Fig. 6) or passive (T1(b) in Fig. 6) solutions. T1(a) drivers that use no energy storage component normally operate by altering the number of LEDs in the string following the grid voltage waveform. These drivers are proposed to eliminate the need for conventional bulky, limited lifetime, and expensive ac-supplied LED drivers. Fig. 11 shows an example of T1(a) drivers presented in [65] and [82] for high ac voltages using a rectifier bridge. There is a linear current regulator in series with LEDs all the time to control the current and eventually shape it to achieve a low power factor. The voltage difference between the LED string and input voltage appears across the linear regulator. Even though the losses in the regulator can be more than losses in a conventional power electronics driver,

TABLE 1. Analog and PWM dimming methods.

PARAMETER	ANALOG DIMMING	PWM DIMMING
Shift in Color Temperature	Dimming produces visible color shift	Relatively constant color over all dim levels
Dimming range	Fairly limited in most designs	Can achieve very high contrast ratios
Flexibility	Changes to dim range by hardware adjustment	Changes to dim range by software adjustment
Efficiency	Better than PWM at lower dim levels	Lower efficiency at high peak currents
EMC	Usual issues with switching supplies	Shunt switch could exhibit hard edges leading to EMI
Relative Cost	Usually cheaper	More expensive

in applications with no isolation requirement and size and cost limitations, the use of ac-LEDs is promising. In [83], it is suggested to add a switched-LED module, shown in Fig. 11, series with the main LED string to reduce the voltage across the linear regulator. As the input voltage increases, this switched LED module adjusts the number of LEDs to minimize the voltage across the linear regulator. For example, the time interval of t_1 to t_2 in Fig. 11(b) will be divided into six sub-intervals and at the beginning of each interval, the number of auxiliary LEDs will increase by one. Therefore, v_{C1} will reduce greatly and the efficiency is increased.

In applications where dimming is not required, it is possible to use T1(b) drivers shown in Fig. 6, to increase the efficiency and reduce the possibility of flicker and cost without using controllers. Due to the self-rectifying ac-LED modules, as shown in Fig. 3, T1(b), the rectifier bridge is not needed anymore [85]. Both T1(a) and T1(b) drivers are well compatible with phase cut dimming of the ac source. T1(b) based light engines dim linearly with leading and trailing-edge dimmers provided that the minimum load conditions of the dimmer are maintained. Ac-LED modules provide low cost, small size, mechanical design flexibility, low THD, and seamless dimming compatibility with phase cut dimmers. They, however, suffer from lower performance, limited component choices, higher PCB layout challenges, lower LED utilization, lower power factors, and a higher probability of flicker.

2) T1(c) AND T2 - PFC-BASED AC-LED MODULE DRIVERS

Ac-LED modules can be fed with frequencies higher than grid frequency [86], [87]. The block diagram of single-stage or two-stages-based LED drivers are identified by T1(c) and T2 labels in Fig. 6. Topology example of T1(c) and T2 LED based systems are shown in Fig. 12 and Fig. 13 [84], [88]. These types of drivers normally provide low component counts and higher reliability. In these drivers, to decrease the size of C_B, larger ΔV_{CB} or higher V_{CB} can be selected. Selecting high V_{CB} can impose a high voltage stress on all the converter switches and diodes and selecting larger ΔV_{CB} is preferred.

E. AC-SUPPLIED DC-LED MODULE DRIVER SYSTEMS

In order to properly feed dc-LED modules from ac mains, many solutions have been proposed in the literature with various trade-offs between lifetime, power quality, efficiency, reliability, design flexibility, safety concerns, cost, and size. Based on the number of stages, the type of each stage, and the location of the energy storage component, ac-supplied dc-LED module driver systems can be divided into three types: Single-stage drivers, Two series stages drivers, and Auxiliary DFPD circuit drivers. Here these types and their sub-types are described.

1) TYPE 3 - AC-SUPPLIED SINGLE-STAGE DRIVER SYSTEMS

In this type of ac-supplied dc-LED systems, apart from filters and rectifier bridge, only one stage is used in the system. Single-stage solutions presented in the literature can be categorized into five sub-types, based on the type of the stage and the location of the energy storage. In the first sub-type, T3(a) in Fig. 6 also known as passive LED drivers, a stage containing energy storage inductors are placed after the diode bridge and filters in which no active component is used for regulating LED current. Fig. 14 shows typical passive LED drivers with a valley-fill circuit to improve the input PF, THD, and output voltage ripple presented in [89] and [61]. The input inductor limits the load power and sensitivity against transients of the ac mains voltage. The output ripple can be further reduced using coupled inductors as in Fig. 14(c) [90]. The passive LED drivers cannot regulate the LED current against input voltage variations, and changes in parameters due to temperature. The current drawn from the grid has harmonics and the power factor may not be acceptable. Thus, passive LED drivers have applications in far-to-reach locations where low maintenance is more important than high performance.

In the second sub-type, T3(b), a linear current regulator stage is used to regulate LED-module current. This type of driver is considered the conventional passive solution for supplying dc-LED modules from ac mains. These drivers are based on placing C_B right after the diode bridge and filters. In order to provide an LED module with smooth dc power and avoid flickering, the capacitor must be large enough. Considering the cost pressure, typically electrolytic capacitors are used in these drivers. As there is no input current shaping mechanism in these drivers, their input current is pulsating and contains considerable harmonics. As a result, the PF of these drivers are limited, and they can marginally pass class D limit [91]. To reduce the size of C_B, large ΔV_{CB} can be selected and the Linear LED CR can suppress the side effect of high voltage ripple by adjusting the amount of resistance. However, in this case, the dissipation will increase significantly. The linear LED CR block shown by label T3(b),

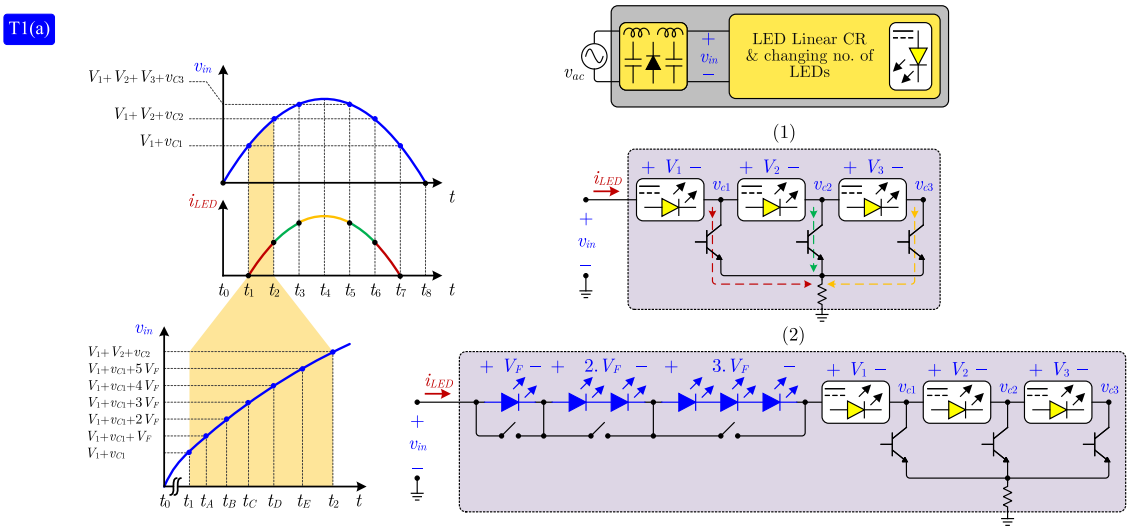

FIGURE 11. T1(a) ac-supplied LED drivers. (1) The driver circuit before adding the switched-LED module [82] and [65]. (2) The driver circuit with three LED strings in the switched-LED module [83].

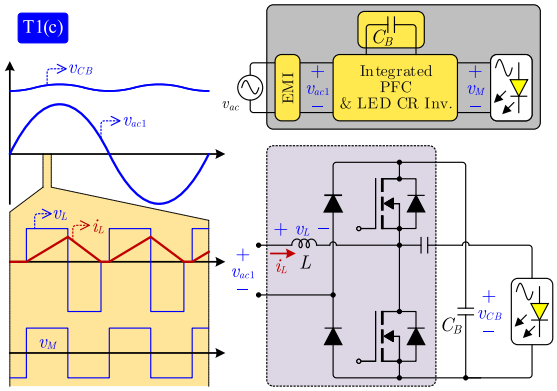

FIGURE 12. T1(c) ac-supplied high-frequency ac-LED driver [84].

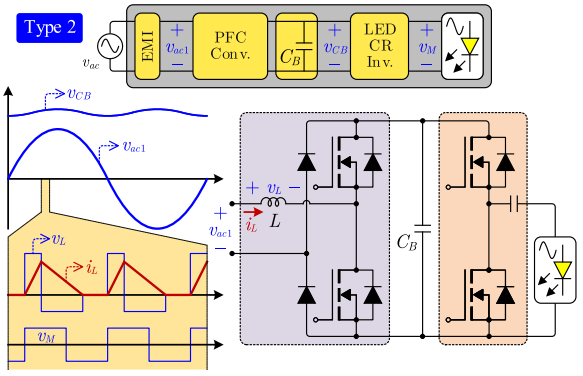

FIGURE 13. Type 2 ac-supplied high-frequency ac-LED driver [84].

in Fig. 6 can be implemented by using a simple current limit resistor as shown in Fig. 15. This circuit is suitable for high-voltage LED modules as for low-voltage LED modules the current limit resistor conduction loss is considerably high, making the system efficiency too low. For low-voltage LED modules, a low-frequency step-down transformer can be added to the front end of the driver [92]. Although the resistor conduction losses will be reduced, its loss in addition to the core loss introduced by the transformer still limits the efficiency of the system. In order to add the dimming capability to this type of driver, a linear CR can be used as the linear LED CR block [93], [94]. However, replacing the resistor with the linear CR cannot improve the efficiency of the system.

Single-stage CR converter-based drivers, T3(c) in Fig. 6, are the conventional and simplest approach to implement a high-efficiency ac-supplied dc-LED module driver. As shown in the block diagram of these drivers, an energy storage capacitor followed by an LED CR Converter is used. By selecting larger ΔV_{CB}, smaller C_B can be selected and the LED CR Converter can suppress the side effects of high ΔV_{CB} and control the current fed to the LED module. Also, in applications where CV LED drivers are needed, the dc-dc converter can also be used to control the voltage placed on the LED modules. The efficiency and component count of this kind of driver are acceptable. However, the power quality is low and the size of required C_B is usually high which makes it challenging to comply with IEC 61000-3-2 in terms of the input current waveform and also to implement the driver without electrolytic capacitors, especially in high power applications. Fig. 16 shows an example of this type of converters which is presented in [96]. In [97] and [98], switched capacitor technique is used to improve the power quality of this type of drivers.

To address T3(c) drivers problems, single-stage power factor correction (PFC) converter-based drivers, T3(d) shown in Fig. 6, can be used. As shown in the block diagram, a PFC converter is placed as the interface between the ac input and the LED module. C_B is connected in parallel with the LED module. Reference [99] provides an overview of general PFC

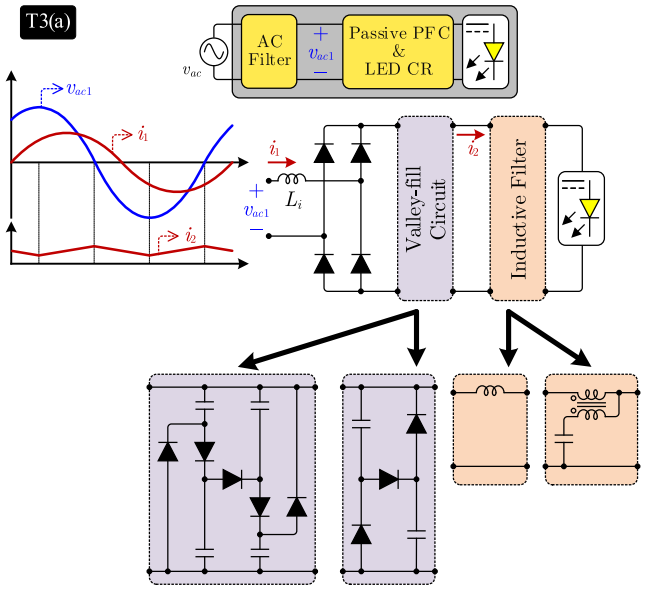

FIGURE 14. T3(a) ac-supplied passive dc-LED driver [61].

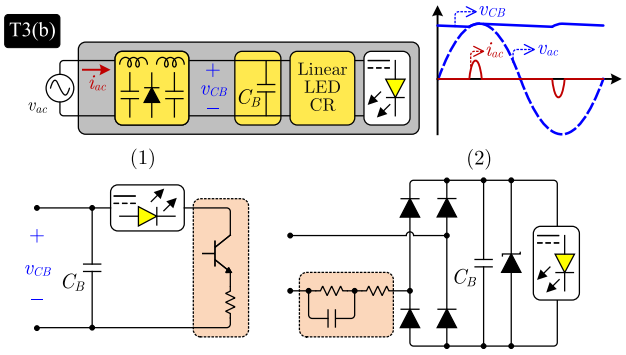

FIGURE 15. T3(b) ac-supplied single-stage linear LED CR-based drivers. (1) [91], [94]. (2) [95].

architectures and this paper only focuses on the smaller subset commonly used in LED drivers. An extensive study on PFC topologies with galvanic isolation can be found in [100]. As, the allowed level of harmonic currents generated by the electric load is limited and regulated [101], normally a bulk capacitor energy storage often of electrolytic type is used in parallel with the LED string or sometimes with an inductor in series with the LEDs to reduce double frequency ac power oscillations on the LEDs. Although the size of C_B can be reduced by increasing V_{CB}, a high voltage will be placed on the LED module which limits the application of this type of drivers.

In this type of drivers, a flyback converter, shown in Fig. 17, and its derivatives are widely used as the PFC converter due to their circuit and control simplicity, galvanic isolation, and their ability to achieve unity PF by operating in discontinuous conduction mode (DCM) [56], [102], [103], [104]. In addition to the flyback converter, in [105] a bridgeless single-stage driver based on the SEPIC topology is proposed that is suitable for floating LEDs. Fewer components, fewer conduction losses, lower switch voltage stress and EMI

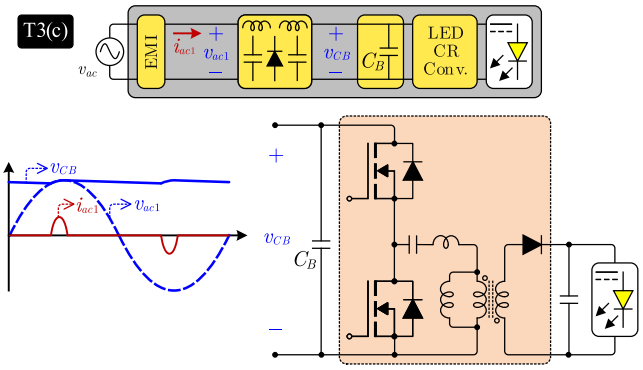

FIGURE 16. T3(c) ac-supplied single-stage LED CR converter based driver [96].

are among the advantages of this driver. Further discussions on this type of drivers are presented in [106]. However, the main problem of this type of drivers is that they are unable to remove electrolytic capacitors while ensuring low double frequency ripple and low voltage on LED modules.

The last sub-type of single-stage ac-supplied dc-LED modules is the one with a PFC converter integrated with a CR converter stage, T3(e) in Fig. 6. This type of drivers is achieved by integrating two series stages in T4 systems and placing C_B inside the integrated converter. The "PFC & LED CR Conv." stage shown in the block diagram, is responsible for both shaping the input current and regulating the LED current. As a result, this type of systems can offer a near unity PF, low THD as well as low LED double frequency ripple while using smaller C_B. Hence, in low-power applications, electrolytic-capacitor-less (ECL) ac-supplied systems can be easily implemented using these drivers. However, as the power rating of the system rises, it becomes challenging to maintain the input THD and the LED current ripple in the acceptable range and use a low amount of capacitance while having low V_{CB}.

A systematic categorization of converters that can be used as the "PFC & LED CR Conv." stage in T3(e) systems is given in [130]. In addition to many dc-dc converters, as a unique topology, flyback converter and its variations are commonly used in T3(e) LED drivers. In [110], a flyback driver with C_B at primary side is proposed as shown in Fig. 18(1). In this converter, a PFC boost stage is integrated with the dc-dc flyback stage. The PFC boost stage operates in DCM, while the flyback operates at the critical conduction mode. Although efficient, this converter imposes high voltages across C_B to obtain low THD. An improved variation of this circuit using a variable boost inductor is reported in [131] adequate for the universal input voltage-range (90–270Vrms) applications at the expense of a relatively complex magnetic inductor design.

Many other converters have been also proposed based on integration of two converters. The integration of a PFC buck-boost and a flyback converter in [119], shown in Fig. 18(9), a PFC buck-boost and a modified flyback converter with a voltage doubler rectifier output in [132], a buck-boost PFC and a resonant LLC converter, [120], shown in

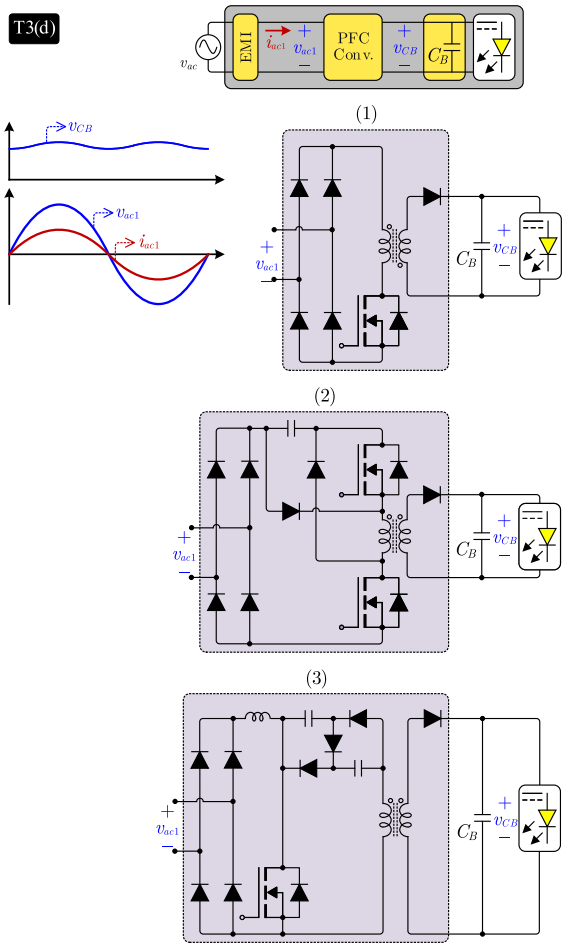

FIGURE 17. T3(d) ac-supplied single-stage PFC converter-based LED drivers. (1) [107]. (2) [108]. (3) [109].

Fig. 18(10), a buck-boost PFC and a class-E converter, [112], shown in Fig. 18(11), and a buck-boost and a resonant converter in [121], shown in Fig. 18(12) are proposed. The buck-boost PFC operates in DCM to achieve a high input power factor as the duty ratio is almost constant. In addition to boost or buck-boost PFC, in [133] and [134] the Sheppard Taylor converter has been used as a single-stage PFC ac-dc converter. This converter is a cascade of a modified boost stage and a buck stage, with the two stages sharing the same active switch. This converter can provide high PF and output regulation provided that the modified boost converter part operates in discontinuous mode and the buck converter part operates in CCM. This topology has an inverted output and can also accommodate an isolation transformer if needed.

A bridge-less single-stage driver based on the SEPIC topology is proposed in [105] that is suitable for floating LEDs. Fewer components, less conduction losses, lower switch voltage stress and EMI are among the advantages of this driver. In [111], shown in Fig. 18(2) and [124], shown in Fig. 18(15), and [135] two-switch drivers are suggested based on a soft-switching asymmetrical half-bridge topology. The boost converter operates in DCM to achieve near unity PF with advantages such as constant-frequency operation, soft-switching, low component count and low voltage stress across the switches.

In [136], a two-switch single-stage driver with coupled inductors is introduced which integrates a dual buck–boost PFC with coupled inductors and a half-bridge LLC dc–dc resonant converter into a single-stage topology. The coupled inductors are operated in the DCM to obtain near unity PF. The half-bridge-type LLC resonant converter achieves soft-switching on both the switches and rectifier diodes. The disadvantage of switch sharing is that only two degrees of freedom exist: switching frequency and duty cycle. This reduces the design flexibility and can lead to higher losses due to the extra stress on the shared switches. Similar topologies are reported in [137]. In [138], a boost-forward driver with a shared switch is presented. Due to its simple structure and few inexpensive components, this circuit is suitable for low-voltage applications where a reasonable output filter size can be achieved. At higher output voltages a low ripple requirement can lead to large and expensive output inductors. In [139] a single-stage driver is presented based on a two-switch forward converter. This converter has an auxiliary circuit to get a reduced V_{CB}. Operating in the DCM, this circuit provides high PF at the expense of increased current stress on the power circuit components. This topology is also adequate for lower power applications (<100W). In [114], Fig. 18(4), another single-stage driver is presented based on a two-switch forward converter with a simpler transformer and a modified output filter to reduce the ripple. Smaller output capacitance can be utilized as the output inductor current ripple is significantly reduced.

Various bridge-less PFC topologies are also proposed, some depicted in Fig. 18(5)-(8), [115], [116], [117], [118], [140], [141]. Having no input diode bridge and the presence of only one diode in each switching cycle allows lower conduction loss compared to bridge-based PFCs. These features are achieved at the expense of more complexity and more serious EMI issues due to the increased common-mode noise [142]. To reduce the THD, the PFC should have a low pass-filter characteristic with 10-20 Hz bandwidth. This results in slow output voltage dynamics for the PFC which can cause perceivable effects in the LED lights. If the specification requires better light uniformity, a second stage is often needed.

2) TYPE 4 - AC-SUPPLIED TWO SERIES STAGES DRIVER SYSTEMS

The single-stage approaches, T3, usually face challenges to fully comply with requirements on the power factor, THD, life span, efficiency, and output current ripple. Multiple-stage approaches, on the other hand, can introduce more design flexibility in achieving the aforementioned performance factors. Hence, for specific applications and high power levels where these requirements are more challenging, the focus has been shifted to developing multi-stage structures systems.

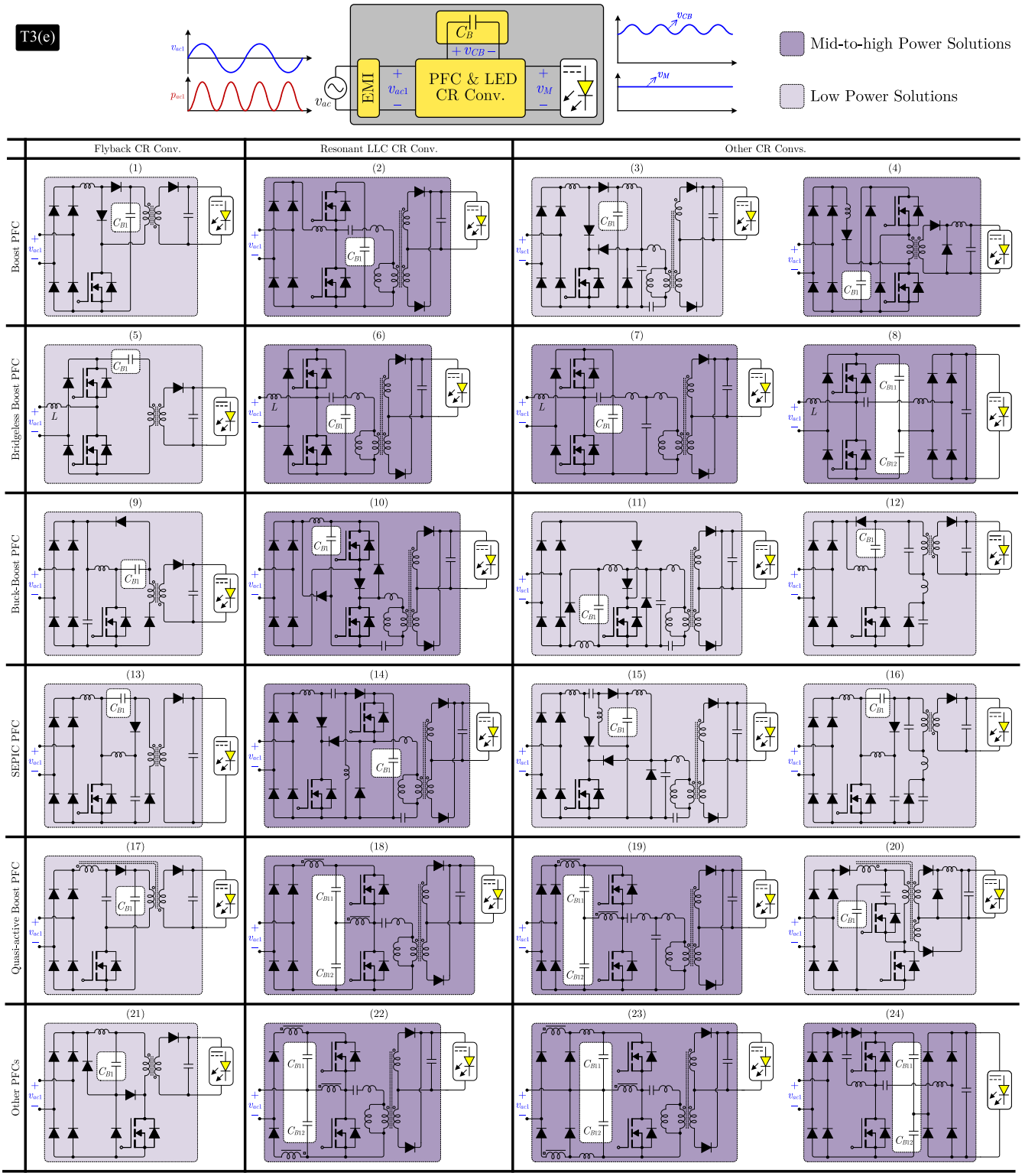

FIGURE 18. T3(e) ac-supplied single-stage PFC and LED CR converter-based drivers presented in the literature. (1) [110]. (2) [111]. (3) based on [112] and [113]. (4) [114]. (5) [115]. (6) [116]. (7) [117]. (8) [118]. (9) [119], (10) [120]. (11) [112]. (12) [121]. (13) [122]. (14) [123]. (15) [124]. (16) based on [121]. (17) based on [125] and [126]. (18) [126]. (19) based on [126] and [117]. (20) [125]. (21) [127]. (22) based on [126]. (23) based on [126] and [125] and [128]. (24) [129].

In two series approaches, T4 category in Fig. 6, there are independent stages whose objectives are different. The term independent implies that the input power of the LED driver is processed separately in each stage. Each stage is usually

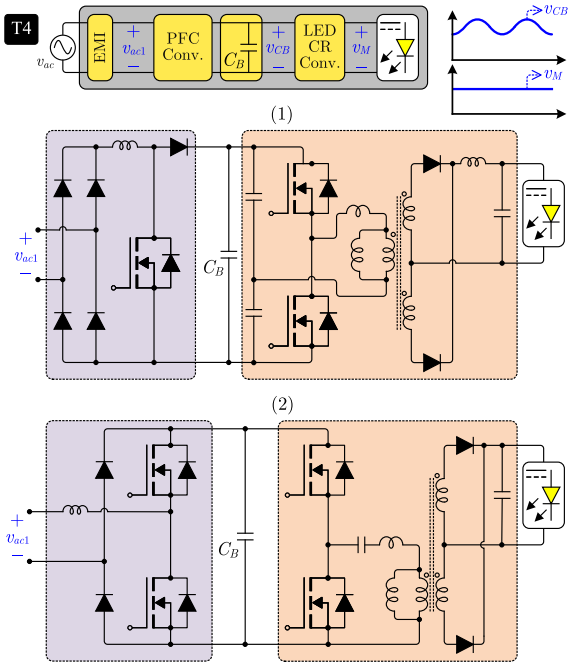

FIGURE 19. T4 ac-supplied two-series stages based LED drivers. Converter (1) [143], [144], [145], converter (2) [146].

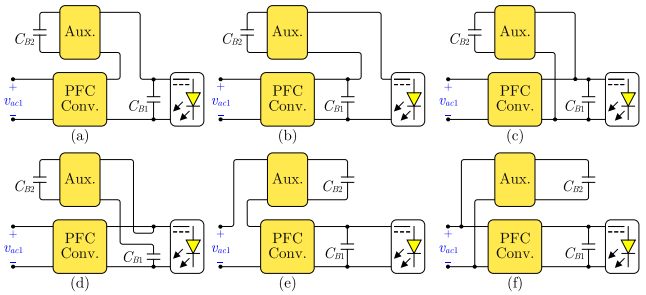

FIGURE 20. Structure diagrams of possible solutions for DFPD through auxiliary circuits. (a) Series connection with the PFC dc side (converter side). (b) Series connection with the PFC circuit dc side (output side). (c) Parallel connection with the dc side of the PFC. (c) Series connection with the dc side of the PFC (capacitor side). (e) Series connection with the ac side of the PFC. (f) Parallel connection with the PFC ac side.

in charge of performing one or two tasks. As a large ΔV_{CB} is usually selected to reduce the C_B size, the grid-side stage which is usually a PFC provides high PF and the LED-side current regulator converter stage regulates the current through LEDs and attenuates the voltage ripples on C_B. PFC and LED CR converters together form the interface between the rectified ac input and the LED string as shown in Fig. 19.

PFC converter ensures that the injection of current harmonics into the line is low due to the quasi-sinusoidal input current waveform [147] to comply with international regulations. In LED drivers, galvanic isolation is often not a requirement for the grid-side stage, thus it is possible to use various non-isolated topologies such as boost, buck-boost, Cuk [148], SEPIC [149] and Zeta [150] as the PFC converter. The topologies with inductive components at the input are often preferred due to less EMI filtering challenges and easier operation with phase cut dimmers.

Boost-type PFC is the most popular with various commercial controllers. Operation in boundary conduction mode (BCM) has gained more popularity due to: (a) soft-switching of the switches is guaranteed. (b) boost inductor is smaller for BCM compared to continuous conduction mode CCM, and (c) a precise measurement of the inductor current is not needed and knowing the zero crossing moment is sufficient [151]. These advantages come at the expense of higher current stresses in both active and passive components and higher conduction losses as well as larger EMI filter sizes. In [143], a boost converter operating in CCM mode is used as the PFC and a half-bridge converter is utilized as the LED CR converter as shown in Fig. 19(1). To improve the efficiency, in [146], the boost converter and the diode bridge is replaced by a bridgeless boost PFC and the half-bridge converter is replaced by a soft-switching resonant LLC converter as shown in Fig. 19(2). The Zeta converter has also a simple control strategy and, when operating in quasi-resonant mode, achieves good efficiency over the whole operating area at the expense of a high voltage on the switch and diode.

For the LED CR Converter, many dc-dc converter topologies can be used. As the first stage, PFC is often non-isolated, the LED-side stage (or a middle stage) provides the isolation. Flyback and LLC converters are the most popular for this purpose.

Having more than one stage provides more flexibility in optimizing each stage for specific tasks toward better LED current regulation, less perceivable flicker, smaller energy storage equipment, and wider dimming range. There are also reports on more than two-stage solutions, e.g. three-stage topologies in [152] and [153]. The purpose is often to provide good overall efficiency across the entire universal input voltage (95 to 305 Vrms). Although a higher number of power processing stages may lead to less overall efficiency, more degrees of freedom can provide better features and may enhance the efficiency of individual stages.

3) TYPE 5 - AC-SUPPLIED AUXILIARY-POWER-DECOUPLING-CIRCUIT-BASED DRIVER SYSTEMS

To further decrease the energy storage capacitor size and improve efficiency, power density and cost issues, ac-supplied LED drivers with auxiliary circuits have been developed, also known as reduced power processing stage topologies. These LED drivers are based on active DFPD methods. In [154], an overview of active DFPD methods and topology derivations is presented. Due to the cost pressure and size limitations in LED applications, only some of the methods presented in [154] can be used in products. In the active DFPD, often a PFC converter is used to perform the power factor correction and deliver power to dc capacitor, and an auxiliary circuit (Aux.) and an additional energy storage capacitor (C_{B2}) is added to perform the DFPD task.

Based on the position of the Aux., six configurations are possible as shown in Fig. 20. The Aux. can be connected to either the dc side of the PFC converter as in Fig. 20(a)-(d), or the ac side of the PFC converter, Fig. 20(e) and (f). Connecting the Aux. to the ac side would expose it to line transients and hence the configurations in Fig. 20(e) and (f) have been rarely used for LED driver applications. Dc side connected auxiliaries are more suitable for LED driver application as they effectively reduce the size of required energy storage capacitance. The Aux. interference between C_{B2} and the rest of the circuit allows selecting large ΔV_{CB2} and/or high V_{CB2} without imposing high voltage stress on the PFC converter. Energy storage capacity of C_{B2} increases and smaller capacitors can be used. Examples of dc side connected Aux. reported in the literature are shown in Fig. 6 T5(a) and T5(c).

In approach T5(a) in Fig. 21, the auxiliary is connected in parallel with the LED module and increases the effective capacitance. Only one energy storage capacitor, C_B, is needed and an inductor, L_f, is added to filter the switching frequency ripple of LED module current. C_B cannot provide any active power and a bidirectional dc-dc converter must be used as the auxiliary circuit [155], [156]. Both high V_{CB} and large ΔV_{CB} can be selected to increase the energy storage capability of C_B and reduce its size. Although selecting high V_{CB} and large ΔV_{CB} does not impose high voltage stress on the PFC converter switches, about 32% of the output power will be processed three times before being delivered to the LED module. As high voltage switches should be used in the bidirectional converter, the theoretical efficiency will have a considerable drop from a conventional single-stage LED driver [157].

To reduce the power processed by the parallel auxiliary circuit, in approach T5(b) in Fig. 22, a three-mode switch is added to the system [159], [162]. When the input power is higher than the power needed by the LED module, C_B gets charged. The energy stored in C_B is delivered to LEDs during line zero-crossing moments when the input power is lower than the power needed by the LED modules. C_B can provide some active power and the auxiliary circuit can be implemented by a unidirectional dc-dc converter.

Approach T5(c) in Fig. 23 is similar to T5(a) only connected in series [160], [161]. An extra energy storage capacitor is needed, Fig. 23, and a large voltage ripple can be selected for both capacitors to reduce their size and avoid high voltage stress. C_{B2} is connected to the auxiliary circuit, a floating capacitor, and it cannot provide active power similar to T5(a). The auxiliary circuit must produce an ac voltage to fully cancel the voltage ripple across C_{B1}. Although the voltage stress on the auxiliary circuit is much lower than the one in previous cases, a full-bridge inverter containing four switches should be used as the auxiliary circuit. To address this problem, a dual-output PFC converter can be used and C_{B2} can be connected to the second output of the PFC converter as in Fig. 24, T5(d) [157], [163], [164]. In this

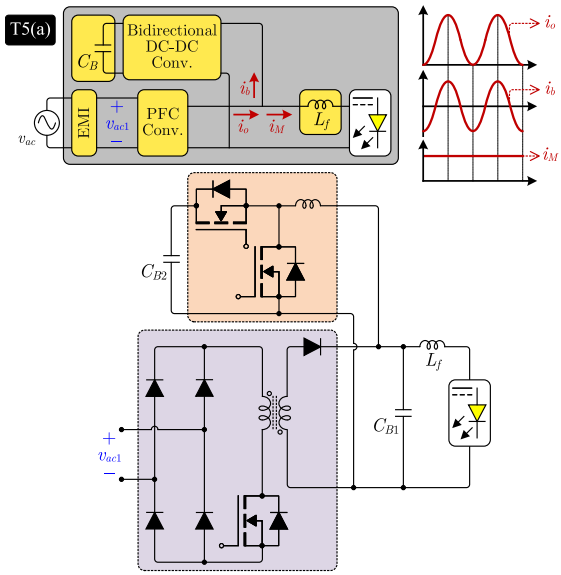

FIGURE 21. T5(a) ac-supplied LED drivers paralleled auxiliary circuit based [155] and [158].

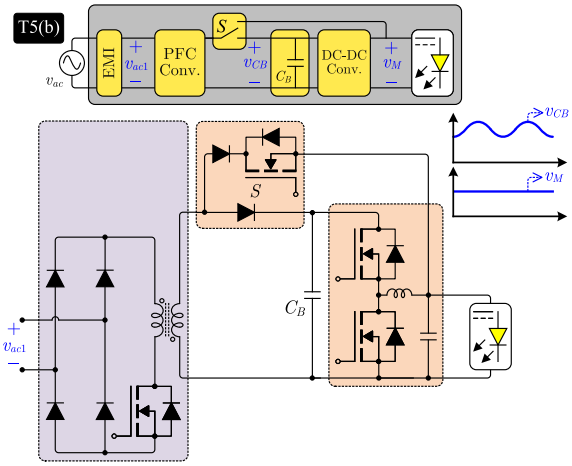

FIGURE 22. T5(b) ac-supplied LED drivers [159].

way, no inverter is needed and the series-connected auxiliary circuit can be realized by a simple dc-dc converter as C_{B2} can provide some active power, and the auxiliary circuit output voltage can have a small dc value. In [165], to reduce the size of the auxiliary circuit, a resonant switched capacitor converter is presented as the auxiliary circuit.

In approach T5(e) in Fig. 25, to reduce the number of required components while allowing large voltage ripple on energy storage capacitors, the series connected auxiliary circuit is integrated with the dual output PFC converter [166].

A brief comparison of ac-supplied LED driving approaches is mentioned in TABLE 3 and TABLE 4.

VI. DC-SUPPLIED LED DRIVING APPROACHES

The dc input LED driver requirements vary in different applications. Two main examples are the drivers for automotive and Power-over-Ethernet (PoE) applications where galvanic

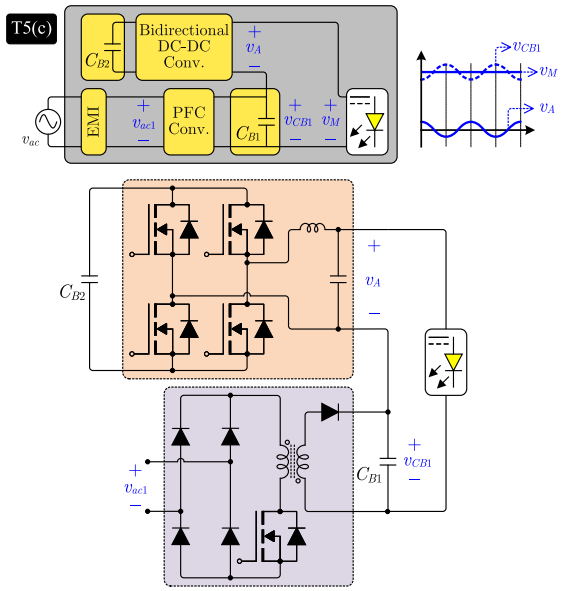

FIGURE 23. T5(c) floating-input series-output two-stage driver [160], [161].

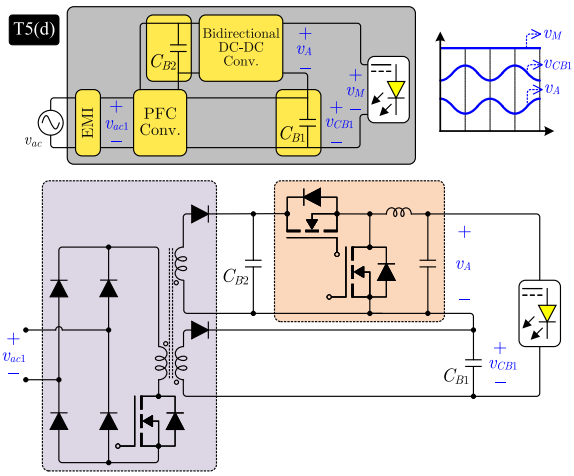

FIGURE 24. T5(d) ac-supplied LED drivers with series connected series-output two-stage driver [157], [162].

isolation is often not required. In such applications, a high level of control integration is desirable to ensure a low external component count toward improved robustness, smaller volume, and ease of design. This also helps the thermal performance of the drivers under high current with minimum PCB area and no expensive thermal management devices which is more important for automotive applications. The input voltage range that an automotive LED driver should tolerate is extremely wide and the survivability to the commonly encountered transients in the automotive environment is of extreme importance [168], [169]. Even though there is a battery in automotive applications, the existence of high power loads such as the engine starter, blower, etc. makes voltage regulation difficult. For example, on a $12V$ vehicle, a cold-crank start can lead to a bus voltage dip of less than

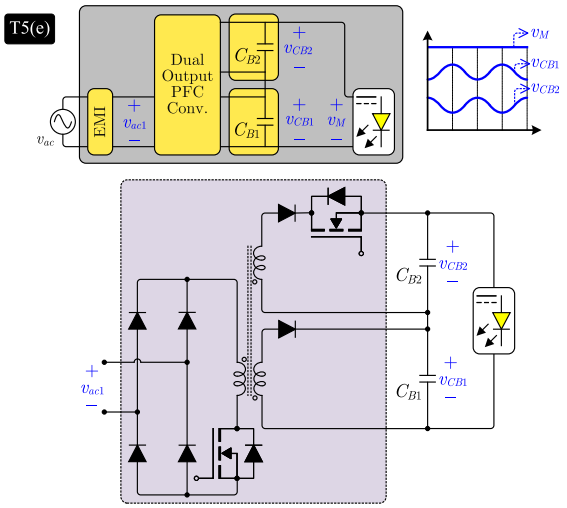

FIGURE 25. T5(e) ac-supplied dual outputs PFC converter based LED drivers [167].

$7V$ and a load dump event can result in a surge voltage above $100V$. A longer over-voltage can also occur from a jump start with a $24V$ battery and there is a possibility of reverse battery connections [170]. In addition, the dc power lines travel long distances in the vehicle and their inductive elements add to the transient severity. Last but not least, the LED driver components should operate efficiently under the automotive temperature range of $-40°C$ to $125°C$. All needs should be carefully considered when designing LED drivers for such applications to maintain flexibility, scalability, efficiency, and low cost. It is often the case that the controllers have integrated protection aspects in order to simplify the product design. These features include open and short LED string diagnostic, slew rate control to eliminate EMI issues, driver to LED cable short circuit detection to the car body, thermal fold-back, over temperature shutdown, as well as overvoltage and undervoltage-lockout.

Similar to ac-supplied LED systems, dc-supplied LED systems presented in the literature can be divided into single-stage, two-series stages, and partial power stages, as shown in Fig. 26. In the following sections, each of these types and their sub-types is described.

A. TYPE 6 - DC-SUPPLIED SINGLE-STAGE DRIVER SYSTEMS

Single-stage dc-supplied LED systems are divided into three sub-types: Linear current regulator-based systems, T6(a), Current regulator converter-based systems T6(b), and Pulsed current regulator converter-based systems T6(c). The current mirror circuit, shown in Fig. 27(1), is a simple example of T6(a) drivers that can be implemented using BJTs or FETs. A current mirror is designed to copy a current through one active device by controlling the current in another active device, to maintain the output current constant. Fig. 27(2) shows Wilson current mirror which has less sensitivity to drain-source variations compared to the basic type.

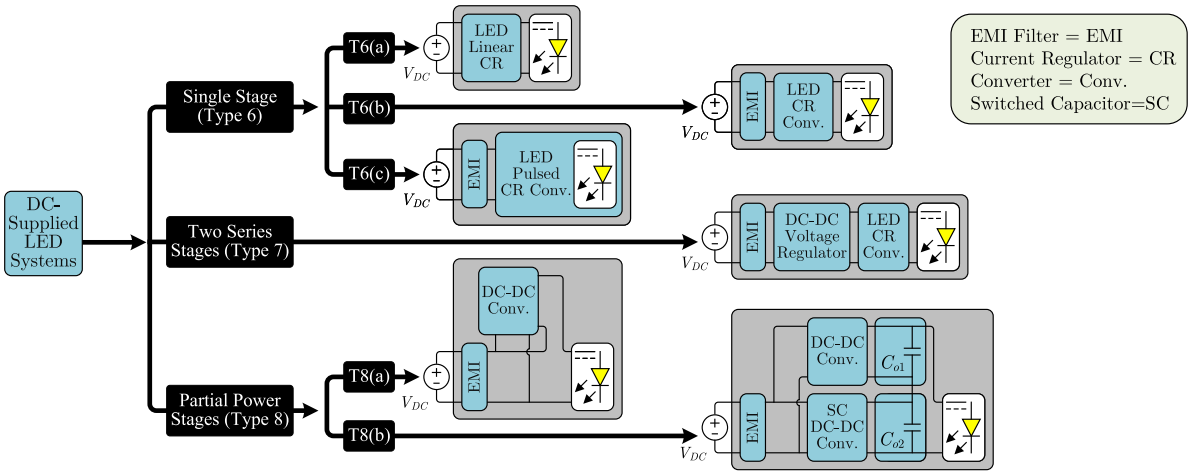

FIGURE 26. Block diagrams of different solutions for dc-supplied LED systems.

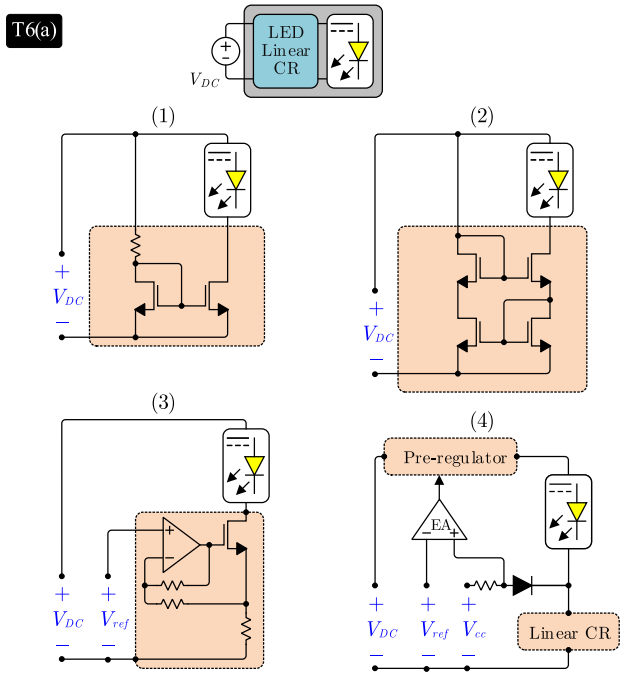

FIGURE 27. Linear Current mirrors for LED drivers. Converters (1), (2) (3) [43], [171], converter (4) [75], [172].

To operate properly, the transistors in a current mirror circuit should remain in the linear region away from saturation. This leads to unwanted conduction losses especially if the LED current is high. It is also required to avoid any thermal runaway of transistors. The losses are different in the transistor carrying LED current and one in the reference branch, thus the current mirroring becomes temperature dependent. Also due to the large transistor die size required for current and heat distribution when LED current exceeds 100mA, the current mirror becomes unfeasible.

To drive high-current LEDs, the linear current regulator shown in Fig. 27(3) can be used. In this circuit, the LED current is sensed using a small sensing resistor and the transistor operates in a linear region to keep the current constant via the feedback loop. This circuit can be used as the second stage in a two-series stage structure, type 7. In case of having a pre-regulator as in Fig. 27(4), the second loop can be implemented to minimize the voltage across the active switch in the linear regulator in order to minimize losses [75]. This approach is robust however requires the sensing resistors and extra circuitry to feed the low-offset op-amp, which is often cost-prohibitive.

The second sub-type of single-stage dc-supplied systems is labeled as T6(b) in Fig. 26 and Fig. 28 in which a dc-dc converter is used as the LED current regulator. Based on the input voltage range and the required voltage on the LED module, either step-up, step-down, or step-up/down type non-isolated dc-dc converters can be used.

The conventional boost converter, shown in Fig. 28(2), is the basic step-up dc-dc converter and can provide a desirable continuous input current and non-inverting conversion. When the required voltage on the LED module is much higher than the input voltage, high step-up converters that are variations of the conventional boost converter can be used. Many step-up and high step-up converters are reviewed in [191], [192], and [193]. However, not all of the listed topologies are suitable for high-reliability and cost-sensitive lighting applications. One of the desirable features for a driver is no visible flash of light at the moment of connecting the driver to the power source. Boost-based topologies (which do not use an extra switch to disconnect the input) can have a resonant between the boost inductor and output capacitor when the input is powered up. As the LED string does not draw any current initially, that resonance can be underdamped which leads to an undesirable visible flash of light. Adding an extra switch can solve this issue, however, it is undesirable for efficiency, reliability, and cost.

Many applications, such as lighting systems fed by PoE, require a step-down stage. The conventional buck converter,

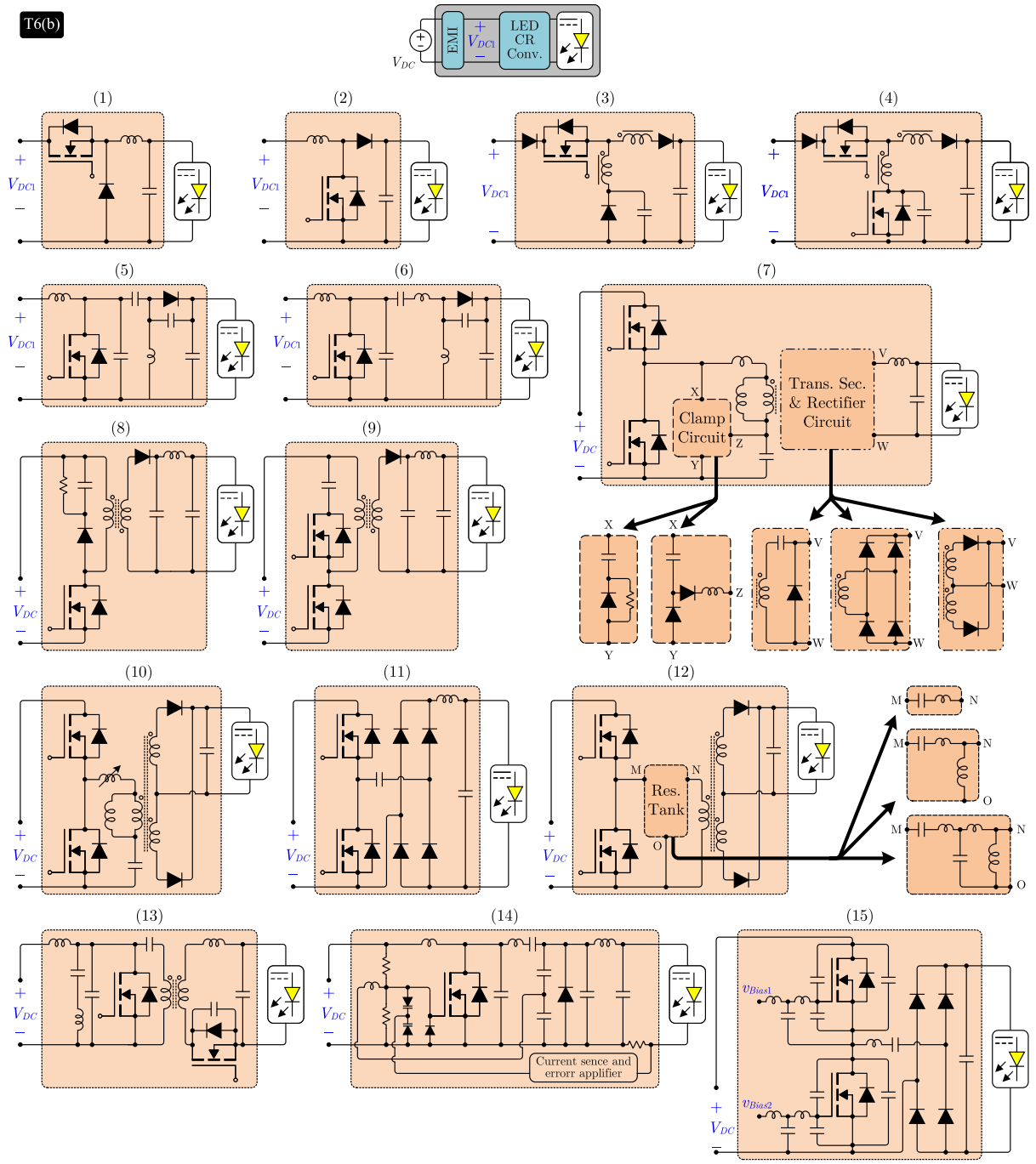

FIGURE 28. T6(b) LED current regulator converters drivers. Converters (1) [173], (2) [174], (3) [175], (4) [176], (5) [177], (6) [178], (7) [179], [180], [181], (8) [182], (9) [183], (10) [184], [185], (11) [186], (12) [187], (13) [188], (14) [189], (15) [190].

shown in Fig. 28(1), can provide continuous output current with low ripple which reduces the output capacitor needed at the LED string [194]. However, it suffers from an extremely short operation duty cycle and high switching loss in applications where extremely low conversion ratios are needed. In this case, high step-down converters which are variants of the conventional buck converter with higher step-down conversion ratios can be used [195], [196], [197], [198].

The conventional non-isolated buck-boost topology which is the basic step-up/down topology is often used for LED drivers when the floating LEDs are permitted with total voltage near the input dc voltage. Cuk converter provides both

continuous input and output currents. SEPIC and Zeta topologies have continuous input and output currents, respectively. Cuk, SEPIC and zeta topologies can operate as step-down or step-up and have their best efficiency at voltage conversion ratios near one.

As there is no galvanic isolation requirement for dc input LED applications, many single-stage topologies can be used. Flyback is a simple variation of buck-boost topology with the added bonus of isolation, as shown in Fig. 28(8). As this topology is widely used, there are various commercially available controllers designed for this converter. When used in critical conduction mode, it is possible to gain a soft turn off of the freewheeling diode with minimum losses, zero voltage commutations of the switch and a decreased EMI over the wide input voltage range [199]. An important feature of the flyback driver is the capability of keeping the output current constant using the primary side current sensor and controller [200], [201]. It is also possible to increase the efficiency by synchronous rectification on the secondary side [202], integrated self-driving [182], dual transformers [203], regenerative snubbers [204] or resonant clamping [183], the latter is shown in Fig. 28(9). The switch in the flyback converter primary side has to withstand the sum of the maximum input voltage and the reflection of the maximum output voltage back to the primary side. With the use of wide-band-gap devices, flyback can be used for higher powers too. Another limitation is the size of the transformer core which has to store the entire energy before passing it to the secondary side.

Flyback can be combined with other conventional topologies. One common method to simplify the control and gate drive circuitry and to reduce the component count is to share the switches between parts of the circuit with different functionalities [130].

In high-power applications, other isolated converters can be used. In isolated converters, by adjusting the turn ratio of the transformer step-up, step-down or step-up/down converters can be implemented. Among isolated dc-dc converters, half-bridge resonant converters are widely used as they offer low losses, small magnetic components and low EMI emissions. A dc-fed LED driver using a non-resonant asymmetric half-bridge (AHB) is reported in [181] as shown in Fig. 28(7). The secondary side can use center-tapped winding and fewer semiconductors for rectification, or simpler magnetics and more component for full or half bridge rectification. This circuit is robust and has soft-switching for a wide load current range. There are several commercial gate drivers that simplify driving the floating upper switch and maintaining the dead time.

The voltage transition slopes of the AHB ac node can be very different at rising and falling moments which causes EMI. Fig. 28(7) includes a dissipative and non-dissipative snubbers circuit to balance the transformer current during voltage transitions.

Variable inductors are also used in LED drivers [184], [185]. A dc-fed LED driver with an asymmetric half-bridge and a variable inductor has been reported in [205] and [206] as shown in Fig. 28(10). Advantages of this converter include inherent open circuit and short circuit protections, soft-switching, simple dynamics, the possibility of analog and PWM dimming, constant switching frequency operation and high efficiency. However, the design and manufacturing of the variable inductor can be expensive.

An AHB with the switched capacitor concept is reported in [207] shown in Fig. 28(11). It uses a small output inductor to improve the switching behavior of the converter and reduce the impact of the current ripple on the ESR of the output capacitor. Having few components and low cost makes this topology attractive for low-power applications ($<10W$). Fig. 28(12) shows AHB with an LLC network [208]. Both variable frequency control and duty ratio control methods can be applied. Using proper magnetic design it is possible to have a single magnetic component as there is no output inductor. Operating below series resonant frequency the output current can reach low values ($<5\%$ of nominal value) without losing soft-switching. This topology has a limited input voltage range and the frequency variation range can be large which causes EMI filter challenging.

AHB with an LCC network is shown in Fig. 28(12). The LED current control can be achieved by varying the switching frequency above the parallel resonant frequency. Compared to LLC the component count is higher and the transformer is often more expensive [209]. If soft-switching is guaranteed, the converter efficiency becomes frequency independent. Hence, the switching frequency can be increased and as a result, smaller passive components can be used which allows the replacement of bulky and fast-aging capacitors with small magnetic components [178], [210].

Resonant converters can use air-core inductive elements in a very high-frequency range (30 to 300MHz) operation. In this frequency range, the parasitic output capacitance of the switching element is the governing loss mechanism. The main topologies are class E and class DE converters. Class E converter, Fig. 28(6), has a structure similar to Cuk converter with a single switch, two/three inductors, and a capacitor. Having few components in the current path, this topology is suitable for low input voltage applications even though the voltage stress on the switch can reach 3.5 times the dc input [177].

Compared to class E, class $\phi 2$ converter, Fig. 28(13), has an LC circuit across the switch to reduce the switch voltage stress. The size can be similar to class E but the total loss is slightly larger than class E due to the higher resonant currents [188]. Class DE converter uses a full bridge inverter and has lower voltage stress, which makes it more suitable for higher dc voltages and powers. Its power component count is similar to that of class E. The DE converter has better efficiency compared to previous single switch topologies

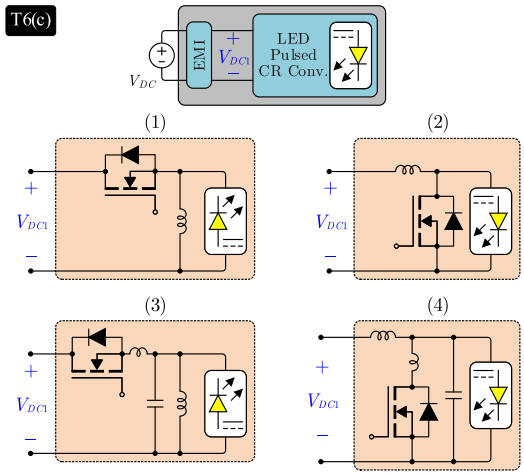

FIGURE 29. T6(c), LED pulsed CR converter drivers. Converters (1), and (2) [211], converters (3), and (4) [212].

provided that the up-side gate drive can be designed properly.

The high-frequency converters can be designed to self-oscillate. This allows the circuit to adjust the switching frequency according to the net effect of all parasitic components of the circuit which makes the system robust against inevitable component tolerances and variations due to temperature and aging. Examples of self-oscillating class E and class DE converters are shown in Fig. 28(14) and Fig. 28(15), respectively [189], [190].

The third sub-type of single-stage dc-supplied systems, T6(c) in Fig. 26, is suitable for applications where LEDs are derived from very low voltages e.g. 1-2V. Fig. 29(1) and (2) show Boost and Buck-boost based variants of this type presented in [211]. As can be seen in the figure, the standard diode used in conventional converter topologies is replaced with an LED while short-circuiting the output of the converter. In this configuration, the LED works both as the load and the rectifier diode of the converter, hence switching the LED at high frequencies (>100 kHz). Although the converter diode and output capacitor are removed in these drivers, a good luminous efficacy can be obtained. However, in this case, the output current shows a negative current peak due to the reverse-recovery effect of the LEDs. In order to reduce the reverse-recovery effect on the LEDs, in [212], the main switch of the converter is replaced with a full-wave resonant switch, which makes it possible to reduce the di/dt during the turn-off of the LED module, therefore the reverse-recovery effect is eliminated. In these drivers, which are shown in Fig. 29 (3) and (4), the dimming of the LEDs is done by means of changing the switching frequency of the converter by varying the turn-off, while keeping a constant turn-on time.

B. TYPE 7 - DC-SUPPLIED TWO CASCADED STAGES DRIVER SYSTEMS

This type of dc-supplied systems is widely used in automotive applications. Considering the wide input voltage range in

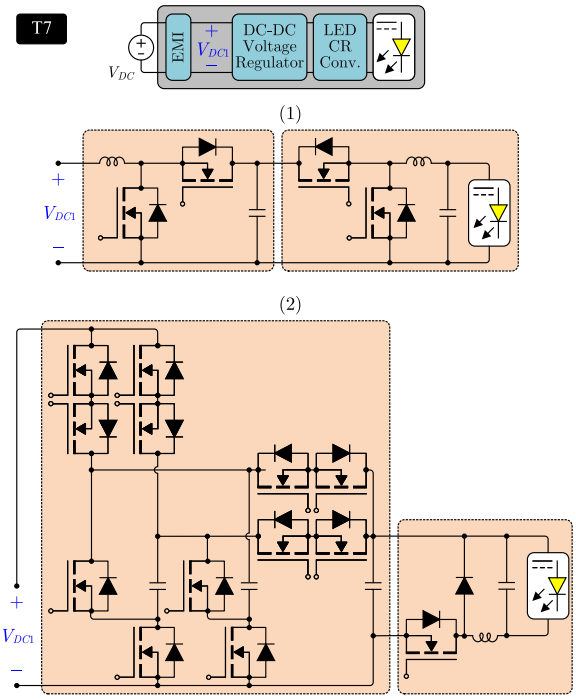

FIGURE 30. T6(b) two series stages LED drivers. Converter (1) [32], converter (2) [213].

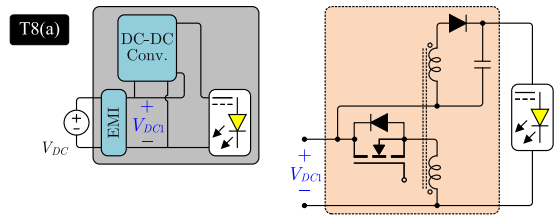

FIGURE 31. T8(a) Partial power processing converter LED drivers [214], [215].

automotive applications, the first stage, which is usually a non-isolated step-up dc-dc converter is used to provide a regulated dc voltage for the second stage. The second stage regulates LED currents and usually, a buck-type converter with low ripple continuous inductor current is used for this stage, as shown in Fig. 30(1). In automotive applications - e.g. for headlights - the optical limitations require several LEDs with a total voltage higher than the battery voltage. A series inductor at the input of step-up converters is desirable as the input current will have low harmonics and the EMI filter becomes smaller, and the short-term disturbances on the vehicle dc bus get heavily damped before reaching the converter.

A method to use high-frequency topologies toward smaller overall sizes is to cascade a low-frequency switched-capacitor pre-regulator (often at fixed voltage gain) with a high-frequency regulating stage, as shown in Fig. 30(2). This approach makes it possible to achieve high efficiency and high power density by maintaining soft charging of the switched capacitor stage and zero voltage switching of the high-frequency regulator stage [213].

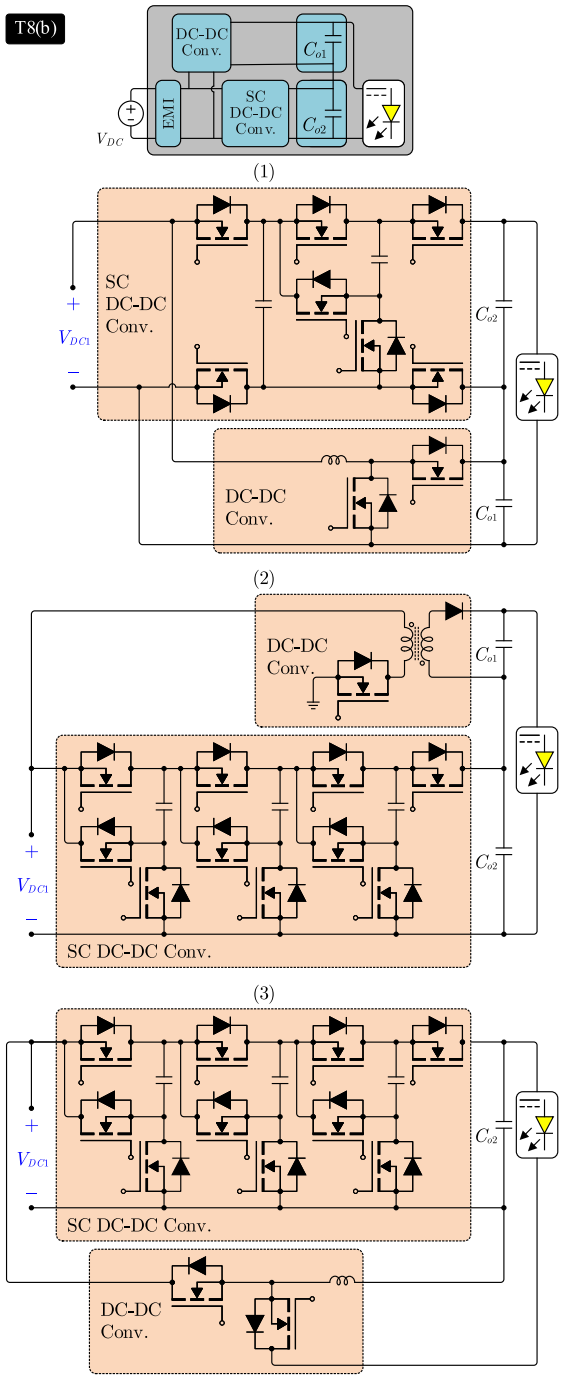

FIGURE 32. T8(b) two partial power converters-based LED drivers. Converter (1) [216], converter (2) [217], converter (3) [218].

C. TYPE 8 - DC-SUPPLIED PARTIAL POWER STAGES

The block diagram of partial power stage dc-supplied LED system is shown by T8 label in Fig. 26. The first sub-type, T8(a) is similar to T6(b) with the difference that the dc-dc converter is used to process only a percentage of the output power. In [214] a driver with a dimming feature is presented. As shown in Fig. 31, the driver consists of a flyback converter in series with the dc-link. By processing a partial power of the driver circuit for current regulation, the loss produced by power conversion can be diminished. The dimming feature is accomplished by means of current amplitude modulation (AM) or double pulse width modulation (DPWM). However, for low to mid-power application, the efficiency of this type of drivers are similar to T6(b) drivers.

The other sub-type of partial power stages systems is shown by T8(b) in Fig. 26. In this sub-type, two partial power stages are used to increase the power density of the system. One of these stages is a switched capacitor (SC) converter and the other one is a dc-dc converter. The high power density SC processes the majority of the power of the system and is left unregulated to maximize its efficiency. The dc-dc converter processes only a small portion of the total power and regulates the output voltage. As a result high power efficiency, small converter volume, and tight output voltage regulation can be achieved. In comparison with other types of drivers, this architecture can reduce the passive component volume and decreases the peak voltage stress of switches. Fig. 32 shows some examples of these drivers [216], [217], and [218]. A brief comparison on dc-supplied LED driving approaches is mentioned in TABLE 5.

TABLE 2. Suggested starting point for topology selection.

Type	A.I	A.II	A.III	A.IV	A.V	A.VI	A.VII	A.IX
T1(a)	✓	✓	–	–	–	–	–	–
T1(b)	✓	–	–	–	–	–	–	–
T1(c)	✓	–	–	–	–	–	–	✓
T2	✓	✓	–	–	–	–	–	–
T3(a)	✓	✓	–	–	–	–	–	–
T3(b)	✓	–	–	–	–	–	–	–
T3(d)	✓	✓	–	–	–	–	–	–
T3(e)	✓	✓	–	–	✓	✓	–	–
T4	✓	✓	–	–	✓	✓	–	–
T5(a)	✓	–	–	–	–	–	–	–
T5(b)	✓	–	–	–	–	–	–	–
T5(c)	–	✓	–	–	–	–	–	–
T5(d)	✓	✓	–	–	–	–	–	–
T5(e)	–	✓	–	–	–	–	–	–
T6(a)	–	–	–	✓	✓	–	–	–
T6(b)	✓	✓	✓	–	✓	–	✓	✓
T6(c)	–	–	–	–	–	–	✓	–
T7	–	✓	–	–	–	–	–	–
T8(a)	–	–	–	–	–	–	✓	✓
T8(b)	–	–	–	–	–	–	✓	✓

VII. SUGGESTED STARTING POINT FOR TOPOLOGY SELECTION

The selection of a driver topology should be carefully decided as it depends on many technical, economical, manufacturing, operational, environmental, and regulatory needs and constraints. These can be the availability of power components, controllers, reliability and component count, manufacturability especially for magnetic components, ease of assembly and less need for testing, as well as the total cost. Authors have developed a topology list to be examined first considering

TABLE 3. Ac-supplied LED drivers comparison.

Type	Ref.	No. of Components (S/D+L+C+T/W)	Switch Stress	Switching Condition	Reported Eff. / PF/ THD	Iso.	Univ. Input
T1(a)	[82]	(10/4+0+0+0/0)	$< V_{l_{max}}$	Hard	90% / 0.998 / 3.5% (at 110V / 35W)	×	×
	[83]	(13/4+0+0+0/0)	$< V_{l_{max}}$	Hard	96.1% / 0.999 / 2.6% (at 110V / 35W)	×	×
	[221]	(10/2+0+0+0/0)	$< V_{l_{max}}$	Hard	82% / 0.998 / 9% (at 110V / 30W)	×	×
	[222]	(4/4+0+0+0/0)	$< V_{l_{max}}$	Hard	90.7% / 0.975 / 22.8% (at 110V / 9W)	×	×
	[223]	(21/4+0+0+0/0)	$< V_{l_{max}}$	Hard	90% / 0.998 / 4.5% (at 110V / 35W)	×	×
	[224]	(3/4+0+0+0/0)	$< V_{l_{max}}$	Hard	90% / 0.96 / – (at 220V / 15W)	×	×
	[225]	(6/4+1+0+0/0)	$< V_{l_{max}}$	Hard	95.1% / 0.986 / – (at 110V / 20W)	×	×
	[226]	(6/4+0+0+0/0)	$< V_{l_{max}}$	Hard	92.2% / 0.996 / 8.6% (at 110V / 22W)	×	×
T1(c)	[84]	(2/2+2+2+0/0)	$\gg V_{l_{max}}$	ZVS	91.67% / 0.978 / 9.2% (at 110V / 100W)	×	×
	[227]	(2/0+1+1+1/2)	$V_{l_{max}}$	ZCS (on)	85% / 0.88 / 13.6% (at 110V / 14W)	✓	×
T2	[62]	(3/5+2+3+0/0)	$< V_{l_{max}}$	ZCS (on) / ZVS	90.7% / – / – (at 220V / 80W)	×	✓
T3(a)	[61]	(0/7+1+3+1/2)	N/A	N/A	91.8% / – / 13.5% (at 220V / 46W)	×	×
	[89]	(0/7+2+3+0/0)	N/A	N/A	93.6% / 0.99 / – (at 220V / 50W)	×	×
	[228]	(0/4+1+4+0/0)	N/A	N/A	95.2% / 0.977 / 10.5% (at 220V / 70W)	×	×
	[229]	(0/7+1+6+0/0)	N/A	N/A	98% / 0.99 / 4.28% (at 220V / 70W)	×	×
T3(b)	[92]	(0/4+0+1+1/2)+1R	N/A	N/A	49% / 0.59 / 40.6% (at 220V / 10W)	✓	×
T3(c)	[96]	(2/5+0+3+1/2)	$V_{l_{max}}$	ZVS	86 / – / – (at 220V / 6W)	✓	×
T3(d)	[108]	(2/7+1+3+1/2)	$\gg V_{l_{max}}$	ZCS (on)	91.2% / 0.98 / 15% (at 220V / 100W)	✓	✓
	[109]	(1/9+2+5+1/2)	$\gg V_{l_{max}}$	ZCS (on)	90.8% / 0.975 / – (at 110V / 50W)	✓	✓
	[230]	(1/6+1+2+1/2)	$\gg V_{l_{max}}$	ZCS (on)	90% / 0.991 / 13.26% (at 110V / 12.5W)	✓	✓
	[231]	(1/7+4+4+0/0)	$\gg V_{l_{max}}$	ZCS (on)	91.5% / 0.995 / 4.1% (at 220V / 42W)	✓	✓
	[232]	(1/6+1+2+1/2)	$\gg V_{l_{max}}$	ZCS (on)	94% / 0.956 / 27.27% (at 100V / 60W)	×	✓
	[233]	(1/6+1+3+1/2)+1R	$\gg V_{l_{max}}$	ZCS (on)	89.7% / 0.997 / – (at 110V / 9.5W)	✓	✓
	[231]	(1/7+4+4+0/0)	$\gg V_{l_{max}}$	ZCS/ZVS	91.5% / 0.999 / 4.1% (at 220V / 42W)	×	✓
	[234]	(1/5+2+1+0/0)	$\gg V_{l_{max}}$	ZVS	90.6% / 0.96 / – (at 100V / 22W)	×	×
T3(e)	[110]	(1/7+2+3+1/2)	$\gg V_{l_{max}}$	ZCS (on)	80.5% / 0.932 / – (at 220V / 60W)	✓	×
	[235]	(1/7+3+5+1/2)	$\gg V_{l_{max}}$	ZCS (on)	87.8% / 0.99 / 16.28% (at 100V / 96W)	✓	✓
	[236]	(1/7+2+3+1/2)	$\gg V_{l_{max}}$	ZCS (on)	83.2% / 0.812 / 57.49% (at 110V / 24W)	✓	×
	[111]	(2/6+3+4+1/3)	$\gg V_{l_{max}}$	ZVS	90.9% / 0.98 / – (at 110V / 75W)	✓	×
	[237]	(4/8+4+4+1/3)	$\gg V_{l_{max}}$	ZVS	91% / 0.989 / – (at 220V / 300W)	✓	✓
	[238]	(2/8+4+6+1/3)	$\gg V_{l_{max}}$	ZVS	– / 0.99 / 10% (at 110V / 144W)	✓	×
	[114]	(2/9+3+5+2/4)	$\gg V_{l_{max}}$	ZCS (on)	89% / 0.989 / – (at 110V / 33.6W)	✓	×
	[239]	(2/8+2+5+1/2)	$> V_{l_{max}}$	ZVS	93.1% / 0.99 / 14.6% (at 220V / 90W)	✓	×
	[240]	(1/8+4+5+0/0)	$\gg V_{l_{max}}$	ZCS (on)	87.8% / 0.989 / 9.61% (at 120V / 47W) (2 Str.)	×	×
	[116]	(2/4+3+4+1/3)	$\gg V_{l_{max}}$	ZVS	93.05% / 0.994 / 7.27% (at 115V / 144W)	✓	×
	[117]	(2/6+5+6+1/3)	$\gg V_{l_{max}}$	ZVS	92.8% / 0.992 / 7% (at 110V / 100W)	✓	×
	[118]	(2/6+3+5+0/0)	$\gg V_{l_{max}}$	ZVS	92.4% / 0.977 / 20.4% (at 220V / 100W)	×	✓
	[241]	(2/6+3+4+0/0)	$\gg V_{l_{max}}$	ZVS	94.3% / 0.99 / 10.9% (at 127V / 42W)	×	✓
	[119]	(1/7+2+4+1/2)	$\gg V_{l_{max}}$	ZCS (on)	85% / 0.99 / 8% (at 110V / 8W)	✓	✓
	[132]	(1/8+2+5+1/2)	$\gg V_{l_{max}}$	ZCS (on)	88.5% / 0.992 / – (at 220V / 120W)	✓	×
	[242]	(1/7+3+3+0/0)	$\gg V_{l_{max}}$	ZCS (on)	85% / 0.96 / 28% (at 220V / 70W)	×	×

the requirements, TABLE 2. This list is entirely based on the authors' experience and it may be helpful for product engineers to narrow down their search for adequate driver topologies.

TABLE 4. Ac-supplied LED drivers comparison.

Type	Ref.	No. of Components (S/D+L+C+T/W)	Switch Stress	Switching Condition	Reported Eff. / PF/ THD	Iso.	Univ. Input
	[112]	(1/10+4+5+1/3)	$\gg V_{l_{max}}$	ZCS (on)	90.8% / 0.994 / 5.4% (at $110V$ / $100W$)	✓	×
	[121]	(1/7+3+5+1/2)	$\gg V_{l_{max}}$	ZCS	92% / 0.999 / 2.6% (at $220V$ / $21W$)	✓	×
	[243]	(1/7+3+3+0/0)	$\gg V_{l_{max}}$	Hard	89.5% / 0.995 / 3.5% (at $110V$ / $100W$)	×	×
	[244]	(2/6+2+3+1/2)	$\gg V_{l_{max}}$	ZVS	93% / 0.99 / 5.2% (at $110V$ / $100W$)	×	×
	[245]	(1/8+3+3+0/0)	$\gg V_{l_{max}}$	ZCS (on)	85.82% / 0.957 / 14.7% (at $127V$ / $50W$)	×	×
	[122]	(1/7+3+4+1/2)	$\gg V_{l_{max}}$	ZCS (on)	91.6% / 0.992 / 12.6% (at $220V$ / $21W$)	✓	×
	[123]	(2/10+3+5+1/3)	$\gg V_{l_{max}}$	ZVS	92% / 0.995 / 6% (at $220V$ / $100W$)	✓	×
	[124]	(1/10+5+6+1/3)	$\gg V_{l_{max}}$	ZCS (on)	91.2% / 0.995 / 5.2% (at $110V$ / $100W$)	✓	×
	[246]	(2/4+4+3+0/0)	$\gg V_{l_{max}}$	Hard	93.8% / 0.997 / 10.4% (at $110V$ / $100W$)	×	×
	[126]	(2/7+2+5+2/5)	$V_{l_{max}}$	ZVS	91.4% / 0.992 / 8% (at $220V$ & $150W$)	✓	×
	[247]	(2/8+1+5+2/4)	$V_{l_{max}}$	ZCS	89.4% / 0.98 / 16.4% (at $220V$ / $50W$)	✓	×
	[127]	(1/8+2+3+1/2)	$\gg V_{l_{max}}$	ZCS (on)	89% / 0.96 / 16% (at $110V$ / $25W$)	✓	✓
	[248]	(3/9+3+3+1/2)	$\gg V_{l_{max}}$	ZCS (on)	86% / – / – (at $230V$ / $100W$)	×	✓
	[249]	(3/9+3+3+1/2)	$V_{l_{max}}$	Hard	89.22% / 0.93 / 14% (at $110V$ / $12W$)	×	✓
	[250]	(1/12+2+3+1/3)	$\gg V_{l_{max}}$	Hard	90% / 0.99 / – (at $110V$ / $60W$)	✓	✓
	[251]	(1/9+2+5+1/2)	$\gg V_{l_{max}}$	ZCS (on)	87% / 0.99 / – (at $110V$ / $20W$)	✓	×
	[252]	(1/9+2+4+1/3)	$\gg V_{l_{max}}$	ZCS (on)	80% / 0.997 / 2.5% (at $110V$ / $25W$)	✓	×
	[253]	(1/8+2+3+1/2)	$\gg V_{l_{max}}$	ZCS (on)	91.1% / 0.97 / 22.3% (at $220V$ / $105W$)	×	×
T4	[143]	(3/7+3+4+1/3)	$V_{l_{max}}$	ZVS/Hard	90.96% / 0.994 / 3.31% (at $115V$ / $130W$)	✓	✓
	[254]	(17/0+3+8+1/2)	$V_{l_{max}}$	ZVS/Hard	90% / – / – (at $120V$ / $480W$)	✓	✓
	[255]	(3/9+3+3+1/2)	$> V_{l_{max}}$	ZCS (on)	– / 0.99 / 10% (at $220V$ / $50W$)	✓	✓
	[256]	(2/7+3+4+0/0)	$V_{l_{max}}$	ZCS (on)	85.4% / 0.94 / – (at $110V$ / $15W$)	×	×
	[257]	(3/8+0+4+3/6)	$\gg V_{l_{max}}$	ZCS (on) / Hard	92.3% / 0.95 / 9% (at $220V$ / $130W$)	✓	✓
T5(a)	[155]	(3/5+3+3+1/2)	$\gg V_{l_{max}}$	ZCS (on) / Hard	87.7% / – / – (at $110V$ / $20W$)	✓	✓
	[258]	(3/5+3+3+1/2)	$\gg V_{l_{max}}$	ZCS (on) / Hard	– / – / – (at $110V$ / $20W$)	✓	✓
	[259]	(5/7+2+3+1/3)	$\gg V_{l_{max}}$	ZCS (on) / Hard	80.5% / – / – (at $110V$ / $33.6W$)	✓	✓
T5(b)	[159]	(3/6+1+3+1/3)	$\gg V_{l_{max}}$	Hard	66% / 0.99 / 14% (at $110V$ / $13.5W$)	✓	✓
	[260]	(2/8+3+3+1/3)	$\gg V_{l_{max}}$	ZCS (on)	89.5% / 0.96 / 25% (at $110V$ / $20W$)	✓	✓
	[261]	(3/7+1+3+1/3)	$\gg V_{l_{max}}$	ZCS (on)	80% / 0.995 / – (at $110V$ / $13.5W$)	✓	✓
	[262]	(3/7+1+3+1/3)	$\gg V_{l_{max}}$	ZCS (on) / Hard	82.5% / 0.94 / 6.5% (at $110V$ / $15W$)	✓	×
	[263]	(3/7+3+3+0/0)	$\gg V_{l_{max}}$	ZCS (on) / Hard	91% / 0.998 / 3.5% (at $110V$ / $16W$)	×	×
T5(c)	[160]	(6/5+3+5+1/2)	$\gg V_{l_{max}}$	ZVS / Hard	91% / 0.992 / – (at $110V$ / $100W$)	✓	×
	[161]	(6/5+3+5+1/2)	$\gg V_{l_{max}}$	ZVS / Hard	91% / 0.992 / 4.5% (at $110V$ / $100W$)	✓	✓
T5(d)	[162]	(3/6+2+4+1/3)	$\gg V_{l_{max}}$	ZCS (on) / Hard	85.5% / 0.99 / 6% (at $110V$ / $35W$)	✓	✓
	[164]	(3/6+2+5+1/2)	$\gg V_{l_{max}}$	ZCS (on) / Hard	87.5% / – / – (at $110V$ / $10W$)	×	✓
	[163]	(6/6+3+5+1/3)	$\gg V_{l_{max}}$	ZVS	90.6% / 0.992 / – (at $110V$ / $100W$)	✓	✓
	[166]	(2/7+1+4+2/5)	$\gg V_{l_{max}}$	ZCS (on)	85.5% / 0.99 / 5.5% (at $110V$ / $30W$)	✓	✓
	[264]	(2/7+2+3+1/3)	$\gg V_{l_{max}}$	ZCS (on)	84% / 0.98 / – (at $220V$ / $20W$)	✓	✓
	[265]	(2/7+2+4+1/3)	$\gg V_{l_{max}}$	Hard	90% / 0.999 / 9% (at $110V$ / $20W$)	✓	×
T5(e)	[167]	(2/6+1+3+1/3)	$\gg V_{l_{max}}$	ZCS (on) / Hard	86% / 0.97 / 17.8% (at $110V$ / $8.5W$)	✓	✓
	[266]	(2/6+1+3+1/3)	$\gg V_{l_{max}}$	ZCS (on) / Hard	88.2% / – / – (at $110V$ / $23W$)	✓	✓

TABLE 5. Dc-supplied LED drivers comparison.

Type	Ref.	No. of components (S/D+L+C+T/W)	Switch Stress	Switching Condition	Reported Eff.(%)	Iso.	Com. Gnd.	Gain
T6(a)	[75]	(5/6+1+4+1/2)	$\gg V_{in_{max}}$	Hard	87% (4 Str.) (at $30V$ / 120kHz / $-$)	×	✓	<1 & >1
T6(b)	[17]	(4/0+2+5+0/0)	$V_{in_{max}}$	ZVS	89.5% (at $14V$ / 2MHz / $10W$)	×	✓	<1 & >1
	[35]	(4/0+2+4+0/0)	$V_{in_{max}}$	ZVS	91.8% (at $14V$ / 2MHz / $13W$)	×	✓	<1 & >1
	[36]	(3/1+0+1+1/2)	$\gg V_{in_{max}}$	ZVS	98.2% (at $13.5V$ / 100kHz / $13W$)	×	✓	<1 & >1
	[173]	(1/1+1+1+0/0)	$V_{in_{max}}$	Hard	86.8% (at $12V$ / 500kHz / $3.6W$)	×	✓	<1
	[267]	(2/2+1+4+1/2)	$< V_{o_{max}}$	ZVS	93% (at $24V$ / 85kHz / $135W$)	×	✓	>1
	[175]	(1/3+0+3+1/2)	$\gg V_{in_{max}}$	ZCS	91% (at $12V$ / 200kHz / $8W$)	×	✓	<1
	[176]	(2/2+0+2+1/2)	$\gg V_{in_{max}}$	ZCS	90.3% (at $12V$ / 100kHz / $26W$)	×	✓	>1
	[177]	(1/1+2+5+0/0)	$\gg V_{in_{max}}$	ZVS	84% (at $40V$ / 51MHz / $5W$)	×	✓	<1
	[179]	(6/0+1+4+1/2)	$V_{in_{max}}$	ZCS	94.8% (at $400V$ / 200kHz / $100W$)	✓	×	<1
	[181]	(2/2+1+3+1/3)	$V_{in_{max}}$	ZVS	94.5% (at $400V$ / 114kHz / $40W$)	✓	×	<1
	[268]	(3/2+2+3+1/3)+1R	$V_{in_{max}}$	ZVS	95.1% (at $400V$ / 100kHz / $180W$)	✓	×	<1
	[269]	(2/1+1+2+1/2)	$V_{in_{max}}$	ZVS	95.3% (at $400V$ / 400kHz / $160W$)	✓	×	<1
	[184]	(2/2+1+2+1/3)	$V_{in_{max}}$	ZVS	90.5% (at $400V$ / 100kHz / $33W$)	✓	×	<1
	[185]	(2/2+1+2+0/0)	$V_{in_{max}}$	ZVS	94% (at $48V$ / 100kHz / $22W$)	×	✓	>1
	[186]	(2/4+1+2+0/0)	$V_{in_{max}}$	ZCS (on)	75% (at $24V$ / 130kHz / $4.58W$)	×	×	<1
	[187]	(2/4+1+4+1/2)	$V_{in_{max}}$	ZVS	96.5% (at $400V$ / 100kHz / $100W$)(2 Str.)	✓	×	<1
	[188]	(2/0+3+6+1/2)	$\gg V_{in_{max}}$	ZVS	82% (at $18V$ / 10MHz / $10W$)	✓	×	<1
	[189]	(1/2+4+6+0/0)	$V_{in_{max}}$	ZVS	89% (at $6V$ / 120MHz / $9W$)	×	✓	>1
	[270]	(6/0+1+3+0/0)	$\gg V_{in_{max}}$	ZVS	92.8% (at $6V$ / 300kHz / $6W$)	×	✓	>1
	[40]	(2/0+0+3+2/4)	$\gg V_{in_{max}}$	ZVS	93.5% (at $12V$ / 2.4MHz / $30W$)	✓	×	<1 & >1
	[41]	(4/0+0+5+2/4)	$\gg V_{in_{max}}$	ZVS	89.6% (at $12V$ / 1.8MHz / $6W$)	✓	×	<1 & >1
	[42]	(2/2+3+6+2/4)	$\gg V_{in_{max}}$	ZVS	92% (at $12V$ / 10kHz / $30W$)	✓	×	>1
T6(c)	[213]	(1/0+1+0+0/0)	$\gg V_{in_{max}}$	Hard	85% (at $1.5V$ / 600kHz / $1W$)	×	✓	>1
	[214]	(1/0+2+1+0/0)	$\gg V_{in_{max}}$	ZCS	94.5% (at $12V$ / 265kHz / $7.5W$)	×	✓	>1
T7	[215]	(1/2+0+1+1/2)	$< V_{in_{max}}$	ZVS	96% (at $50V$ / 50kHz & $3-30$MHz / $30W$)	×	×	<1
	[39]	(24/0+3+5+1/2)	$V_{in_{max}}$ & $\gg V_{in_{max}}$	ZVS	92.1% (at $13V$ / 250kHz / $20W$)	×	✓	<1
T8(a)	[216]	(1/2+0+1+1/2)	$\gg V_{in_{max}}$	Hard	95.9% (at $48V$ / 50kHz / $48W$)	×	✓	>1
T8(b)	[218]	(9/0+1+4+0/0)	$\gg V_{in_{max}}$	Hard	90% (at $4V$ / 270kHz & 1080kHz / $260mW$)	×	✓	>1
	[219]	(11/1+0+5+1/2)	$\gg V_{in_{max}}$	Hard	90.2% (at $12V$ / 500kHz / $13.75W$)	×	✓	>1
	[220]	(14/0+1+4+0/0)	$\gg V_{in_{max}}$	Hard	93% (3 Strings) (at $3.7V$ / 565kHz & 1131kHz / $-$)	×	×	>1
	[271]	(6/0+1+4+0/0)	$\ll V_{in_{max}}$	Hard	92% (at $24V$ / 1MHz / $5W$)	×	✓	<1
	[272]	(6/0+2+3+0/0)	$\ll V_{o_{max}}$	ZVS	93.5% (at $4.2V$ / 2MHz / $1.9W$)	×	✓	>1
	[273]	(10/0+1+3+0/0)	$\ll V_{o_{max}}$	Hard	91.15% (at $3.7V$ / 100kHz & 1MHz / $0.9W$)	×	✓	>1

VIII. CONCLUSION

As LEDs continue to evolve the lighting industry, the selection of the right drivers to satisfy the needs of the ever-growing list of applications gets more important. This review provides an overall picture of diverse applications and their technical and economical needs including material cost and operational conditions. It also overviews drivers fed from ac and dc sources and their shared and different

considerations. Driver topologies are categorized and their shared properties, constraints, and differences with generic power supplies are discussed. Finally, a high-level suggested list of starting topologies per application is provided.

REFERENCES

[1] R. D. Dupuis and M. R. Krames, "History, development, and applications of high-brightness visible light-emitting diodes," *J. Lightw. Technol.*, vol. 26, no. 9, pp. 1154–1171, May 2008, doi: 10.1109/JLT.2008.923628.

[2] V. K. Khanna, *Fundamentals of Solid-State Lighting: LEDs, OLEDs, and Their Applications in Illumination and Displays*. Boca Raton, FL, USA: CRC Press, 2014.

[3] M. R. Krames, O. B. Shchekin, R. Mueller-Mach, G. O. Mueller, L. Zhou, G. Harbers, and M. G. Craford, "Status and future of high-power light-emitting diodes for solid-state lighting," *J. Display Technol.*, vol. 3, no. 2, pp. 160–175, Jun. 2007.

[4] G. Chen, M. Craven, A. Kim, A. Munkholm, S. Watanabe, M. Camras, W. Götz, and F. Steranka, "Performance of high-power III-nitride light emitting diodes," *Phys. Status Solidi A*, vol. 205, no. 5, pp. 1086–1092, May 2008.

[5] S. Liu and X. Luo, *LED Packaging for Lighting Applications: Design, Manufacturing, and Testing*. Hoboken, NJ, USA: Wiley, 2011.

[6] X. Li, Z. Ghassemlooy, S. Zvanovec, M. Zhang, and A. Burton, "Equivalent circuit model of high power LEDs for VLC systems," in *Proc. 2nd West Asian Colloq. Opt. Wireless Commun. (WACOWC)*, Apr. 2019, pp. 90–95.

[7] *American National Standard for Light-Emitting Diode Drivers—Methods of Measurement*, Standard ANSI C82.16-2015, National Electrical Manufacturers Association, Nov. 2015.

[8] *Phase-Cut Dimming for Solid State Lighting—Basic Compatibility*, Standard NEMA SSL 7A-2015, National Electrical Manufacturers Association, Jan. 2016.

[9] S. Pimputkar, J. S. Speck, S. P. DenBaars, and S. Nakamura, "Prospects for LED lighting," *Nature Photon.*, vol. 3, no. 4, pp. 180–182, Apr. 2009.

[10] Y. Narukawa, M. Ichikawa, D. Sanga, M. Sano, and T. Mukai, "White light emitting diodes with super-high luminous efficacy," *J. Phys. D, Appl. Phys.*, vol. 43, no. 35, 2010, Art. no. 354002.

[11] E. F. Schubert, T. Gessmann, and J. K. Kim, *Light Emitting Diodes*. Hoboken, NJ, USA: Wiley, 2005.

[12] J. S. Kim, P. E. Jeon, Y. H. Park, J. C. Choi, H. L. Park, G. C. Kim, and T. W. Kim, "White-light generation through ultraviolet-emitting diode and white-emitting phosphor," *Appl. Phys. Lett.*, vol. 85, no. 17, pp. 3696–3698, Oct. 2004.

[13] N. Kimura, K. Sakuma, S. Hirafune, K. Asano, N. Hirosaki, and R.-J. Xie, "Extrahigh color rendering white light-emitting diode lamps using oxynitride and nitride phosphors excited by blue light-emitting diode," *Appl. Phys. Lett.*, vol. 90, no. 5, Jan. 2007, Art. no. 051109.

[14] D. Li, G. Yu, S.-H. Chen, and Y.-C. Hsiao, "Curved display device," U.S. Patent 9 763 346, Sep. 12, 2017.

[15] J. D. Bullough, "LEDs in automotive lighting," in *Nitride Semiconductor Light-Emitting Diodes (LEDs)*, J. Huang, H.-C. Kuo, and S.-C. Shen, Eds. Woodhead Publishing, 2014, ch. 20, pp. 595–605, doi: 10.1533/9780857099303.3.595.

[16] J. Moisel, "Requirements for future high resolution ADB modules," in *Proc. 11th Int. Symp. Automot. Lighting (ISAL)*, vol. 16. Munich, Germany: Herbert Utz Verlag, 2015, p. 161.

[17] S. Mukherjee, A. Sepahvand, and D. Maksimović, "High-frequency LC^3L resonant DC–DC converter for automotive LED driver applications," in *Proc. IEEE Appl. Power Electron. Conf. Expo. (APEC)*, Mar. 2018, pp. 797–802.

[18] M. Schratz, C. Gupta, T. J. Struhs, and K. Gray, "A new way to see the light: Improving light quality with cost-effective LED technology," *IEEE Ind. Appl. Mag.*, vol. 22, no. 4, pp. 55–62, Jul. 2016.

[19] M. Schratz, C. Gupta, T. Struhs, and K. Gray, "Reducing energy and maintenance costs while improving light quality and reliability with led lighting technology," in *Proc. Conf. Rec. Annu. IEEE Pulp Paper Ind. Tech. Conf. (PPIC)*, Jun. 2013, pp. 43–49.

[20] R. C. Morrow, "LED lighting in horticulture," *HortScience*, vol. 43, no. 7, pp. 1947–1950, 2008.

[21] F. Kalantari, O. M. Tahir, R. A. Joni, and E. Fatemi, "Opportunities and challenges in sustainability of vertical farming: A review," *J. Landscape Ecol.*, vol. 11, no. 1, pp. 35–60, Jan. 2018.

[22] H. J. Vreman and D. K. Stevenson, "Devices for treating circadian rhythm disorders using LED's," U.S. Patent 6 350 275, Feb. 26, 2002.

[23] L. H. Koh, Y. K. Tan, Z. Z. Wang, and K. J. Tseng, "An energy-efficient low voltage DC grid powered smart LED lighting system," in *Proc. 37th Annu. Conf. IEEE Ind. Electron. Soc. (IECON)*, Nov. 2011, pp. 2883–2888.

[24] *Lighting Science: Nomenclature and Definitions for Illuminating Engineering*, Standard ANSI/IES LS-1-22, 2021.

[25] Illuminating Engineering Society, *IES Lighting Handbook*, 10th ed. New York, NY, USA: Illuminating Engineering Society, 2017.

[26] A. Szalai, T. Szabó, P. Horváth, A. Timár, and A. Poppe, "Smart SSL: Application of IoT/CPS design platforms in LED-based street-lighting luminaires," in *Proc. IEEE Lighting Conf. Visegrad Countries (Lumen V4)*, Sep. 2016, pp. 1–6.

[27] P. T. Daely, H. T. Reda, G. B. Satrya, J. W. Kim, and S. Y. Shin, "Design of smart LED streetlight system for smart city with web-based management system," *IEEE Sensors J.*, vol. 17, no. 18, pp. 6100–6110, Sep. 2017.

[28] A. C. C. Chun, H. Ramiah, and S. Mekhilef, "Wide power dynamic range CMOS RF-DC rectifier for RF energy harvesting system: A review," *IEEE Access*, vol. 10, pp. 23948–23963, 2022.

[29] H. H. R. Sherazi, D. Zorbas, and B. O'Flynn, "A comprehensive survey on RF energy harvesting: Applications and performance determinants," *Sensors*, vol. 22, no. 8, p. 2990, Apr. 2022.

[30] H. H. Ibrahim, M. J. Singh, S. S. Al-Bawri, S. K. Ibrahim, M. T. Islam, A. Alzamil, and M. S. Islam, "Radio frequency energy harvesting technologies: A comprehensive review on designing, methodologies, and potential applications," *Sensors*, vol. 22, no. 11, p. 4144, May 2022.

[31] L.-G. Tran, H.-K. Cha, and W.-T. Park, "RF power harvesting: A review on designing methodologies and applications," *Micro Nano Syst. Lett.*, vol. 5, no. 1, pp. 1–16, Dec. 2017.

[32] I. K. Hsu. (2018). LED drivers for automotive exterior lighting applications. Texas Instruments. [Online]. Available: https://www.ti.com/lit/pdf/SLPY006B

[33] S. Saponara, G. Pasetti, N. Costantino, F. Tinfena, P. D'Abramo, and L. Fanucci, "A flexible LED driver for automotive lighting applications: IC design and experimental characterization," *IEEE Trans. Power Electron.*, vol. 27, no. 3, pp. 1071–1075, Mar. 2012.

[34] Y. Qu, W. Shu, and J. S. Chang, "A low-EMI, high-reliability PWM-based dual-phase LED driver for automotive lighting," *IEEE J. Emerg. Sel. Topics Power Electron.*, vol. 6, no. 3, pp. 1179–1189, Mar. 2018.

[35] M. Khatua, A. Kumar, D. Maksimović, and K. K. Afridi, "A high-frequency LCLC network based resonant DC–DC converter for automotive LED driver applications," in *Proc. IEEE 19th Workshop Control Model. for Power Electron. (COMPEL)*, Jun. 2018, pp. 1–7.

[36] S.-N. Lin, T.-Y. Lee, Z.-Y. He, Y.-C. Hsieh, Y.-N. Chang, and C.-S. Moo, "An LED driver with wide operation range for automotive lighting," in *Proc. IEEE Int. Conf. Ind. Technol. (ICIT)*, Feb. 2019, pp. 1–4.

[37] C. Song, H. Kweon, U. Lee, J. Kim, S. Yang, and J. Park, "Modeling of conducted EMI noise in an automotive LED driver module with DC/DC converters," in *Proc. Int. Symp. Electromagn. Compat. (EMC EUROPE)*, Sep. 2019, pp. 1009–1013.

[38] P. Horsky, J. Plojhar, and J. Daniel, "Adaptive peak average current control LED driver for automotive lighting," *IEEE Solid-State Circuits Lett.*, vol. 2, no. 9, pp. 199–202, Sep. 2019.

[39] S. Mukherjee, V. Yousefzadeh, A. Sepahvand, M. Doshi, and D. Maksimovic, "A two-stage automotive LED driver with multiple outputs," *IEEE Trans. Power Electron.*, vol. 36, no. 12, pp. 14175–14186, Dec. 2021.

[40] A. Sepahvand, M. Doshi, V. Yousefzadeh, J. Patterson, K. K. Afridi, and D. Maksimović, "High-frequency ZVS Ćuk converter for automotive LED driver applications using planar integrated magnetics," in *Proc. IEEE Appl. Power Electron. Conf. Expo. (APEC)*, Mar. 2017, pp. 2467–2474.

[41] A. Sepahvand, M. Doshi, V. Yousefzadeh, J. Patterson, K. K. Afridi, and D. Maksimovic, "Automotive LED driver based on high frequency zero voltage switching integrated magnetics Ćuk converter," in *Proc. IEEE Energy Convers. Congr. Expo. (ECCE)*, Sep. 2016, pp. 1–8.

[42] Y. Wang, S. Gao, Y. Guan, J. Huang, D. Xu, and W. Wang, "A single-stage LED driver based on double LLC resonant tanks for automobile headlight with digital control," *IEEE Trans. Transport. Electrific.*, vol. 2, no. 3, pp. 357–368, Sep. 2016.

[43] K. Macalanda, "Fundamentals to automotive LED driver circuits," Texas Instrum., Dallas, TX, USA, Tech. Rep. SLYY163, 2019.

[44] H. Z. Cummins and H. L. Swinney, "III light beating spectroscopy," in *Progress in Optics*, vol. 8. Amsterdam, The Netherlands: Elsevier, 1970, pp. 133–200.

[45] E. Kiyoi, "The state of UV-LED curing: An investigation of chemistry and applications," RadTech Rep., 2013, vol. 2, pp. 59–63. [Online]. Available: https://radtech.org/magazinearchives/Publications/RadTechReport/jun-2013/The%20State%20of%20UV-LED%20Curing%20-%20An%20Investigation%20of%20Chemistry%20and%20Applications.pdf

[46] H. Wang and T. Hu, "Multichannel sequential display LED driver with optimal transient performance and efficiency via synchronous integral control," *IET Power Electron.*, vol. 13, no. 15, pp. 3226–3233, Nov. 2020.

[47] A. Agrawal, A. Shrivastava, and K. C. Jana, "A universal input, single-stage AC–DC LED driver for an auditorium light," *J. Circuits, Syst. Comput.*, vol. 28, no. 2, Feb. 2019, Art. no. 1950024.

[48] Texas Instruments. (2015). *LP8557 High-Efficiency LED Backlight Driver For Tablets*. [Online]. Available: https://www.ti.com/lit/gpn/LP8557?keyMatch=UV%20LED%20DRIVER

[49] D. Allen and M. Allen, "LED assemblies and light strings containing same," U.S. Patent 7 344 275, Mar. 18, 2008.

[50] J. Cho, J. Jung, J. H. Chae, H. Kim, H. Kim, J. W. Lee, S. Yoon, C. Sone, T. Jang, Y. Park, and E. Yoon, "Alternating-current light emitting diodes with a diode bridge circuitry," *Jpn. J. Appl. Phys.*, vol. 46, no. 48, pp. L1194–L1196, Dec. 2007.

[51] G. A. Onushkin et al., "Efficient alternating current operated white light-emitting diode chip," *IEEE Photon. Technol. Lett.*, vol. 21, no. 1, pp. 33–35, Jan. 1, 2009, doi: 10.1109/LPT.2008.2008204.

[52] Maxim Integrated. (2019). *LED Drivers for Automotive Applications Design Guide*. [Online]. Available: https://www.analog.com/media/en/technical-documentation/tech-articles/led-drivers-for-automotive-applications-design-guide.pdf

[53] Y.-T. Huang, Y.-T. Chen, Y.-H. Liu, H.-C. Hsiao, and W.-T. Tsai, "Compact-size and high-conversion-efficiency regulator for alternating-current-operated light-emitting diodes," *IEEE Trans. Ind. Electron.*, vol. 58, no. 9, pp. 4130–4135, Sep. 2011.

[54] M. Khatib, "Ballast resistor calculation: Current matching in parallel LEDs," Texas Instrum., Dallas, TX, USA, Tech. Rep. SLVA325, 2009.

[55] D. Hong and H. Cha, "LED current balancing scheme using current-fed quasi-Z-source converter," *IEEE Trans. Power Electron.*, vol. 36, no. 12, pp. 14187–14194, Dec. 2021.

[56] Y. Wang, J. M. Alonso, and X. Ruan, "A review of LED drivers and related technologies," *IEEE Trans. Ind. Electron.*, vol. 64, no. 7, pp. 5754–5765, Jul. 2017.

[57] Y. Hu and M. M. Jovanović, "A new current-balancing method for paralleled LED strings," in *Proc. 26th Annu. IEEE Appl. Power Electron. Conf. Expo. (APEC)*, Mar. 2011, pp. 705–712.

[58] R. Zhang and H. S.-H. Chung, "Paralleled LED strings: An overview of current-balancing techniques," *IEEE Ind. Electron. Mag.*, vol. 9, no. 2, pp. 17–23, Jun. 2015.

[59] H.-H. Yen, W.-Y. Yeh, and H.-C. Kuo, "GaN alternating current light-emitting device," *Phys. Status Solidi A*, vol. 204, no. 6, pp. 2077–2081, Jun. 2007.

[60] S. M. Baddela and D. S. Zinger, "Parallel connected LEDs operated at high frequency to improve current sharing," in *Proc. Conf. Rec. IEEE Ind. Appl. Conf., 39th IAS Annu. Meeting*, vol. 3, Oct. 2004, pp. 1677–1681.

[61] W. Chen, S. N. Li, and S. Y. R. Hui, "A comparative study on the circuit topologies for offline passive light-emitting diode (LED) drivers with long lifetime & high efficiency," in *Proc. IEEE Energy Convers. Congr. Expo.*, Sep. 2010, pp. 724–730.

[62] C.-L. Kuo, T.-J. Liang, K.-H. Chen, and J.-F. Chen, "Design and implementation of high frequency AC-LED driver with digital dimming," in *Proc. IEEE Int. Symp. Circuits Syst.*, May 2010, pp. 3713–3716.

[63] C.-C. Wang, K.-H. Wu, Y.-C. Liu, C.-Y. Yang, M. M. Alam, Y.-K. Lo, and H.-J. Chiu, "Study and implementation of an improved-power factor alternating-current-light emitting diode driver," *IET Power Electron.*, vol. 8, no. 7, pp. 1156–1163, 2015.

[64] (2012). *AC-LED Lighting Products Find Niche, Perhaps More*. [Online]. Available: https://www.analog.com/media/en/technical-documentation/tech-articles/led-drivers-for-automotive-applications-design-guide.pdf

[65] Exar Corporation. (2014). *Datasheet iML8684 Three Terminal Current Controller*. [Online]. Available: https://www.maxlinear.com/ds/xr46084.pdf

[66] *Phase-Cut Dimming for Solid State Lighting: Basic Compatibility*, Standard NEMA SSL 7A-2015, 2016, pp. 1–35.

[67] T. Jiang, H. Zeng, J. Zhang, and Z. Qian, "A primary side feedforward control scheme for low power LED driver compatible with TRIAC dimmer," in *Proc. 27th Annu. IEEE Appl. Power Electron. Conf. Expo. (APEC)*, Feb. 2012, pp. 963–968.

[68] B. Lehman and A. J. Wilkins, "Designing to mitigate effects of flicker in LED lighting: Reducing risks to health and safety," *IEEE Power Electron. Mag.*, vol. 1, no. 3, pp. 18–26, Sep. 2014.

[69] R. Zhang and H. S.-H. Chung, "A TRIAC-dimmable LED lamp driver with wide dimming range," *IEEE Trans. Power Electron.*, vol. 29, no. 3, pp. 1434–1446, Mar. 2014.

[70] H. Eom, C.-C. Lee, T.-Y. Yang, and S. Yang, "Design optimization of TRIAC-dimmable AC-DC converter in LED lighting," in *Proc. 27th Annu. IEEE Appl. Power Electron. Conf. Expo. (APEC)*, Feb. 2012, pp. 831–835.

[71] L. Yan, B. Chen, and J. Zheng, "A new TRIAC dimmable LED driver control method achieves high-PF and quality-of-light," in *Proc. 27th Annu. IEEE Appl. Power Electron. Conf. Expo. (APEC)*, Feb. 2012, pp. 969–974.

[72] M. Kadota, H. Shoji, H. Hirose, A. Hatakeyama, and K. Wada, "A turn-off delay controlled bleeder circuit for single-stage TRIAC dimmable LED driver with small-scale implementation and low output current ripple," *IEEE Trans. Power Electron.*, vol. 34, no. 10, pp. 10069–10081, Oct. 2019.

[73] P.-Y. Wu, T.-J. Liang, W.-J. Tseng, and C.-Y. Chen, "Design and implementation of active bleeder for TRIAC dimmable LED driver," in *Proc. IEEE 4th Int. Future Energy Electron. Conf. (IFEEC)*, Nov. 2019, pp. 1–7.

[74] B.-H. Yeom, S.-S. Hong, and T.-W. Kim, "A study on LED driver compatible with TRIAC-dimmer employing active bleeder," *Trans. Korean Inst. Power Electron.*, vol. 19, no. 4, pp. 297–302, Aug. 2014.

[75] Y. Hu and M. M. Jovanovic, "LED driver with self-adaptive drive voltage," *IEEE Trans. Power Electron.*, vol. 23, no. 6, pp. 3116–3125, Nov. 2008.

[76] Z. Ye, F. Greenfeld, and Z. Liang, "Single-stage offline SEPIC converter with power factor correction to drive high brightness LEDs," in *Proc. 24th Annu. IEEE Appl. Power Electron. Conf. Expo.*, Feb. 2009, pp. 546–553.

[77] K. Zhou, J. G. Zhang, S. Yuvarajan, and D. F. Weng, "Quasi-active power factor correction circuit for HB LED driver," *IEEE Trans. Power Electron.*, vol. 23, no. 3, pp. 1410–1415, May 2008.

[78] H.-J. Chiu, Y.-K. Lo, J.-T. Chen, S.-J. Cheng, C.-Y. Lin, and S.-C. Mou, "A high-efficiency dimmable LED driver for low-power lighting applications," *IEEE Trans. Ind. Electron.*, vol. 57, no. 2, pp. 735–743, Feb. 2010.

[79] K. H. Loo, W.-K. Lun, S.-C. Tan, Y. M. Lai, and C. K. Tse, "On driving techniques for LEDs: Toward a generalized methodology," *IEEE Trans. Power Electron.*, vol. 24, no. 12, pp. 2967–2976, Dec. 2009.

[80] W. Chen and S. Y. R. Hui, "A dimmable light-emitting diode (LED) driver with mag-amp postregulators for multistring applications," *IEEE Trans. Power Electron.*, vol. 26, no. 6, pp. 1714–1722, Jun. 2011.

[81] Q. Wang, T. Li, and Q.-H. He, "Dimmable and cost-effective DC driving technique for flicker mitigation in LED lighting," *J. Display Technol.*, vol. 10, no. 9, pp. 766–774, Sep. 2014.

[82] K. I. Hwu and W. C. Tu, "Dimmable driver for light-emitting diode with total harmonic distortion improved," *IET Power Electron.*, vol. 5, no. 1, pp. 59–67, 2012.

[83] K. I. Hwu, W. C. Tu, and Y. T. Fang, "Dimmable AC LED driver with efficiency improved based on switched LED module," *J. Display Technol.*, vol. 10, no. 3, pp. 171–181, Mar. 2014.

[84] G.-C. Tseng, K.-H. Wu, H.-J. Chiu, and Y.-K. Lo, "Single-stage high power-factor bridgeless AC-LED driver for lighting applications," in *Proc. Int. Conf. Renew. Energy Res. Appl. (ICRERA)*, Nov. 2012, pp. 1–6.

[85] Z. Fan, H. Jiang, and J. Lin, "Heterogeneous integrated high voltage DC/AC light emitter," U.S. Patent 7 221 044, May 22, 2007.

[86] B.-G. Kang, Y. Choi, and S.-K. Chung, "High frequency AC-LED driving for street light," in *Proc. 9th Int. Conf. Power Electron. ECCE Asia (ICPE-ECCE Asia)*, Jun. 2015, pp. 1246–1251.

[87] P. D. Teodosescu, M. Bojan, and R. Marschalko, "Resonant LED driver with inherent constant current and power factor correction," *Electron. Lett.*, vol. 50, no. 15, pp. 1086–1088, Jul. 2014.

[88] K.-H. Wu, H.-J. Chiu, and Y.-K. Lo, "A single-stage high power-factor bridgeless AC-LED driver for lighting applications," *Int. J. Circuit Theory Appl.*, vol. 42, no. 1, pp. 96–109, Jan. 2014.

[89] S. Y. Hui, S. N. Li, X. H. Tao, W. Chen, and M. W. Ng, "A novel passive offline LED driver with long lifetime," *IEEE Trans. Power Electron.*, vol. 25, no. 10, pp. 2665–2672, Oct. 2010.
[90] R. S. Y. Hui, "Apparatus and methods of operation of passive led lighting equipment," U.S. Patent 12 429 792, Oct. 28, 2010.
[91] P. Richman, "Wave factors for rectifiers with capacitor input filters, and other high crest-factor loads," *IEEE Trans. Ind. Electron. Control Instrum.*, vol. IECI-21, no. 4, pp. 235–241, Nov. 1974.
[92] J. M. Alonso, D. Gacio, A. J. Calleja, J. Ribas, and E. L. Corominas, "A study on LED retrofit solutions for low-voltage halogen cycle lamps," *IEEE Trans. Ind. Appl.*, vol. 48, no. 5, pp. 1673–1682, Sep. 2012.
[93] *SOT-89 TO-252 Low Cost Constant Current Linear LED Driver IC Chip F5111 F5112 ODM Solutions*, Aolittel Technol., Dongguan, China. [Online]. Available: http://aolittel.sell.everychina.com/p-109240896-sot-89-to-252-low-cost-constant-current-linear-led-driver-ic-chip-f5111-f5112.html
[94] TI. (2014). *TPS92410 Switch-Controlled, Direct Drive, Linear Controller for Offline LED Drivers*. [Online]. Available: https://www.ti.com/lit/gpn/tps92410
[95] J. J. Yu, "Integrated LED bulb," U.S. Patent 7 661 852, Feb. 16, 2010.
[96] S. Buso, G. Spiazzi, and F. Sichirollo, "Study of the asymmetrical half-bridge flyback converter as an effective line-fed solid-state lamp driver," *IEEE Trans. Ind. Electron.*, vol. 61, no. 12, pp. 6730–6738, Dec. 2014.
[97] E. Eloi, E. M. Sá Jr., R. L. D. Santos, P. A. Miranda, and F. L. M. Antunes, "Single stage switched capacitor LED driver with high power factor and reduced current ripple," in *Proc. IEEE Appl. Power Electron. Conf. Expo. (APEC)*, Mar. 2015, pp. 906–912.
[98] M. A. M. Oninda, G. Sarowar, and M. M. H. Galib, "Single-phase switched capacitor AC-DC step down converters for improved power quality," in *Proc. IEEE Region 10 Hum. Technol. Conf. (R10-HTC)*, Dec. 2017, pp. 520–523.
[99] B. Singh, B. N. Singh, A. Chandra, K. Al-Haddad, A. Pandey, and D. P. Kothari, "A review of single-phase improved power quality AC-DC converters," *IEEE Trans. Ind. Electron.*, vol. 50, no. 5, pp. 962–981, Oct. 2003.
[100] B. Singh, S. Singh, A. Chandra, and K. Al-Haddad, "Comprehensive study of single-phase AC-DC power factor corrected converters with high-frequency isolation," *IEEE Trans. Ind. Informat.*, vol. 7, no. 4, pp. 540–556, Nov. 2011.
[101] *Electromagnetic Compatibility (EMC)—Part 3–2: Limits-Limits for Harmonic Current Emissions (Equipment Input Current 16A Perphase)*, Standard IEC 61000-3-2:2014, 2014.
[102] C. Branas, F. J. Azcondo, and J. M. Alonso, "Solid-state lighting: A system review," *IEEE Ind. Electron. Mag.*, vol. 7, no. 4, pp. 6–14, Dec. 2013.
[103] P. S. Almeida, D. Camponogara, M. D. Costa, H. Braga, and J. M. Alonso, "Matching LED and driver life spans: A review of different techniques," *IEEE Ind. Electron. Mag.*, vol. 9, no. 2, pp. 36–47, Jun. 2015.
[104] S. Li, S.-C. Tan, C. K. Lee, E. Waffenschmidt, S. Y. Hui, and C. K. Tse, "A survey, classification, and critical review of light-emitting diode drivers," *IEEE Trans. Power Electron.*, vol. 31, no. 2, pp. 1503–1516, Feb. 2016.
[105] E. H. Ismail, "Bridgeless SEPIC rectifier with unity power factor and reduced conduction losses," *IEEE Trans. Ind. Electron.*, vol. 56, no. 4, pp. 1147–1157, Apr. 2009.
[106] I. Castro, A. Vazquez, M. Arias, D. G. Lamar, M. M. Hernando, and J. Sebastian, "A review on flicker-free AC–DC LED drivers for single-phase and three-phase AC power grids," *IEEE Trans. Power Electron.*, vol. 34, no. 10, pp. 10035–10057, Oct. 2019.
[107] R. Watson, G. C. Hua, and F. C. Lee, "Characterization of an active clamp flyback topology for power factor correction applications," *IEEE Trans. Power Electron.*, vol. 11, no. 1, pp. 191–198, Jan. 1996.
[108] K.-W. Siu and Y.-S. Lee, "A novel high-efficiency flyback power-factor-correction circuit with regenerative clamping and soft switching," *IEEE Trans. Circuits Syst. I, Fundam. Theory Appl.*, vol. 47, no. 3, pp. 350–356, Mar. 2000.
[109] H. Ma, W. Yu, Q. Feng, J.-S. Lai, and C. Zheng, "A novel SEPIC-derived PFC pre-regulator without electrolytic capacitor for PWM dimming LED lighting application based on valley fill circuit," in *Proc. IEEE Energy Convers. Congr. Expo.*, Sep. 2011, pp. 2310–2317.
[110] Z. Bo, Y. Xu, X. Ming, C. Qiaoliang, and W. Zhaoan, "Design of boost-flyback single-stage PFC converter for LED power supply without electrolytic capacitor for energy-storage," in *Proc. IEEE 6th Int. Power Electron. Motion Control Conf.*, May 2009, pp. 1668–1671.
[111] S.-Y. Chen, Z. R. Li, and C.-L. Chen, "Analysis and design of single-stage AC/DC *LLC* resonant converter," *IEEE Trans. Ind. Electron.*, vol. 59, no. 3, pp. 1538–1544, Mar. 2012.
[112] Y. Wang, J. Huang, W. Wang, and D. Xu, "A single-stage single-switch LED driver based on class-E converter," *IEEE Trans. Ind. Appl.*, vol. 52, no. 3, pp. 2618–2626, May/Jun. 2016.
[113] Y. Wang, F. Li, Y. Qiu, S. Gao, Y. Guan, and D. Xu, "A single-stage LED driver based on flyback and modified class-E resonant converters with low-voltage stress," *IEEE Trans. Ind. Electron.*, vol. 66, no. 11, pp. 8463–8473, Nov. 2019.
[114] S.-W. Lee and H.-L. Do, "Boost-integrated two-switch forward AC–DC LED driver with high power factor and ripple-free output inductor current," *IEEE Trans. Ind. Electron.*, vol. 64, no. 7, pp. 5789–5796, Jul. 2017.
[115] W.-Y. Choi and M.-K. Yang, "High-efficiency isolated SEPIC converter with reduced conduction losses for LED displays," *Int. J. Electron.*, vol. 101, no. 11, pp. 1495–1502, Nov. 2014.
[116] C.-A. Cheng, C.-H. Chang, T.-Y. Chung, and F.-L. Yang, "Design and implementation of a single-stage driver for supplying an LED street-lighting module with power factor corrections," *IEEE Trans. Power Electron.*, vol. 30, no. 2, pp. 956–966, Feb. 2015.
[117] Y. Wang, X. Deng, Y. Wang, and D. Xu, "Single-stage bridgeless LED driver based on a CLCL resonant converter," *IEEE Trans. Ind. Appl.*, vol. 54, no. 2, pp. 1832–1841, Mar./Apr. 2018.
[118] P. S. Almeida, H. A. C. Braga, M. A. D. Costa, and J. M. Alonso, "Offline soft-switched LED driver based on an integrated bridgeless boost–asymmetrical half-bridge converter," *IEEE Trans. Ind. Appl.*, vol. 51, no. 1, pp. 761–769, Jan./Feb. 2015.
[119] Y.-C. Li and C.-L. Chen, "A novel single-stage high-power-factor AC-to-DC LED driving circuit with leakage inductance energy recycling," *IEEE Trans. Ind. Electron.*, vol. 59, no. 2, pp. 793–802, Feb. 2012.
[120] J.-L. Lin, W.-K. Yao, and S.-P. Yang, "Analysis and design for a novel single-stage high power factor correction diagonal half-bridge forward AC–DC converter," *IEEE Trans. Circuits Syst. I, Reg. Papers*, vol. 53, no. 10, pp. 2274–2286, Oct. 2006.
[121] B. Poorali, E. Adib, and H. Farzanehfard, "A single-stage single-switch soft-switching power-factor-correction LED driver," *IEEE Trans. Power Electron.*, vol. 32, no. 10, pp. 7932–7940, Oct. 2017.
[122] B. Poorali and E. Adib, "Analysis of the integrated SEPIC-flyback converter as a single-stage single-switch power-factor-correction LED driver," *IEEE Trans. Ind. Electron.*, vol. 63, no. 6, pp. 3562–3570, Jun. 2016.
[123] Y. Wang, N. Qi, Y. Guan, C. Cecati, and D. Xu, "A single-stage LED driver based on SEPIC and LLC circuits," *IEEE Trans. Ind. Electron.*, vol. 64, no. 7, pp. 5766–5776, Jul. 2017.
[124] Y. Wang, Y. Guan, K. Ren, W. Wang, and D. Xu, "A single-stage LED driver based on BCM boost circuit and *LLC* converter for street lighting system," *IEEE Trans. Ind. Electron.*, vol. 62, no. 9, pp. 5446–5457, Sep. 2015.
[125] Y.-M. Liu and L.-K. Chang, "Single-stage soft-switching AC–DC converter with input-current shaping for universal line applications," *IEEE Trans. Ind. Electron.*, vol. 56, no. 2, pp. 467–479, Feb. 2009.
[126] S. Mangkalajan, C. Ekkaravarodome, K. Jirasereeamornkul, P. Thounthong, K. Higuchi, and M. K. Kazimierczuk, "A single-stage LED driver based on ZCDS class-E current-driven rectifier as a PFC for street-lighting applications," *IEEE Trans. Power Electron.*, vol. 33, no. 10, pp. 8710–8727, Oct. 2018.
[127] G. Z. Abdelmessih, J. M. Alonso, and M. A. D. Costa, "Loss analysis for efficiency improvement of the integrated buck–flyback LED driver," *IEEE Trans. Ind. Appl.*, vol. 54, no. 6, pp. 6543–6553, Nov. 2018.
[128] M. Esteki, D. Darvishrahimabadi, M. Shahabbasi, and S. A. Khajehoddin, "An electrolytic-capacitor-less PFC LED driver with low DC-bus voltage stress for high power streetlighting applications," *IEEE Trans. Power Electron.*, vol. 38, no. 5, pp. 6294–6310, May 2023.
[129] C. Ekkaravarodome, V. Chunkag, K. Jirasereeamornkul, and M. K. Kazimierczuk, "Class-D zero-current-switching rectifier as power-factor corrector for lighting applications," *IEEE Trans. Power Electron.*, vol. 29, no. 9, pp. 4938–4948, Sep. 2014.
[130] R. Redl, L. Balogh, and N. O. Sokal, "A new family of single-stage isolated power-factor correctors with fast regulation of the output voltage," in *Proc. 25th Annu. IEEE Power Electron. Spec. Conf. (PESC)*, vol. 2, Jun. 1994, pp. 1137–1144.

[131] Y. Hu, L. Huber, and M. M. Jovanović, "Single-stage, universal-input AC/DC LED driver with current-controlled variable PFC boost inductor," *IEEE Trans. Power Electron.*, vol. 27, no. 3, pp. 1579–1588, Mar. 2012.

[132] Q. Luo, J. Huang, Q. He, K. Ma, and L. Zhou, "Analysis and design of a single-stage isolated AC–DC LED driver with a voltage doubler rectifier," *IEEE Trans. Ind. Electron.*, vol. 64, no. 7, pp. 5807–5817, Jul. 2017.

[133] C. K. Tse and M. H. L. Chow, "New single-stage PFC regulator using the Sheppard–Taylor topology," *IEEE Trans. Power Electron.*, vol. 13, no. 5, pp. 842–851, Sep. 1998.

[134] M. Rezanejad, M. Dargahi, S. Lesan, A. R. Noee, and M. Karami, "New switching method for Sheppard–Taylor PFC converter," in *Proc. IEEE 2nd Int. Power Energy Conf.*, Dec. 2008, pp. 793–796.

[135] T.-F. Wu, J.-C. Hung, S.-Y. Tseng, and Y.-M. Chen, "A single-stage fast regulator with PFC based on an asymmetrical half-bridge topology," *IEEE Trans. Ind. Electron.*, vol. 52, no. 1, pp. 139–150, Feb. 2005.

[136] C.-A. Cheng, H.-L. Cheng, and T.-Y. Chung, "A novel single-stage high-power-factor LED street-lighting driver with coupled inductors," *IEEE Trans. Ind. Appl.*, vol. 50, no. 5, pp. 3037–3045, Sep./Oct. 2014.

[137] J. Ma, X. Wei, L. Hu, and J. Zhang, "LED driver based on boost circuit and LLC converter," *IEEE Access*, vol. 6, pp. 49588–49600, 2018.

[138] J.-Y. Lee, J.-F. Chen, H.-Y. Shen, and S.-F. Hong, "Single-stage single-switch high-power-factor boost-forward converter with FM and PWM composite control," in *Proc. Int. Symp. Comput., Consum. Control*, Jun. 2012, pp. 353–356.

[139] W. Guo and P. K. Jain, "Design optimization for steady state and dynamic performance of a single-stage power factor corrected AC-DC converter," in *Proc. 19th Annu. IEEE Appl. Power Electron. Conf. Expo. (APEC)*, vol. 2, Feb. 2004, pp. 1206–1212.

[140] M. Mahdavi and H. Farzanehfard, "Zero-current-transition bridgeless PFC without extra voltage and current stress," *IEEE Trans. Ind. Electron.*, vol. 56, no. 7, pp. 2540–2547, Jul. 2009.

[141] B. Zhao, A. Abramovitz, and K. Smedley, "Family of bridgeless buck-boost PFC rectifiers," *IEEE Trans. Power Electron.*, vol. 30, no. 12, pp. 6524–6527, Dec. 2015.

[142] P. Kong, S. Wang, and F. C. Lee, "Common mode EMI noise suppression for bridgeless PFC converters," *IEEE Trans. Power Electron.*, vol. 23, no. 1, pp. 291–297, Jan. 2008.

[143] C. Spini, "48 V–130 W high-efficiency converter with PFC for LED street lighting applications," ST Microelectron., Geneva, Switzerland, Appl. Note AN3106, 2012.

[144] *Lighting Solutions to Maximize Energy Efficiency*, Fairchild Semicond., Sunnyvale, CA, USA, 2009.

[145] *Energy-Efficient Solutions for Offline LED Lighting and General Illumination*, ST Microelectron., Geneva, Switzerland, 2012, pp. 1–27.

[146] H. Ma, J.-S. Lai, C. Zheng, and P. Sun, "A high-efficiency quasi-single-stage bridgeless electrolytic capacitor-free high-power AC–DC driver for supplying multiple LED strings in parallel," *IEEE Trans. Power Electron.*, vol. 31, no. 8, pp. 5825–5836, Aug. 2016.

[147] O. Garcia, J. A. Cobos, R. Prieto, P. Alou, and J. Uceda, "Power factor correction: A survey," in *Proc. IEEE 32nd Annu. Power Electron. Spec. Conf.*, Vancouver, BC, Canada, vol. 1, 2001, pp. 8–13, doi: 10.1109/PESC.2001.953987.

[148] R. D. Middlebrook and S. Cuk, "A general unified approach to modelling switching-converter power stages," in *Proc. IEEE Power Electron. Spec. Conf.*, Jun. 1976, pp. 18–34.

[149] F. S. Dos Reis, J. Sebastian, and J. Uceda, "Characterization of conducted noise generation for Sepic, Cuk and Boost converters working as power factor preregulators," in *Proc. 19th Annu. Conf. IEEE Ind. Electron. (IECON)*, Nov. 1993, pp. 965–970.

[150] H. Zhang, Y. Zhang, and X. Ma, "Distortion behavior analysis of general pulse-width modulated zeta PFC converter operating in continuous conduction mode," *IEEE Trans. Power Electron.*, vol. 27, no. 10, pp. 4212–4223, Oct. 2012.

[151] L. Rossetto, G. Spiazzi, and P. Tenti, "Control techniques for power factor correction converters," in *Proc. PEMC*, 1994, vol. 94, no. 9, pp. 1310–1318.

[152] X. Qu, S. C. Wong, and K. T. Chi, "Noncascading structure for electronic ballast design for multiple LED lamps with independent brightness control," *IEEE Trans. Power Electron.*, vol. 25, no. 2, pp. 331–340, Mar. 2010.

[153] M. Arias, M. F. Díaz, D. G. Lamar, D. Balocco, A. A. Diallo, and J. Sebastián, "High-efficiency asymmetrical half-bridge converter without electrolytic capacitor for low-output-voltage AC–DC LED drivers," *IEEE Trans. Power Electron.*, vol. 28, no. 5, pp. 2539–2550, May 2013.

[154] H. Wang, H. Wang, G. Zhu, and F. Blaabjerg, "An overview of capacitive DC-links-topology derivation and scalability analysis," *IEEE Trans. Power Electron.*, vol. 35, no. 2, pp. 1805–1829, Feb. 2020.

[155] S. Wang, X. Ruan, K. Yao, S.-C. Tan, Y. Yang, and Z. Ye, "A flicker-free electrolytic capacitor-less AC–DC LED driver," *IEEE Trans. Power Electron.*, vol. 27, no. 11, pp. 4540–4548, Nov. 2012.

[156] Q. Hu and R. Zane, "Minimizing required energy storage in off-line LED drivers based on series-input converter modules," *IEEE Trans. Power Electron.*, vol. 26, no. 10, pp. 2887–2895, Oct. 2011.

[157] P. Fang, B. White, C. Fiorentino, and Y.-F. Liu, "Zero ripple single stage AC-DC LED driver with unity power factor," in *Proc. IEEE Energy Convers. Congr. Expo. (ECCE)*, Sep. 2013, pp. 3452–3458.

[158] Y. Yang, X. Ruan, L. Zhang, J. He, and Z. Ye, "Feed-forward scheme for an electrolytic capacitor-less AC/DC LED driver to reduce output current ripple," *IEEE Trans. Power Electron.*, vol. 29, no. 10, pp. 5508–5517, Oct. 2014.

[159] F. Wang, L. Li, Y. Zhong, and X. Shu, "Flyback-based three-port topologies for electrolytic capacitor-less LED drivers," *IEEE Trans. Ind. Electron.*, vol. 64, no. 7, pp. 5818–5827, Jul. 2017.

[160] Y. Qiu, H. Wang, L. Wang, Y.-F. Liu, and P. C. Sen, "Current-ripple-based control strategy to achieve low-frequency ripple cancellation in single-stage high-power LED driver," in *Proc. IEEE Energy Convers. Congr. Expo. (ECCE)*, Sep. 2015, pp. 5316–5322.

[161] Y. Qiu, L. Wang, H. Wang, Y.-F. Liu, and P. C. Sen, "Bipolar ripple cancellation method to achieve single-stage electrolytic-capacitor-less high-power LED driver," *IEEE J. Emerg. Sel. Topics Power Electron.*, vol. 3, no. 3, pp. 698–713, Sep. 2015.

[162] P. Fang, Y.-F. Liu, and P. C. Sen, "A flicker-free single-stage offline LED driver with high power factor," *IEEE J. Emerg. Sel. Topics Power Electron.*, vol. 3, no. 3, pp. 654–665, Sep. 2015.

[163] Y. Qiu, H. Wang, Z. Hu, L. Wang, Y.-F. Liu, and P. C. Sen, "Electrolytic-capacitor-less high-power LED driver," in *Proc. IEEE Energy Convers. Congr. Expo. (ECCE)*, Sep. 2014, pp. 3612–3619.

[164] P. Fang and Y. F. Liu, "An electrolytic capacitor-free single stage Buck–Boost LED driver and its integrated solution," in *Proc. IEEE Appl. Power Electron. Conf. Expo. (APEC)*, Mar. 2014, pp. 1394–1401.

[165] Z. Shan, X. Chen, S. Fan, G. Yuan, and C. K. Tse, "Resonant switched-capacitor auxiliary circuit for active power decoupling in electrolytic capacitor-less AC/DC LED drivers," in *Proc. IEEE Energy Convers. Congr. Expo. (ECCE)*, Sep. 2019, pp. 866–871.

[166] P. Fang, Y.-J. Qiu, H. Wang, and Y.-F. Liu, "A single-stage primary-side-controlled off-line flyback LED driver with ripple cancellation," *IEEE Trans. Power Electron.*, vol. 32, no. 6, pp. 4700–4715, Jun. 2017.

[167] P. Fang and Y. F. Liu, "Energy channeling LED driver technology to achieve flicker-free operation with true single stage power factor correction," *IEEE Trans. Power Electron.*, vol. 32, no. 5, pp. 3892–3907, May 2017.

[168] *Road Vehicles—Electrical Disturbances From Conduction and Coupling—Part 2: Electrical Transient Conduction Along Supply Lines Only*, ISO Standard 7637-2:2011, International Organization for Standardization, 2011.

[169] B. Wen, D. Sarafianos, R. A. McMahon, and S. Pickering, "Understanding automotive electrical network voltage transients," in *Proc. 8th IET Int. Conf. Power Electron., Mach. Drives (PEMD)*, Glasgow, U.K., 2016, pp. 1–6, doi: 10.1049/cp.2016.0197.

[170] M. Corbett and P. McCambridge, "Transient suppression in the automotive environment," Automot. Electron. Des., Appl. Note 9312, Jul. 1999, pp. 49–60.

[171] S.-C. Hsia, M.-H. Sheu, and S.-Y. Lai, "Chip implementation of high-efficient light-emitting diode dimming driver for high-power light-emitting diode lighting system," *IET Power Electron.*, vol. 8, no. 6, pp. 1043–1051, Jun. 2015.

[172] Y. Hu and M. M. Jovanovic, "A novel LED driver with adaptive drive voltage," in *Proc. 23rd Annu. IEEE Appl. Power Electron. Conf. Expo.*, Feb. 2008, pp. 565–571.

[173] W. K. Lun, K. H. Loo, S. C. Tan, Y. M. Lai, and C. K. Tse, "Bilevel current driving technique for LEDs," *IEEE Trans. Power Electron.*, vol. 24, no. 12, pp. 2920–2932, Dec. 2009.

[174] X. Xu and X. Wu, "High dimming ratio LED driver with fast transient boost converter," in *Proc. IEEE Power Electron. Spec. Conf.*, Jun. 2008, pp. 4192–4195.

[175] F. Pouladi, H. Farzanehfard, E. Adib, and H. Le Sage, "Single-switch soft-switching LED driver suitable for battery-operated systems," *IEEE Trans. Ind. Electron.*, vol. 66, no. 4, pp. 2726–2734, Apr. 2019.

[176] F. Pouladi, H. Farzanehfard, and E. Adib, "Battery operated soft switching resonant Buck–Boost LED driver with single magnetic element," *IEEE Trans. Power Electron.*, vol. 34, no. 3, pp. 2704–2711, Mar. 2019.
[177] M. P. Madsen, A. Knott, and M. A. E. Andersen, "Very high frequency resonant DC/DC converters for LED lighting," in *Proc. 28th Annu. IEEE Appl. Power Electron. Conf. Expo. (APEC)*, Mar. 2013, pp. 835–839.
[178] D. J. Perreault, J. Hu, J. M. Rivas, Y. Han, O. Leitermann, R. C. N. Pilawa-Podgurski, A. Sagneri, and C. R. Sullivan, "Opportunities and challenges in very high frequency power conversion," in *Proc. 24th Annu. IEEE Appl. Power Electron. Conf. Expo.*, Feb. 2009, pp. 1–14.
[179] J. Zhang, J. Wang, G. Zhang, and Z. Qian, "A hybrid driving scheme for full-bridge synchronous rectifier in LLC resonant converter," *IEEE Trans. Power Electron.*, vol. 27, no. 11, pp. 4549–4561, Nov. 2012.
[180] C. Ye, P. Das, and S. K. Sahoo, "Peak current control of multichannel LED driver with selective dimming," *IEEE Trans. Ind. Electron.*, vol. 66, no. 5, pp. 3446–3457, May 2019.
[181] M. Arias, D. G. Lamar, F. F. Linera, D. Balocco, A. A. Diallo, and J. N. Sebastián, "Design of a soft-switching asymmetrical half-bridge converter as second stage of an LED driver for street lighting application," *IEEE Trans. Power Electron.*, vol. 27, no. 3, pp. 1608–1621, Mar. 2012.
[182] N. Rouger, J. C. Crébier, and S. Catellani, "High-efficiency and fully integrated self-powering technique for intelligent switch-based flyback converters," *IEEE Trans. Ind. Appl.*, vol. 44, no. 3, pp. 826–835, May 2008.
[183] D. A. Smith, "Multi-resonant clamped flyback converter," U.S. Patent 5 430 633, Jul. 4, 1995.
[184] J. M. Alonso, M. S. Perdigão, M. A. D. Costa, G. Martínez, and R. Osorio, "Analysis and experiments on a single-inductor half-bridge LED driver with magnetic control," *IEEE Trans. Power Electron.*, vol. 32, no. 12, pp. 9179–9190, Dec. 2017.
[185] M. Martins, M. S. Perdigão, A. M. S. Mendes, R. A. Pinto, and J. M. Alonso, "Analysis, design, and experimentation of a dimmable resonant-switched-capacitor LED driver with variable inductor control," *IEEE Trans. Power Electron.*, vol. 32, no. 4, pp. 3051–3062, Apr. 2016.
[186] E. E. D. S. Filho, P. H. A. Miranda, E. M. Sá, and F. L. M. Antunes, "A LED driver with switched capacitor," *IEEE Trans. Ind. Appl.*, vol. 50, no. 5, pp. 3046–3054, Sep. 2014.
[187] X. Wu, J. Zhang, and Z. Qian, "A simple two-channel LED driver with automatic precise current sharing," *IEEE Trans. Ind. Electron.*, vol. 58, no. 10, pp. 4783–4788, Oct. 2011.
[188] X. Ren, Y. Zhou, D. Wang, X. Zou, and Z. Zhang, "A 10-MHz isolated synchronous class-Φ_2 resonant converter," *IEEE Trans. Power Electron.*, vol. 31, no. 12, pp. 8317–8328, Dec. 2016.
[189] A. Knott, T. M. Andersen, P. Kamby, J. A. Pedersen, M. P. Madsen, M. Kovacevic, and M. A. Andersen, "Evolution of very high frequency power supplies," *IEEE J. Emerg. Sel. Topics Power Electron.*, vol. 2, no. 3, pp. 386–394, Sep. 2014.
[190] M. P. Madsen, J. A. Pedersen, A. Knott, and M. A. E. Andersen, "Self-oscillating resonant gate drive for resonant inverters and rectifiers composed solely of passive components," in *Proc. 29thIEEE Appl. Power Electron. Conf. Expo. (APEC)*, Mar. 2014, pp. 2029–2035.
[191] M. Forouzesh, Y. P. Siwakoti, S. A. Gorji, F. Blaabjerg, and B. Lehman, "Step-up DC–DC converters: A comprehensive review of voltage-boosting techniques, topologies, and applications," *IEEE Trans. Power Electron.*, vol. 32, no. 12, pp. 9143–9178, Dec. 2017.
[192] S. A. Arshadi, E. Adib, H. Farzanehfard, and M. Esteki, "New high step-up DC–DC converter for photovoltaic grid-connected applications," in *Proc. 6th Power Electron., Drive Syst. Technol. Conf. (PEDSTC)*, Feb. 2015, pp. 189–194.
[193] A. M. S. S. Andrade, E. Mattos, L. Schuch, H. L. Hey, and M. L. da Silva Martins, "Synthesis and comparative analysis of very high step-up DC–DC converters adopting coupled-inductor and voltage multiplier cells," *IEEE Trans. Power Electron.*, vol. 33, no. 7, pp. 5880–5897, Jul. 2018.
[194] M. G. Kim, "High-performance current-mode-controller design of buck LED driver with slope compensation," *IEEE Trans. Power Electron.*, vol. 33, no. 1, pp. 641–649, Jan. 2018.
[195] S. Khalili, M. Esteki, M. Packnezhad, H. Farzanehfard, and S. A. Khajehoddin, "Fully soft-switched non-isolated high step-down DC–DC converter with reduced voltage stress and expanding capability," *IEEE J. Emerg. Sel. Topics Power Electron.*, vol. 11, no. 1, pp. 796–805, Feb. 2023.
[196] N. Molavi, M. Esteki, E. Adib, and H. Farzanehfard, "High step-up/down DC–DC bidirectional converter with low switch voltage stress," in *Proc. 6th Power Electron., Drive Syst. Technol. Conf. (PEDSTC)*, Feb. 2015, pp. 162–167.
[197] M. Hajiheidari, H. Farzanehfard, and M. Esteki, "Asymmetric ZVS buck converters with high-step-down conversion ratio," *IEEE Trans. Ind. Electron.*, vol. 68, no. 9, pp. 7957–7964, Sep. 2021.
[198] M. Esteki, B. Poorali, E. Adib, and H. Farzanehfard, "Interleaved buck converter with continuous input current, extremely low output current ripple, low switching losses, and improved step-down conversion ratio," *IEEE Trans. Ind. Electron.*, vol. 62, no. 8, pp. 4769–4776, Aug. 2015.
[199] G. Spiazzi, D. Tagliavia, and S. Spampinato, "DC–DC flyback converters in the critical conduction mode: A re-examination," in *Proc. Conf. Rec. IEEE Ind. Appl. Conf. 35th IAS Annu. Meeting World Conf. Ind. Appl. Electr. Energy*, vol. 4, Oct. 2000, pp. 2426–2432.
[200] H.-H. Chou, Y.-S. Hwang, and J.-J. Chen, "An adaptive output current estimation circuit for a primary-side controlled LED driver," *IEEE Trans. Power Electron.*, vol. 28, no. 10, pp. 4811–4819, Oct. 2013.
[201] X. Xie, Z. Lan, and C. Zhao, "A new primary side controlled high power factor single-stage flyback LED driver," in *Proc. IEEE Energy Convers. Congr. Expo. (ECCE)*, Sep. 2012, pp. 3575–3580.
[202] K. I. Hwu, Y. T. Yau, and L.-L. Lee, "Powering LED using high-efficiency SR flyback converter," *IEEE Trans. Ind. Appl.*, vol. 47, no. 1, pp. 376–386, Jan./Feb. 2011.
[203] Y. B. Weng and Y. Xing, "A dual-transformer flyback converter in critical conduction mode," in *Proc. 4th Int. Power Electron. Motion Control Conf. (IPEMC)*, vol. 3, 2004, pp. 1074–1079.
[204] C. Y. Inaba, Y. Konishi, H. Tanimatsu, K. Hirachi, and M. Nakaoka, "Soft switching PWM DC–DC flyback converter with transformer–assisted pulse current regenerative passive resonant snubbers," in *Proc. 5th Int. Conf. Power Electron. Drive Syst. (PEDS)*, 2003, pp. 882–887.
[205] M. S. Perdigão, M. F. Menke, Á. R. Seidel, R. A. Pinto, and J. M. Alonso, "A review on variable inductors and variable transformers: Applications to lighting drivers," *IEEE Trans. Ind. Appl.*, vol. 52, no. 1, pp. 531–547, Jan. 2016.
[206] J. M. Alonso, M. Perdigao, M. A. D. Costa, G. Martínez, and R. Osorio, "Analysis and design of a novel variable-inductor-based LED driver for DC lighting grids," in *Proc. IEEE Ind. Appl. Soc. Annu. Meeting*, Oct. 2016, pp. 1–8.
[207] E. E. D. S. Filho, F. L. M. Antunes, P. H. A. Miranda, and E. M. Sá, "A LED driver with switched capacitor," in *Proc. 10th IEEE/IAS Int. Conf. Ind. Appl.*, Nov. 2012, pp. 1–6.
[208] L. Zuo, H. Qin, L. Ma, and T. Fang, "Design and implementation of LLC half-bridge LED driver based on NCP1396," in *Proc. Int. Conf. Electr. Control Eng.*, Sep. 2011, pp. 4424–4426.
[209] K. Chen, P. Xiao, A. Johnsen, and R. E. Saenz, "Turn-on optimization for class D series–parallel *LCC*-type constant current high-power LED driver design based on traditional fluorescent control IC," *IEEE Trans. Power Electron.*, vol. 31, no. 7, pp. 4732–4741, Jul. 2016.
[210] B. Akhlaghi, M. Esteki, and H. Farzanehfard, "Family of zero voltage transition interleaved converters with low voltage and current stress," *IET Power Electron.*, vol. 11, no. 12, pp. 1886–1893, Oct. 2018.
[211] I. Castro, A. Vazquez, D. G. Aller, M. Arias, D. G. Lamar, and J. Sebastian, "On supplying LEDs from very low DC voltages with high-frequency AC-LED drivers," *IEEE Trans. Power Electron.*, vol. 34, no. 6, pp. 5711–5719, Jun. 2019.
[212] I. Castro, D. G. Lamar, S. Lopez, K. Martin, M. Arias, and J. Sebastian, "A family of high frequency AC-LED drivers based on ZCS-QRCs," *IEEE Trans. Power Electron.*, vol. 33, no. 10, pp. 8728–8740, Oct. 2018.
[213] S. Lim, J. Ranson, D. M. Otten, and D. J. Perreault, "Two-stage power conversion architecture suitable for wide range input voltage," *IEEE Trans. Power Electron.*, vol. 30, no. 2, pp. 805–816, Feb. 2015.
[214] C.-S. Moo, Y.-J. Chen, Y.-J. Li, and H.-C. Yen, "A dimmable LED driver with partial power regulation," in *Proc. 41st Annu. Conf. IEEE Ind. Electron. Soc. (IECON)*, Nov. 2015, pp. 672–677.
[215] N. G. F. D. Santos, J. R. R. Zientarski, and M. L. da Silva Martins, "A review of series-connected partial power converters for DC–DC applications," *IEEE J. Emerg. Sel. Topics Power Electron.*, vol. 10, no. 6, pp. 7825–7838, Dec. 2021.
[216] T. McRae, A. Prodić, G. Lisi, W. McIntrye, and A. Aguilar, "Hybrid serial-output converter for integrated LED lighting applications," in *Proc. IEEE Appl. Power Electron. Conf. Expo. (APEC)*, Mar. 2016, pp. 2540–2544.
[217] T. McRae and A. Prodić, "Hybrid serial-output converter topology for volume and weight restricted LED lighting applications," in *Proc. 9th Int. Conf. Power Electron. ECCE Asia (ICPE-ECCE Asia)*, Jun. 2015, pp. 1311–1316.

[218] T. McRae, A. Prodić, S. Chakraborty, W. McIntyre, and A. Aguilar, "A hybrid multioutput divided power converter for LED applications," *IEEE J. Emerg. Sel. Topics Power Electron.*, vol. 8, no. 3, pp. 2041–2055, Sep. 2020.

[219] K. I. Hwu and W. C. Tu, "Controllable and dimmable AC LED driver based on FPGA to achieve high PF and low THD," *IEEE Trans. Ind. Informat.*, vol. 9, no. 3, pp. 1330–1342, Aug. 2013.

[220] H. Gao, K. Sun, J. Chen, X. Wu, Y. Leng, J. Xi, and L. He, "An electrolytic-capacitorless and inductorless AC direct LED driver with power compensation," in *Proc. IEEE 2nd Int. Future Energy Electron. Conf. (IFEEC)*, Nov. 2015, pp. 1–5.

[221] K. I. Hwu and J.-J. Shieh, "Dimmable AC LED driver based on series drive," *J. Display Technol.*, vol. 12, no. 10, pp. 1097–1105, Oct. 2016.

[222] C. Liu, X.-Q. Lai, H.-S. He, and H.-X. Du, "Sectional linear LED driver for optimised efficiency in lighting applications," *IET Power Electron.*, vol. 9, no. 4, pp. 825–834, 2016.

[223] Y. Gao, L. Li, K.-H. Chong, and P. K. T. Mok, "A hybrid LED driver with improved efficiency," *IEEE J. Solid-State Circuits*, vol. 55, no. 8, pp. 2129–2139, Aug. 2020.

[224] J. Kim, J. Lee, and S. Park, "A soft self-commutating method using minimum control circuitry for multiple-string LED drivers," in *IEEE Int. Solid-State Circuits Conf. (ISSCC) Dig. Tech. Papers*, Feb. 2013, pp. 376–377.

[225] Y.-T. Yau, K.-I. Hwu, and C.-W. Wang, "Bridgeless isolated AC LED driver," *Processes*, vol. 9, no. 7, p. 1173, Jul. 2021.

[226] E. S. Lee, B. H. Choi, J. P. Cheon, G. C. Lim, B. C. Kim, and C. T. Rim, "Temperature-robust LC^3 passive LED drivers with low THD, high efficiency and PF, and long life," *IEEE J. Emerg. Sel. Topics Power Electron.*, vol. 3, no. 3, pp. 829–840, Sep. 2015.

[227] D. Venkatesh and S. V. Thazhathu, "Design and analysis of an integrated LC^3–valley fill passive LED driver," *Int. J. Electron.*, vol. 105, no. 12, pp. 2052–2065, Dec. 2018.

[228] D. G. Lamar, M. Arias, M. M. Hernando, and J. Sebastian, "Using the loss-free resistor concept to design a simple AC–DC HB-LED driver for retrofit lamp applications," *IEEE Trans. Ind. Appl.*, vol. 51, no. 3, pp. 2300–2311, May/Jun. 2014.

[229] I. Burgardt, E. A. Junior, C. H. Illa Font, and C. B. Nascimento, "Dimmable flicker-free power LEDs lighting system based on a SEPIC rectifier using a regenerative snubber," *IET Power Electron.*, vol. 9, no. 5, pp. 891–899, Apr. 2016.

[230] Y.-C. Liu, F.-C. Syu, H.-C. Hsieh, K. A. Kim, and H.-J. Chiu, "Hybrid switched-inductor buck PFC converter for high-efficiency LED drivers," *IEEE Trans. Circuits Syst. II, Exp. Briefs*, vol. 65, no. 8, pp. 1069–1073, Aug. 2018.

[231] S. Bandyopadhyay, B. Neidorff, D. Freeman, and A. P. Chandrakasan, "90.6% efficient 11 MHz 22 W LED driver using GaN FETs and burst-mode controller with 0.96 power factor," in *IEEE Int. Solid-State Circuits Conf. (ISSCC) Dig. Tech. Papers*, Feb. 2013, pp. 368–369.

[232] S.-W. Lee and H.-L. Do, "A single-switch AC–DC LED driver based on a boost-flyback PFC converter with lossless snubber," *IEEE Trans. Power Electron.*, vol. 32, no. 2, pp. 1375–1384, Feb. 2017.

[233] D. G. Lamar, M. Arias, A. Fernandez, J. A. Villarejo, and J. Sebastian, "Active input current shaper without an electrolytic capacitor for retrofit lamps applications," *IEEE Trans. Power Electron.*, vol. 32, no. 5, pp. 3908–3919, May 2017.

[234] J. Yi, H. Ma, X. Li, S. Lu, and J. Xu, "A novel hybrid PFM/IAPWM control strategy and optimal design for single-stage interleaved boost-LLC AC–DC converter with quasi-constant bus voltage," *IEEE Trans. Ind. Electron.*, vol. 68, no. 9, pp. 8116–8127, Sep. 2021.

[235] C.-A. Cheng, H.-L. Cheng, C.-H. Chang, F.-L. Yang, and T.-Y. Chung, "A single-stage LED driver for street-lighting applications with interleaving PFC feature," in *Proc. Int. Symp. Next-Gener. Electron.*, Feb. 2013, pp. 150–152.

[236] Z. P. da Fonseca, A. J. Perin, E. A. Junior, and C. B. Nascimento, "Single-stage high power factor converters requiring low DC-link capacitance to drive power LEDs," *IEEE Trans. Ind. Electron.*, vol. 64, no. 5, pp. 3557–3567, May 2017.

[237] X. Liu, X. Li, Q. Zhou, and J. Xu, "Flicker-free single switch multi-string LED driver with high power factor and current balancing," *IEEE Trans. Power Electron.*, vol. 34, no. 7, pp. 6747–6759, Jul. 2019.

[238] A. Malschitzky, E. Agostini, and C. B. Nascimento, "Integrated bridgeless-boost nonresonant half-bridge converter employing hybrid modulation strategy for LED driver applications," *IEEE Trans. Ind. Electron.*, vol. 68, no. 9, pp. 8049–8060, Sep. 2021.

[239] J. M. Alonso, D. Gacio, J. Garcia, M. Rico-Secades, and M. A. D. Costa, "Analysis and design of the integrated double buck-boost converter operating in full DCM for LED lighting applications," in *Proc. 37th Annu. Conf. IEEE Ind. Electron. Soc. (IECON)*, Nov. 2011, pp. 2889–2894.

[240] S. Li, W. Qi, J. Wu, S.-C. Tan, and S.-Y. Hui, "Minimum active switch requirements for single-phase PFC rectifiers without electrolytic capacitors," *IEEE Trans. Power Electron.*, vol. 34, no. 6, pp. 5524–5536, Jun. 2019.

[241] H.-L. Cheng and C.-W. Lin, "Design and implementation of a high-power-factor LED driver with zero-voltage switching-on characteristics," *IEEE Trans. Power Electron.*, vol. 29, no. 9, pp. 4949–4958, Sep. 2014.

[242] C. Gobbato, S. V. Kohler, I. H. de Souza, G. W. Denardin, and J. de Pelegrini Lopes, "Integrated topology of DC–DC converter for LED street lighting system based on modular drivers," *IEEE Trans. Ind. Appl.*, vol. 54, no. 4, pp. 3881–3889, Jul./Aug. 2018.

[243] H. Ma, Y. Li, J.-S. Lai, C. Zheng, and J. Xu, "An improved bridgeless SEPIC converter without circulating losses and input-voltage sensing," *IEEE J. Emerg. Sel. Topics Power Electron.*, vol. 6, no. 3, pp. 1447–1455, Sep. 2018.

[244] H. Khalilian, H. Farzanehfard, E. Adib, and M. Esteki, "Analysis of a new single-stage soft-switching power-factor-correction LED driver with low DC-bus voltage," *IEEE Trans. Ind. Electron.*, vol. 65, no. 5, pp. 3858–3865, May 2018.

[245] G. Z. Abdelmessih and J. M. Alonso, "A new active hybrid-series-parallel PWM dimming scheme for off-line integrated LED drivers with high efficiency and fast dynamics," in *Proc. IEEE Ind. Appl. Soc. Annu. Meeting*, Oct. 2016, pp. 1–8.

[246] H.-A. Ahn, S.-K. Hong, and O.-K. Kwon, "A highly accurate current LED lamp driver with removal of low-frequency flicker using average current control method," *IEEE Trans. Power Electron.*, vol. 33, no. 10, pp. 8741–8753, Oct. 2018.

[247] L. Wang, B. Zhang, and D. Qiu, "A novel valley-fill single-stage boost-forward converter with optimized performance in universal-line range for dimmable LED lighting," *IEEE Trans. Ind. Electron.*, vol. 64, no. 4, pp. 2770–2778, Apr. 2017.

[248] P. TianFu, C. HuangJen, C. ShihJen, and C. ShihYen, "An improved single-stage flyback PFC converter for high-luminance lighting LED lamps," in *Proc. 8th Int. Conf. Electron. Meas. Instrum.*, Aug. 2007, pp. 4-212–4-215.

[249] G. Z. Abdelmessih, J. M. Alonso, and W.-T. Tsai, "Analysis and experimentation on a new high power factor off-line LED driver based on interleaved integrated buck flyback converter," *IEEE Trans. Ind. Appl.*, vol. 55, no. 4, pp. 4359–4369, Jul. 2019.

[250] G. G. Pereira, M. A. D. Costa, J. M. Alonso, M. F. De Melo, and C. H. Barriquello, "LED driver based on input current shaper without electrolytic capacitor," *IEEE Trans. Ind. Electron.*, vol. 64, no. 6, pp. 4520–4529, Jun. 2017.

[251] S. Pervaiz, A. Kumar, and K. K. Afridi, "GaN-based high-power-density electrolytic-free universal input led driver," *IEEE Trans. Ind. Appl.*, vol. 54, no. 4, pp. 3890–3901, Jul./Aug. 2018.

[252] F. Zhang, J. Ni, and Y. Yu, "High power factor AC–DC LED driver with film capacitors," *IEEE Trans. Power Electron.*, vol. 28, no. 10, pp. 4831–4840, Oct. 2013.

[253] H.-C. Kim, M. C. Choi, S. Kim, and D.-K. Jeong, "An AC–DC LED driver with a two-parallel inverted buck topology for reducing the light flicker in lighting applications to low-risk levels," *IEEE Trans. Power Electron.*, vol. 32, no. 5, pp. 3879–3891, May 2017.

[254] K.-W. Lee, Y.-H. Hsieh, and T.-J. Liang, "A current ripple cancellation circuit for electrolytic capacitor-less AC-DC LED driver," in *Proc. 28th Annu. IEEE Appl. Power Electron. Conf. Expo. (APEC)*, Mar. 2013, pp. 1058–1061.

[255] Y. Zhang and K. Jin, "A single-stage electrolytic capacitor-less AC/DC LED driver," in *Proc. Int. Power Electron. Appl. Conf. Expo.*, Nov. 2014, pp. 881–886.

[256] H. Dong, X. Xie, L. Jiang, Z. Jin, and X. Zhao, "An electrolytic capacitor-less high power factor LED driver based on a 'one-and-a-half stage' forward-flyback topology," *IEEE Trans. Power Electron.*, vol. 33, no. 2, pp. 1572–1584, Feb. 2018.

[257] W. Chen and S. Y. R. Hui, "Elimination of an electrolytic capacitor in AC/DC light-emitting diode (LED) driver with high input power factor and constant output current," *IEEE Trans. Power Electron.*, vol. 27, no. 3, pp. 1598–1607, Mar. 2012.

[258] P. Fang, B. Sheng, S. Webb, Y. Zhang, and Y.-F. Liu, "LED driver achieves electrolytic capacitor-less and flicker-free operation with an energy buffer unit," *IEEE Trans. Power Electron.*, vol. 34, no. 7, pp. 6777–6793, Jul. 2019.

[259] H. Wu, S.-C. Wong, C. K. Tse, S. Y. R. Hui, and Q. Chen, "Single-phase LED drivers with minimal power processing, constant output current, input power factor correction, and without electrolytic capacitor," *IEEE Trans. Power Electron.*, vol. 33, no. 7, pp. 6159–6170, Jul. 2018.
[260] H. Valipour, G. Rezazadeh, and M. R. Zolghadri, "Flicker-free electrolytic capacitor-less universal input offline LED driver with PFC," *IEEE Trans. Power Electron.*, vol. 31, no. 9, pp. 6553–6561, Sep. 2016.
[261] G.-C. Jane, Y.-L. Lin, H.-J. Chiu, and Y.-K. Lo, "Dimmable light-emitting diode driver with cascaded current regulator and voltage source," *IET Power Electron.*, vol. 8, no. 7, pp. 1305–1311, Jul. 2015.
[262] Z. Shan, X. Chen, J. Jatskevich, and C. K. Tse, "AC–DC LED driver with an additional active rectifier and a unidirectional auxiliary circuit for AC power ripple isolation," *IEEE Trans. Power Electron.*, vol. 34, no. 1, pp. 685–699, Jan. 2019.
[263] K.-B. Park, G.-W. Moon, and M.-J. Youn, "Nonisolated high step-up stacked converter based on boost-integrated isolated converter," *IEEE Trans. Power Electron.*, vol. 26, no. 2, pp. 577–587, Feb. 2011.
[264] J.-I. Baek, J.-K. Kim, J.-B. Lee, H.-S. Youn, and G.-W. Moon, "Integrated asymmetrical half-bridge zeta (AHBZ) converter for DC/DC stage of LED driver with wide output voltage range and low output current," *IEEE Trans. Ind. Electron.*, vol. 62, no. 12, pp. 7489–7498, Dec. 2015.
[265] G. Spiazzi and S. Buso, "Extended analysis of the asymmetrical half-bridge flyback converter," *IEEE Trans. Power Electron.*, vol. 36, no. 7, pp. 7956–7964, Jul. 2021.
[266] S. Marconi, G. Spiazzi, A. Bevilacqua, and M. Galvano, "A novel integrated step-up hybrid converter with wide conversion ratio," *IEEE Trans. Power Electron.*, vol. 35, no. 3, pp. 2764–2775, Mar. 2020.
[267] T. McRae, N. Vukadinović, and A. Prodić, "Low-volume hybrid tap-connected SC-buck converter with shared output capacitor," in *Proc. IEEE Appl. Power Electron. Conf. Expo. (APEC)*, Mar. 2017, pp. 2222–2227.
[268] M. Huang, Y. Lu, T. Hu, and R. P. Martins, "A hybrid boost converter with cross-connected flying capacitors," *IEEE J. Solid-State Circuits*, vol. 56, no. 7, pp. 2102–2112, Jul. 2021.
[269] N. Pal, A. Fish, W. McIntyre, N. Griesert, G. Winter, T. Eichhorn, R. Pilawa-Podgurski, and P. K. Hanumolu, "A 91.15% efficient 2.3–5-V input 10–35-V output hybrid boost converter for LED-driver applications," *IEEE J. Solid-State Circuits*, vol. 56, no. 11, pp. 3499–3510, Nov. 2021.

MORTEZA ESTEKI (Student Member, IEEE) received the B.Sc. degree in electrical engineering from the University of Bonab, East Azerbaijan, Iran, in 2012, and the M.Sc. degree in electrical engineering (electronics) from the Isfahan University of Technology (IUT), Isfahan, Iran, in 2015. He is currently pursuing the Ph.D. degree in electrical engineering with the University of Alberta, Edmonton, AB, Canada.

He was a Research Assistant and a Laboratory Engineer with the Department of Electrical and Computer Engineering, IUT, from 2015 to 2019. He has authored or coauthored more than 30 technical papers published in journals and conference proceedings. His current research interests include high-frequency high-power-density DC–DC, AC–DC, and DC–AC converters, renewable energy, and modeling and control.

Mr. Esteki received numerous awards and scholarships, including the Best Master of Science Thesis Award in Electrical and Computer Engineering in Iran, awarded by the IEEE Iran Section, in 2016, the Alberta Graduate Excellence Scholarship, in 2020, the Dr. William Youdelis Graduate Scholarship in Engineering, in 2021, and the Alberta Innovates Graduate Student Scholarship, in 2021 and 2022.

S. ALI KHAJEHODDIN (Senior Member, IEEE) received the Ph.D. degree in electrical engineering from Queens University, Kingston, Canada, in April 2010. Prior to his Ph.D. degree, he had co-founded a start-up company that was focused on the development and production of power analyzers and smart metering products for smart grid applications. For his doctoral research with Queen's University, he concentrated on the design and implementation of compact and durable microinverters for photovoltaic (PV) grid-connected systems; leading to the spin off of SPARQ Systems Inc., where he was a Lead Research and Development Engineer toward mass production and commercialization of microinverters, from 2010 to 2013. He is currently a Professor with the University of Alberta, Edmonton, Canada. His current research interests include design and implementation of high-power density power converters based on novel modeling techniques, topologies, and controllers for energy systems.

He was a recipient of several awards, including Second Place Paper Award from the IEEE TRANSACTIONS ON POWER ELECTRONICS, in 2022. He is also an Associate Editor of IEEE TRANSACTIONS ON POWER ELECTRONICS, IEEE TRANSACTIONS ON TRANSPORTATION ELECTRIFICATION, and *Journal of Emerging and Selected Topics in Power Electronics*.

ALIREZA SAFAEE (Senior Member, IEEE) received the Ph.D. degree in power electronics from Queen's University, in 2015.

From 1997 to 2005, he was a Design Engineer/ the Manager of Manabe Taghzyeh Electronic Company, where he played a major role in establishing automotive lighting products for national automakers. He designed controllers for tail lights and brake lights, completed the standard compliance processes, and later launched the product lines. He also designed 10kW inverters for emergency lightings of metro stations, with extreme safety, and security considerations. These systems are still in operation. From 2011 to 2014, he was with Bombardier Transportation working on projects that required lighting systems development (via collaboration with vendors) for rail wayside lighting and for train vehicle interior lighting. From 2014 to 2017, he was a Senior Key Expert with the OSRAM Sylvania Research Center working on steerable automotive lighting systems, street lighting LED drivers that could energize IoT sensing systems, micro LED displays, and tail lights for EVs. He contributed to a first-of-a-kind high-precision flicker measurement tool. His designs are used in several products and granted more than ten patents. Since 2017, he has been with Apple Inc., developing power supplies and displays.

YUNWEI (RYAN) LI (Fellow, IEEE) received the Ph.D. degree from Nanyang Technological University, Singapore.

In 2005, he was a Visiting Scholar with Aalborg University, Denmark. From 2006 to 2007, he was a Postdoctoral Research Fellow with Ryerson University, Canada. In 2007, he was with Rockwell Automation Canada, before he joined the University of Alberta, Canada, in 2007, where he is currently a Professor and the Interim Department.

Dr. Li received the Richard M. Bass Outstanding Young Power Electronics Engineer Award from IEEE PELS, in 2013. He is recognized as a Highly Cited Researcher by the Web of Science Group. He serves as the Editor-in-Chief for IEEE TRANSACTIONS ON POWER ELECTRONICS LETTERS. Prior to that, he was an Associate Editor for IEEE TRANSACTIONS ON POWER ELECTRONICS, IEEE TRANSACTIONS ON INDUSTRIAL ELECTRONICS, IEEE TRANSACTIONS ON SMART GRID, and IEEE JOURNAL OF EMERGING AND SELECTED TOPICS IN POWER ELECTRONICS. He served as the General Chair for IEEE Energy Conversion Congress of Exposition (ECCE), in 2020. He is an AdCom Member at Large for IEEE Power Electronics Society (PELS) (2021–2023).